MOLECULAR MECHANISMS OF ADHESION OF PLANKTONIC AND BIOFILM-DISPERSED *ESCHERICHIA COLI* CELLS TO SILICON NITRIDE INVESTIGATED BY ATOMIC FORCE MICROSCOPE

AYŞE ÖRDEK

Master's Thesis

Graduate School

Izmir University of Economics

İzmir

2021

MOLECULAR MECHANISMS OF ADHESION OF PLANKTONIC AND BIOFILM-DISPERSED *ESCHERICHIA COLI* CELLS TO SILICON NITRIDE INVESTIGATED BY ATOMIC FORCE MICROSCOPE

AYŞE ÖRDEK

A Thesis Submitted to
The Graduate School of Izmir University of Economics
Master of Science Program in Bioengineering

İzmir
2021

ABSTRACT

MOLECULAR MECHANISMS OF ADHESION OF PLANKTONIC AND BIOFILM-DISPERSED *ESCHERICHIA COLI* CELLS TO SILICON NITRIDE INVESTIGATED BY ATOMIC FORCE MICROSCOPE

Ördek, Ayşe

Master of Science Program in Bioengineering

Advisor: Asst. Prof. Dr. Fatma Pınar Gördesli Duatepe

February, 2021

Targetting c-di GMP pathways by using nitric oxide donor sodium nitroprusside (SNP), thereby inducing biofilm dispersal, is a widely used strategy in combating biofilms. However, recent studies have shown that bacteria, which are thought to have entered the planktonic mode after biofilm dispersal, actually possess different properties and are more lethal than their planktonic counterparts. This situation indicates that improved strategies are needed to control the adhesion of biofilm-dispersed cells to surfaces and their development into new biofilms. However, little is known regarding the molecular adhesion properties of biofilm-dispersed cells in comparison to planktonic cells. In this dissertation, to reveal the differences between molecular adhesions of planktonic and biofilm-dispersed *E. coli* cells (as functions of different SNP concentration added to biofilm cultures grown in batch and continuous systems), their adhesion forces to model inert surfaces of silicon nitride in water were

measured by atomic force microscope (AFM). In addition, bacterial dimensions and the lengths of their surface biopolymers were determined using AFM. Higher values of bacterial dimensions, molecular adhesion strengths, and heterogeneities in the AFM data correlated with higher intracellular c-di GMP amounts. In particular, the use of 0.5 μM and 2.5 mM (toxic) SNP concentrations caused significant increases in the molecular adhesion and c-di GMP amounts of biofilm-dispersed cells from batch cultures. Considering the role of c-di GMP in biofilm dispersion, the investigation of molecular adhesion mechanisms of c-di GMP induced biofilm-dispersed cells will contribute to the elimination of gaps in the literature and the development of biofilm-combating methods.

Keywords: Biofilm dispersion, molecular adhesion, adhesion force, atomic force microscope (AFM), c-di GMP, sodium nitroprusside (SNP)

ÖZET

PLANKTONİK VE BİYOFİLMDEN DAĞILMIŞ *ESCHERICHIA COLI* HÜCRELERİNİN SİLİKON NİTRATA OLAN ADEZYONLARININ MOLEKÜLER MEKANİZMALARININ ATOMİK KUVVET MİKROSKOBU İLE İNCELENMESİ

Ördek, Ayşe

Biyomühendislik Tezli Yüksek Lisans Programı

Tez Danışmanı: Dr. Öğr. Üyesi Fatma Pınar GÖRDESLİ DUATEPE

Şubat, 2021

Nitrik oksit verici sodyum nitroprusit (SNP) kullanarak, c-di GMP yolaklarının hedeflenmesi ve böylece biyofilm dağılımının sağlanması biyofilmlerle mücadelede yaygın olarak kullanılan bir stratejidir. Ancak son araştırmalar biyofilm dağıldıktan sonra planktonik moda girdiği düşünülen bakterilerin aslında planktonik muadillerinden farklı özelliklere sahip olduğunu ve daha öldürücü olduğunu göstermiştir. Bu durum, biyofilmden dağılmış hücrelerin yüzeylere adezyonunu ve yeni biyofilmlere dönüşmesini kontrol etmek için geliştirilmiş stratejilere ihtiyaç olduğunu göstermektedir. Ancak planktonik hücrelere kıyasla biyofilmden dağılmış hücrelerin moleküler adezyon özellikleri hakkında çok az bilgi bulunmaktadır. Bu çalışmada, planktonik ve biyofilmden dağılmış *E. coli* hücrelerinin (kesikli ve sürekli sistem biyofilmlerine eklenen farklı SNP konsantrasyonunun fonksiyonları olarak)

moleküler adezyonları arasındaki farkları ortaya çıkarmak amacıyla su içinde model silikon nitrat yüzeylerine uyguladıkları adezyon kuvvetleri atomik kuvvet mikroskobu (AKM) ile ölçülmüştür. Ek olarak, bakteri boyutları ve yüzey biyopolimerlerinin uzunlukları da belirlenmiştir. Yüksek değerlerdeki bakteri boyutları, adezyon kuvvetleri ve AKM verilerindeki heterojenlik, yüksek değerdeki hücre içi c-di GMP miktarlarıyla korelasyon göstermiştir. Özellikle 0.5 μM ve 2.5 mM (toksik) konsantrasyonlarda SNP kullanımının biyofilmden dağılmış hücrelerin moleküler adezyonunda ve c-di GMP miktarlarında önemli artışlara neden olduğu görülmüştür.Biyofilm dağılımında c-di GMP'nin rolü göz önüne alındığında, c-di GMP kaynaklı biyofilmden dağılmış hücrelerin moleküler adezyon mekanizmalarının araştırılması, literatürdeki boşlukların giderilmesine ve biyofilmle mücadele yöntemlerinin geliştirilmesine katkı sağlayacaktır.

Anahtar Kelimeler: Biyofilm dağılımı, moleküler adezyon, adezyon kuvveti, atomik kuvvet mikroskobu (AKM), c-di GMP, sodyum nitroprusit (SNP)

ACKNOWLEDGEMENTS

Foremost, my most sincere thanks to Asst. Prof. Dr. Fatma Pınar GÖRDESLİ DUATEPE, for giving me the opportunity to study in this project, for her strong support throughout my master's education and for being such an inspirational supervisor. Her knowledge and experiences are very valuable for me.

I am so thankful to my project partner, Gamze Nur ASPAR, who my lovely friend and confidante, who best teammate with her skills and kindness for her endless support, and patience during almost all of my master's education. Her presence and support are my great chance.

I would like to thank for their support to Dünya KILAVUZ, Beyza KANAT, Mesoud ABEDINIFAR, Saygın PORTAKAL, Çağatay KIRMIZIAY, Sahra TABAKOĞLU, Erdem OKUR, Ece SARIYAR and lab friends. I will never forget their help. I would like to say my deepest thanks to my dearest friends Necati Erdem TUĞRAHAN, Betül TORUN, Büşra UÇAR and Elvan Beril PETEK for providing a great support to me during the completion of this thesis. They gave me the motivation I needed to finish this project. Their support and love are very precious to me.

I would like to express my profound thanks to my lovely family, starting with my dear mother Nezihe ÖRDEK, and my dear father Salih ÖRDEK. Their unconditional love and support are my best sources of energy. And of course, I am so thankful to my confidant sisters, Setenay ERYILMAZ and Ceren ÖRDEK, and my new brother Emrullah ERYILMAZ.

Finally, I would like to thank The Scientific and Technological Research Council of Turkey (TUBITAK) for providing us financial support to work on this project coded 118M404 and Izmir University of Economics for hosting this project.

TABLE OF CONTENTS

LIST OF TABLES

LIST OF FIGURES

CHAPTER 1: INTRODUCTION

Bacteria are present in almost every environment such as in the soil, human body, water resources, and even in the radioactive wastes. Depending on the ambient conditions, bacterial cells can be found as either freely-floating *planktonic cells* in fluids or as three-dimensional (3D) complex architectures of communities at the liquid-solid interface, namely as the *biofilms*. Bacteria become resistant to harsh environmental conditions by forming biofilms in the environment. These communities are basically formed by the bacterial cells multiplying within a sticky matrix composed of extracellular polymeric substances (EPSs) on surfaces (Flemming, and Wingender, 2010; Yin et al., 2019). Polysaccharide-based EPS matrix enables the bacterial cells to hold onto each other and to surfaces, and further to form 3D biofilm structure that contains water channels and bacterial layers. Biofilm formation results in significant changes in bacteria such as changes in gene expressions, intercellular communication, protection mechanisms, structural integrity and adhesion ability (Flemming, and Wingender, 2010).

Living in a biofilm structure has several advantages for bacterial cells. One of the important advantages is that the extracellular matrix is protective shield for the bacteria against both physical and chemical external factors. EPS composition can change according to the changes in the environmental conditions, thus ensuring the continuity of protection of bacterial life within the biofilm (Kostakioti et al., 2013). Another important advantage is that it creates an environment that facilitates the exchange of metabolites. The biofilm matrix reduces the diffusivities of small molecules, allowing them to stay in the biofilm longer, thus allowing longer access to nutrients (Flemming, and Wingender, 2010). As a consequence of the advantages of the EPS matrix and multicellular lifestyle, bacteria become resistant to adverse environmental conditions, antibiotics, and disinfection treatments (James et al., 2008). Due to the highly developed resistance to antimicrobial treatments and disinfectants, uncontrolled and unwanted biofilm formations on surfaces causes serious difficulties.

Generally, human body infections are related to the bacterial biofilms. It is known that bacteria can easily attach to implants and form biofilms. This causes an

increase in tissue trauma and treatment costs. Biofilms especially formed on the surfaces of industrial processing equipment in contact with food or water, are the sources of contamination that threaten the quality and safety of products and hence the human health. Additionally, biofilms cause equipment, time, and labor losses in the industry. Consequently, biofilms can cause foodborne or waterborne disease outbreaks that may result in high hospitalization rates and huge economic losses.

Biofilm formation progresses as a process with different stages. Initial stage is the reversible attachment of the planktonic microorganism to the surface. Subsequently, stimulation of bacterial surface biopolymers and initiation of EPS synthesis mediate the permanent attachment of the bacteria to the surface. Then the microcolonies are formed by the proliferation of bacteria which are tightly attached to the surface. Bacteria in microcolonies form mature biofilm structures by proliferation and EPS production (Koo et al., 2017). At this maturation stage, the EPS matrix provides a multifunctional and protective framework for the development of microcolonies (Donlan, 2002). The last stage is the escape of some portion of the bacterial cells from the biofilm structure by using cellular signals. In this process known as the *dispersal stage*, the biofilm-dispersed cells migrate to other surfaces and form new biofilm structures (Koo et al., 2017). This will cause the spread of the biofilm or the transition of acute infections to a chronic state.

Due to high resistance of mature biofilms to antimicrobial agents, previously conducted studies focused mainly on the dispersion of biofilms to eliminate infections. The biofilm dispersion is already a part of the biofilm life-cycle and occurs naturally, as previously mentioned. Researchers have developed methods that mimic this natural dispersion process as a method of combating biofilms. Targeting of cyclic dimeric guanosine monophosphate (c-di GMP) signaling pathways has been shown to trigger the biofilm dispersion. With its applicability both in vivo and in vitro environments, targeting of c-di GMP signaling pathways is accepted as a highly effective approach for the dispersion of biofilms from the surfaces (Chua et al., 2015; Romling et al., 2013).

Intracellular c-di GMP level is particularly effective on the bacterial motility. In other words, c-di GMP level of the bacterium changes during the transition from

the planktonic existence to the biofilm stage. The use of nitric oxide (NO) donors plays an important role in modulating c-di GMP levels. The NO donor sodium nitroprusside (SNP) is the dispersal agent that is commonly used to induce biofilm dispersion. It has been observed that exogeneous NO also provides dispersion of cells from the biofilms formed on the surfaces of water systems, by modulating the c-di GMP levels of the biofilm cells (Barraud et al., 2009).

Although the dispersion of biofilms seems to be an effective method, a study has revealed that these techniques should be reviewed again. In this study, it was observed that the biofilm-dispersed cells are more virulent than the planktonic cells (Chua et al., 2014). With its more resistant and lethal properties, biofilm-dispersed cells can spread the infection. Actually, this study has revealed that biofilm-dispersed cells should not be treated as if they are the planktonic cells, and led to query the safety of an in vivo biofilm dispersion process.

Planktonic and biofilm-dispersed cells have different levels of c-di GMP content, suggesting that there could also be differences in the adhesion capacities of these cells. This is because, c-di GMP controls bacterial motility, EPS-producing exoenzymes and polysaccharides as well as surface associated adhesins. In other words, c-di GMP has significant functions in EPS synthesis and the formation of surface biopolymers that will enable bacteria to adhere to surfaces (Romling et al., 2013), especially in the first stage of the biofilm formation process. In addition, the relationship between the virulence and adhesion capacity of bacteria has been previously reported in the literature (Stones, and Krachler, 2016). Therefore, it can be predicted that biofilm-dispersed cells will probably attach to surfaces more strongly than the planktonic cells. So, new or improved strategies should be used when inducing biofilm dispersal as a strategy to erase biofilms from the surfaces in vivo and in vitro, because more lethal and probably more adhesive cells would be released to the environment instead of the planktonic cells. To develop new and/or improved strategies to reduce biofilm formation, adhesion strengths of biofilm-dispersed cells in comparison to planktonic cells should be first determined especially at the nanoscale, and underlying molecular mechanisms mediating the initial adhesion of these microbes to surfaces should be investigated. It is important to understand the initial bacterial adhesion to a surface, which is the first step in the biofilm formation taking

place at the molecular level. Because the ultimate way to eliminate biofilms from the surfaces is to inhibit the first attachment of the pioneer bacteria to biotic or abiotic surfaces. However, since little is known regarding this important step, most of the strategies developed to combat biofilms aim to disperse mature biofilms, not aim to reduce or eliminate initial bacterial adhesion. This is in part because most of the studies investigating bacterial adhesion to surfaces were done at the macroscale.

Atomic force microscopy (AFM), which can be utilized to examine biological structures in aqueous solutions with three-dimensional imaging at the nanometric scale, is a powerful and preferred technology as well for measuring bacterial adhesion strength directly at the molecular level. It provides excellent application potential for quantitative measurements of bacterial cell morphology and dimensions, amount and diversity of bacterial surface biopolymers, and the interactions of adhesive biopolymers with surfaces in their close native environments (Müller, and Dufrêne, 2011). The use of AFM is of great importance to primarily detail the adhesion properties of the surface biopolymers of planktonic and biofilm-dispersed bacterial cells at the molecular level.

In this dissertation the adhesion strengths of planktonic and biofilm-dispersed *Escherichia coli* (*E. coli*) cells to model inert surfaces of silicon nitride were investigated under water using atomic force microscope. For this purpose, biofilms were formed in batch and continuous systems, and then dispersed cells from the biofilms were obtained by adding different SNP concentrations to the biofilm systems to induce the dispersion by targeting c-di GMP pathways of *E. coli*. The adhesion forces and energies, and pull-off distances (indicators of the lengths of the bacterial surface biopolymers) of planktonic and biofilm-dispersed cells as functions of the SNP concentration added to cultures grown in batch and continuous systems were measured by AFM and analyzed separately. In addition, the height, width and length of the bacterial cells investigated were determined from AFM topographical images taken in water. The hypothesis of this study was that, since molecular bacterial adhesion is controlled by the amount, diversity and the adhesion strength of the surface molecules, different contents of the intracellular c-di GMP in planktonic and biofilm-dispersed bacterial cells will result in the differences in the molecular mechanisms mediating the initial adhesion of the cells to surfaces. Considering the undeniable effect of c-di GMP

on bacterial surface biopolymers and hence on the adhesion, it was thought that the biofilm-dispersed and planktonic cells would have different adhesion properties at the molecular level.

The main subject of this study was to investigate the molecular level adhesion properties of planktonic cells and cells dispersed from biofilms, as well as their intracellular c-di GMP contents. In this direction, the biofilm life-cycle stages and the gained/lost properties of bacteria during this cycle were explained in the next chapter to understand the processes of biofilm formation and dispersion. In addition, the mechanisms of bacterial initial adhesion, which is the basic stage of biofilm formation, as well as measuring bacterial adhesion by AFM were reviewed in Chapter 2. All the experimental procedures followed were described in Chapter 3, including obtaining biofilm dispersed cells from batch and continuous cultures, AFM force measurements and adhesion strength analysis, the extraction procedure of c-di GMP from the bacterial cells investigated, and the measurement of different c-di GMP levels in the bacterial cells using high performance liquid chromatography. The results of all the experiments were presented in Chapter 4. Logical interpretations of the data obtained on bacterial dimensions, adhesion strength, surface heterogeneity, pull-off distances, and c-di GMP levels and their interrelationships were also given in Chapter 4. Finally significant findings and conclusions of this study were given in Chapter 5.

CHAPTER 2: LITERATURE REVIEW

2.1 Nature of biofilms

Biofilms were first shown on the tooth plaque by Van Leeuwenhoek in the 17th century and named as animalcules. However, the *biofilm* term was first mentioned by Costerton et al. in 1978 to describe the cell communities in dental plaques and rivers. After Leeuwenhoek defined the biofilm using his simple microscopes, the studies concentrated on detailed imaging of these structures. In 1969, Jones et al. examined the biofilm structures with electron microscopy and showed that the biofilms contain various cells with different morphologies (Jones et al., 1969). In a previous study examining microbial communities in water systems, it was shown that those communities are highly resistant to disinfectants (Characklis, 1973). Afterwards, various biofilm studies were conducted by different researchers to understand the basic features of this complex structure.

Biofilms can be basically defined as communities formed by microorganisms that prefer to be in groups and attached to a surface rather than freely-floating. They can be seen on many surfaces in nature. The common feature of these surfaces is that they are moist or under water. The solid-water interface provides a habitat which is ideal for microorganisms to attach to the surface (Donlan, 2002). Biofilms can settle in such environments for a very long time. In the fossil records, there is evidence of biofilm formation. Based on this evidence, the fossil evidence of biofilms is thought to date back around 3.25 billion years. Studies on biofilm fossils show that the biofilm formation ability is an ancient feature of prokaryotes. In the evolutionary process, microorganisms have benefited from the advantages of living in communities in order to be more resistant to harsh environmental conditions (Hall-Stoodley et al., 2004). Approximately 99 % of all microorganisms have been observed to form biofilms in various stages of their life (Toyofuku et al., 2016). Among the mentioned microorganisms, especially bacteria and fungi form biofilms that have many common features (Koo et al., 2017). However, the most common type of biofilms observed in the nature is the bacterial biofilms.

2.2 Bacterial biofilms

Bacterial cells can be found in a wide spectrum of environmental niches including human body, water systems, medical and food industries. Bacterial cells can exist as freely-floating planktonic cells in fluids or as three-dimensional (3D) complex architectures on surfaces, namely as the biofilms. (Berlanga, and Guerrero, 2016; Garrett et al., 2008). Biofilm formation is the temporary transition of bacteria from a unicellular lifestyle to a multicellular-like lifestyle. Thanks to this group behavior, bacteria become resistant to adverse environmental conditions. Transition from planktonic life form to biofilm form can also be expressed as the temporal reorganization of bacteria by altering gene expression of complex metabolic regulation processes.

Contact of the bacterial cell and the surface stimulates responses that alter gene expression, triggering gene expression necessary for the formation and maturation of sessile (biofilm) forms. The first step in this genetic regulation is the expression of genes that enable the formation of a matrix composed of extracellular polymeric substances (EPSs) and thus the maturation of the biofilm. EPSs are the construction materials that the bacterial cells secrete into their environment (Di Martino, 2018). The EPS matrix (biofilm matrix) accounts for ~ 90 % of the total biomass of biofilm structure. It is considered as the main component that forms the physiochemical properties of the biofilm. EPS matrix also has important roles in establishing the functional and structural integrity of biofilms (Flemming, Hans-Curt et al., 2000). EPSs consist of ionic or nonionic water-soluble biopolymers such as exo-polysaccharides, proteins, extracellular DNA (eDNA), teichoic acids (TAs), lipids and water (Di Martino, 2018; Karygianni et al., 2020).

Exopolysaccharides, which are the main components of EPSs, can be in hetero-polysaccharide or homo-polysaccharide structure (Di Martino, 2018). Although most of the polysaccharides are neutral, many bacterial EPSs are polyanionic in nature, because they carry negative charges. Bacteria modify EPS composition with respect to changes in the environmental conditions, thereby adapting the biofilm architecture according to the specific environment they are in. The EPS matrix covers the bacterial cells with a protective layer and prevents the diffusion of harmful substances into the bacteria inside the biofilm. It protects the biofilm cells from the host's defense system

(Donlan, 2000), from drying out and from oxidizing agents, radiation effects and other harmful substances such as antibiotics (Flemming, and Wingender, 2010; Kostakioti et al., 2013). It also makes it possible to keep bacteria at close range and allows the DNA exchange and cell-cell interactions. All these features make the EPS matrix as the home of bacterial cells (Flemming, Hans-Curt et al., 2007). In addition, components of the EPS matrix act as adhesins, allowing bacteria to attach to the surface and to each other. Bacteria attached to the surface multiply within the EPS matrix and form the bacterial colonies (Donlan, 2009) and further the 3D biofilm structure.

Biofilm structure can also be expressed as a micro-ecosystem in which bacterial cells find a suitable environment for their vital activities and protect themselves from environmental factors (Kaplan, 2010; Yin et al., 2019). Hence, biofilm structure promotes the colonization of the bacterial cells. Populations in the colonies may consist of a single type or different types of bacteria. The heterogeneity in the populations makes it difficult to combat the biofilm as it requires complex and combined treatment methods (Burmølle et al., 2006). In addition, biofilm structure is an important virulence factor that makes the biofilm resistant to outdoor conditions such as pH change, temperature, nutrient deficiency, and immune host defenses as well as to chemicals such as antibiotics and disinfectants (Koo et al., 2017). Compared to planktonic cells, biofilms have different interactions with other cells and different properties such as phenotypic structures, reproduction rates, antimicrobial resistance rates and gene transcription (Allesen-Holm et al., 2006; Kikuchi et al., 2005; Sihorkar, and Vyas, 2001). Especially, it is noted that biofilms are approximately 500 times more resistant to antibacterial treatments compared to the planktonic bacterial cells (Costerton et al., 1995).

2.2.1 Problems related to bacterial biofilms

Biofilms can develop on almost all biotic and abiotic surfaces such as water systems, food products and food production surfaces, wounds, mucosal surfaces of the host organism, implants and medical devices, and ear channels and tooth surfaces (Figure 1). Due to their high resistance to antimicrobial treatments and ability to re-contaminate surfaces after their dispersion, biofilms cause serious medical and industrial problems (An, and Friedman, 2000). According to the National Institutes of

Health (NIH), it is estimated that biofilms are responsible for 65-80 % of all the infections in the human body (Jamal et al., 2018).

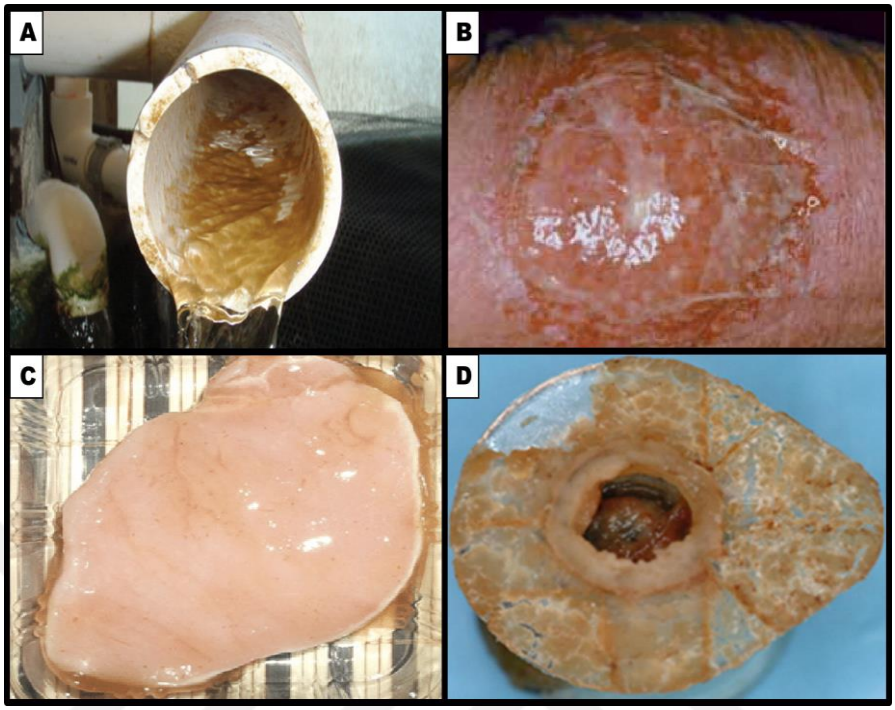

Figure 1. Biofilm formation A) inside a piping system (Source: Getchis et al., 2015), B) on a wound surface (Source: Lenselink, and Andriessen, 2011), C) on a food product (meat surface) (Source: Dochitoiu et al., 2014), D) on voice prosthesis (Source: Knott, 2019).

Catheters , implantable prosthetic devices , and joint replacements are some of the medical devices where bacterial cells can easily hold and form biofilms (Jamal et al., 2018). Treatment of infections that occur on such surfaces is usually done by removing the existing implant. Implant replacement surgeries increase the number of trauma and the cost of treatment (Blanchette, and Wenke, 2018). Another effect of biofilms on health is that it causes chronic wounds. Chronic wounds are a huge burden for the medical world due to their high mortality, morbidity, and treatment costs. Bacterial biofilms stimulate inflammation in the wound area, making this area more resistant to treatment and slowing tissue repair (Wu et al., 2019). James, Swogger et al. examined 50 chronic wound samples and observed that 60 % of the samples had biofilm (James et al., 2008). Approximately 6.5 million people receive treatments for chronic wounds in the United States per year. It is estimated that more than $ 25 billion

is spent each year to treat these wounds. This is of greater importance in diabetic patients. Progressive diabetes can cause ulceration and eventually amputation of body part. So, it can be painful and decrease the quality of life. Dispersion of the chronic wound biofilm by using an effective strategy is very important to make the healing process more effective. However, it should be noted that dispersion of biofilms can also cause new biofilm formations on different environments. This is because, biofilm-dispersed cells in the planktonic forms are released when the mature biofilm is dispersed. Thus, biofilm dispersion must be followed up with an appropriate use of antimicrobials and/or other strategies in the patient. Another disadvantage of bacterial biofilms is the appearance of stench. For example, residues of biofilms formed on the surfaces of teeth such as sulfur compounds can cause bad smell (Washio et al., 2005). In short, biofilms are a major burden on the health system, due to their persistence, high antibiotic resistance, chronic nature, and other unwanted consequences.

Besides causing medical/health problems, biofilms also cause many industrial problems leading to huge economic losses such as congestion and corrosion in the pipes, tanks, processing equipment, and in heat exchangers and contamination on the surfaces of many different packaging materials. The biofilm layer may also act as a barrier and affects negatively the efficiency of heat and fluid transfer (Li et al., 2013). Especially in the food industry, biofilms formed on the surfaces of processing equipment directly transfer to the food surfaces and cause food spoilage. This leads to a short shelf life of food and increases the foodborne diseases and economic losses (Biswas, and Micallef, 2019). Around 1.3 billion tons of food loss occurs annually worldwide, and it has been estimated that one of the main reasons of this loss to be the food spoilage due to biofilms (Marino et al., 2018). Foodborne bacteria such as *Escherichia coli* and *Clostridium botulinum* create biofilms on the surfaces of food processing plants and hence on the food products, and eventually infect humans, causing life-threatening diseases and epidemics (Galié et al., 2018a; Marino et al., 2018). For example, between the years 2007 and 2013, total of 423 foodborne outbreaks associated with *E. coli* were reported in the world. As a result of this epidemic, more than 4,000 infection cases occurred in the Europe, USA and Canada (Galié et al., 2018; EFSA, 2015).

In addition to industrial problems, biofilm formation is frequently encountered in our homes. More than 80 % of the domestic environments examined had bacterial structures. Especially *E. coli*, *Salmonella* and *Campylobacter* cells survive by easily holding on wet surfaces such as sinks and pipes of kitchen and bathroom in our homes (Scott et al., 1984). Biofilms cause pollution and stench in home and natural environments. As a result of biological pollution, natural life is compromised, and diseases multiply. Combating with mature biofilms becomes quite difficult because the biofilm structure is highly resistant to cleaning and disinfection procedures (Galié et al., 2018a; Van Houdt, and Michiels, 2010).

Consequently, biofilms cause significant financial and health problems in different areas such as food, industry, and medicine. For this reason, it is very important to develop strategies appropriate to the field in order to prevent or to eliminate the biofilms. For this purpose, various studies have been carried out and continue to be done today (Blanchette, and Wenke, 2018; Donlan, 2009; Gottenbos et al., 2002; Marino et al., 2018).

2.2.2 Biofilm formation and life-cycle

The level of bacterial cells initially adhering to surfaces and the amount of biofilms that the pioneer bacterial cells form may vary with various factors such as the content and amount of nutrients in the environment (Zeraik, and Nitschke, 2012), pH (Park et al., 2014), temperature (Gordesli, and Abu-Lail, 2012a; Gordesli, and Abu-Lail, 2012c), ionic strength (Gordesli, and Abu-Lail, 2012b) and humidity of the environment (Iturriaga et al., 2007), physiochemical and structural properties of the bacterial cell surface (Choi et al., 2015), the number of bacterial cells initially adhering to the surface and physical and chemical properties of the surface to which the bacterial cells adhere (Song et al., 2015). Regardless of the various factors affecting bacterial adhesion to surfaces, biofilm formation, which is a dynamic process (Donlan, and Costerton, 2002), is generally described by five distinct stages (Figure 2):

(i) Initial attachment of bacterial cells to the surface

- Reversible attachment
- Irreversible attachment

(ii) Growth of bacterial cells and EPS production

(iii) Formation of microcolonies

(iv) Maturation of the biofilm structure

(v) Dispersion of bacterial cells from the biofilm

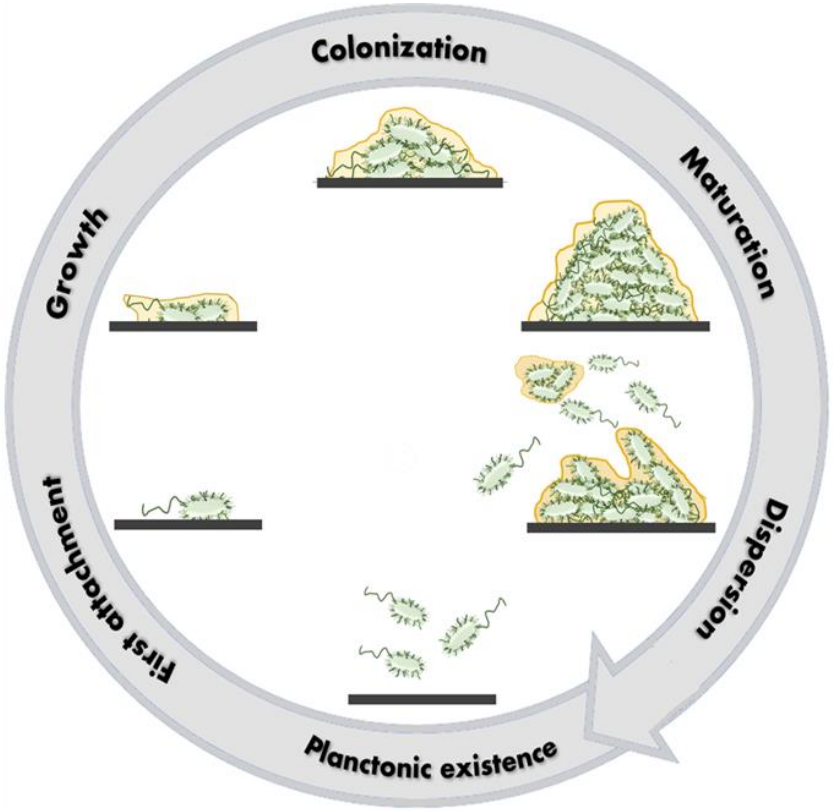

Figure 2. Biofilm life-cycle

The first stage of biofilm formation process is the initial molecular attachment of the bacterial cells to the surface which is mediated by a two-step mechanism. The first step involves long-range non-specific interactions such as electrostatic and Lifshitz-van der Waals interactions. These interactions determine whether the two surfaces can come close enough to molecular contact, so this step is also called reversible bacterial attachment. If the cells could overcome the repulsive long-range interactions and come close to molecular contact with the surface, then specific short-range molecular interactions (ligand-receptor, hydrogen, ionic or covalent bonds) take place and the pioneer bacterial cells irreversibly attach to the surface (Israelachvili, 2011). Irreversible attachment is also consolidated by the bacterial surface biopolymers and surface-associated structures such as, pili, flagella, fimbriae and/or

capsular components. The cellular extensions increase the specific interactions between the bacterial cells and the surface, thereby providing the first contact for bacterial adhesion (Kaplan, 2010). Pioneer bacterial cells that can hold irreversibly onto the surface begin to multiply and produce EPSs, which is the second stage of the biofilm formation process. The EPS matrix holds the bacteria cells together and attaches the bacteria firmly to the surface. Depending on the environmental conditions and the surface properties of the bacterial species, the biofilm matrix to be formed may contain different components such as polysaccharides, proteins, extracellular DNA, water, and ions. It also may contain minerals, corrosion particles or blood components (Donlan, 2002). EPS matrix protects bacteria from adverse environmental conditions and allow them to attach to various surfaces (Koo et al., 2017). It protects against phage attacks, phagocytosis, looting of protozoa, toxic compounds, antibiotics and osmotic pressure (Ruas-Madiedo et al., 2002). Another important feature of EPS matrix is the recognition and adhesion of the cells to the surface. By the virtue of EPS matrix, bacteria can remain stable in the environment and grow predominantly (Donlan, 2002).

The third stage of biofilm formation process is the formation of microcolonies on the surface namely the early biofilm formation. Microcolonies grow using the EPS matrix as a scaffold and form mature biofilms. At this stage, more microorganisms and EPS layers are added on the first layers to create a 3D-dimensional structure. In addition, water channels are created within the biofilm for the exchange of food and waste products. The fourth stage, which is the maturation of the biofilm includes the formation of heterogeneous chemical and physical micro-environments in the EPS matrix and the social interactions of bacterial cells in these environments (Barraud, 2007a). Ambient conditions play a significant role in determining the maturation rate of a biofilm. EPS-producing microorganisms maintain their resistance to harsh environmental changes and can form very thick biofilm structures (Di Martino, 2018; Donlan, 2002). Depending on the bacterial species, biofilms consist of approximately 25 % of bacterial cells and 90 % of the exopolysaccharide matrix (Costerton, 1999). Thanks to this thick protective layer, the biofilm can mature quickly. Within the mature biofilm, there is a vibrant community in preserving the biofilm architecture and actively exchanging and sharing vital products. In this way, the bacteria inside the mature biofilm can reach basic substances such as nutrients and oxygen and continue their vital functions (Kostakioti et al., 2013).

The fifth stage includes the dispersal of individual bacteria and/or bacterial cell clusters from the biofilm structure. Dispersal becomes an option as biofilms mature. As a result of the passive dispersion of biofilms caused by external factors such as shear stress, pressure, as well as environmental changes (nutrient and oxygen availability and increase of toxic products, or other stressful conditions), bacteria tend to spread from the biofilm form to the planktonic entity (Kostakioti et al., 2013). When appropriate environmental conditions are provided, the biofilm-dispersed cells may form new biofilm structures by following the above-mentioned steps (Koo et al., 2017).

Biofilm dispersion is an important stage of the biofilm life-cycle allowing bacterial cells to leave the 3D biofilm environment and to return to the planktonic form of existence. The way of natural biofilm dispersal can be identified with 3 distinct categories: erosion, sloughing, and seeding. Erosion refers to the non-stop release of cells from early biofilm. In the dispersion step of biofilm life-cycle, the separation of large cell groups from the biofilm is called sloughing. Sloughing is a fairly random process because nutrients and oxygen deficiency occur as the biofilm thickens. To minimize this effect, the release of cells from the biofilm is triggered. Seeding refers to the release of cells from cavities formed within the biofilm structure. Erosion, sloughing, and seeding have the potential to create dispersed cells that retain phenotypic characteristics of biofilm (Kaplan, 2010).

2.2.3 Dispersion strategies for bacterial biofilms

The most basic way to inhibit the formation of the biofilm is to prevent the initial attachment of precursor bacterial cells to the surface. However, there is still not an effective strategy to prevent this initial step. This is partly because most of the work done to investigate the bacterial adhesion process has been conducted using macroscale systems with limited resolution. As nanotechnology is still evolving, there is little information available regarding the initial adhesion at the nanoscale. Various methods such as material surface modification, using of surfactants and non-antibiotic coating have been developed to prevent to initial attachment of bacterial cells. However, since the action mechanism of these methods is specific for the bacterial species, it cannot be said that these methods play an effective role in preventing the formation of all biofilm species. In addition, the applicability of these methods is very

limited as it depends on the material and the system (Lebeaux et al., 2014). For these reasons, most of the strategies developed to combat biofilms aim to disperse mature biofilms. The biofilm dispersion is already a part of the biofilm life-cycle and occurs naturally. Researchers have developed methods that mimic this natural dispersion process as a method of combating biofilm. Dispersing of bacterial cells from biofilm is induced by using different techniques. But in general, biofilm dispersion can be classified into two groups: passive and active biofilm dispersion (Figure 3), as will be reviewed in the following section.

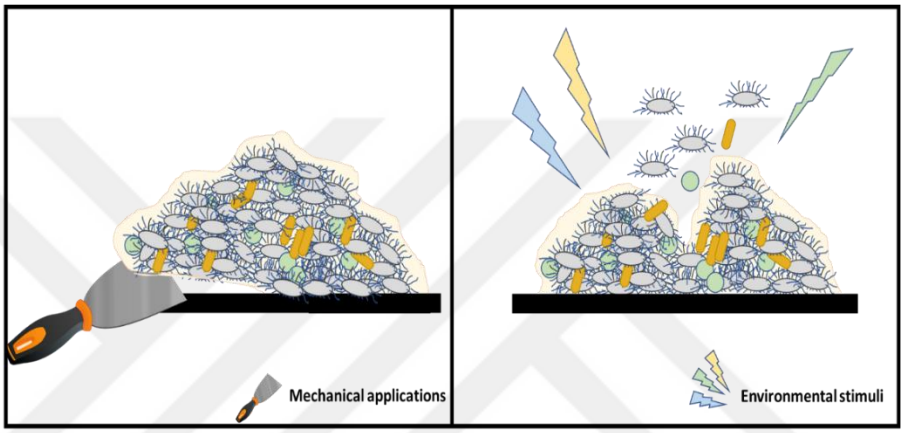

Figure 3. Representation of passive dispersal versus active dispersal. Passive dispersal can be achieved by mechanical applications. Active dispersal can be induced by the changes in the environmental conditions.

2.2.3.1 Passive dispersion

Passive dispersion is the type of dispersion caused by external factors (fluid shear, abrasion, pressure or electric waves and human intervention). For instance, cleaning the plaque formed on the tooth surface by brushing is an example of the passive biofilm dispersal (Fleming, and Rumbaugh, 2017; Kaplan, 2010). Although it seems possible to get rid of biofilms on open surfaces by mechanical methods such as brushing, applying pressure, or scraping, the scraped surface can be damaged and biofilm residues can continue to grow after scraping. In addition, struggling with biofilm on sensitive and closed surfaces requires great effort.

Biofilm layer forms rapidly in pipes and dead-ends in the water system. It is difficult to combat the biofilm layer as it is not possible to reach these points of the building installation mechanically. Planktonic bacteria die with routine disinfection,

but those in the biofilm remain alive (Stoodley et al., 2001). In this regard, the researchers primarily targets biofilm dispersion using pressurized water in long pipe systems. However, due to the strong adhesive structure of the biofilm, it is very difficult to completely disperse the biofilm by mechanical dispersion methods. Biofilm pieces remaining on the pipe surface can form the mature biofilm structure again (Fleming, and Rumbaugh, 2017). Thus, contamination is not eliminated, and the hygienic quality of the water continues to be low.

The possibility of mechanical dispersion is more limited for the biofilm in the body (Fleming, and Rumbaugh, 2017; Koo et al., 2017). The required amount of the shear force or flow rate of the blood for the biofilm dispersion cannot be achieved. Therefore, the most suitable passive dispersion method for biofilms in the body has been seen as the surgery. If the biofilm is formed on an implant placed inside the body or on a tissue, the implant or the infected region can be removed from the body using surgical methods. However, in both cases, it is difficult to completely eliminate the microorganisms, and the remaining bacterial cells can cause new biofilm formations. In addition, healthy surrounding tissues can be damaged during surgery. Surgery is also very costly and can be a difficult process (Blanchette, and Wenke, 2018; Fleming, and Rumbaugh, 2017). High speed micro droplets, water sprays and water jets have been developed for the mechanical breakdown of biofilms. These methods have been used by surgeons for biofilm removal. Fabbri et al., developed mechanical degradation on *Streptococcus mutans* biofilms using water sprays and jets. They showed that the use of water spray allows a significant amount of biofilm to be removed, but the removed biofilm liquefies and spreads on the nearby surfaces (Fabbri et al., 2016) which can initiate the formation of new biofilms.

2.2.3.2 Active dispersion

Active dispersion is the natural disintegration of a biofilm by itself and a step of biofilm life-cycle that ensures the continuity of survival of the bacterial cells. Active dispersal can be triggered by changes in the environmental conditions that cause starvation, accumulation of antimicrobial products, changes in the oxygen levels and increase toxicity in the environment (Kaplan, 2010). Scientists have developed techniques that trigger natural active dispersion to combat biofilms. These techniques, also called inducing active dispersion, can be examined under a few main titles:

- Targeting quorum sensing (QS) mechanisms
- Targeting the EPS matrix
- Targeting c-di GMP signal paths

Quorum sensing (QS) system is defined as the communication system of the bacteria. Bacterial cells in a colony produce and release chemical signal molecules to communicate with each other. When the signal molecule reaches a sufficient concentration with an increase in the bacterial population, bacteria in the biofilm detect the cell density and make changes in the gene expression (Jiang et al., 2019). Thus, cells regulate various features in the population such as symbiosis, EPS production, virulence, bioluminescence production, conjugation, motility, sporulation and biofilm formation (Mangwani et al., 2012). Due to the effects of this system on biofilm formation and other bacterial cell functions, it is used as a target for the development of new treatment strategies and dispersion of biofilms. Basically, QS allows bacteria to control their cell population density and regulate their behavior consequently (Hawver et al., 2016). Signal molecules in QS mechanisms can vary according to the bacterial species. The QS system contains 3 basic signaling molecules, those are: N-acylated-L homoserine lactones (AHL), autoinducing peptides (AIP), and autoinducer-2 (AI-2) molecules.

Gram-negative bacteria produce AHL signaling molecules and these molecules are carried by diffusion through the cell membrane (Figure 4). AIPs are small peptide-structured components produced by Gram-positive bacteria. They are recognized by receptors in the cell membrane. AI-2 molecules are used by both Gram-positive and Gram-negative bacteria. AI-2 molecules, unlike others, provide communication between species (Koo et al., 2017).

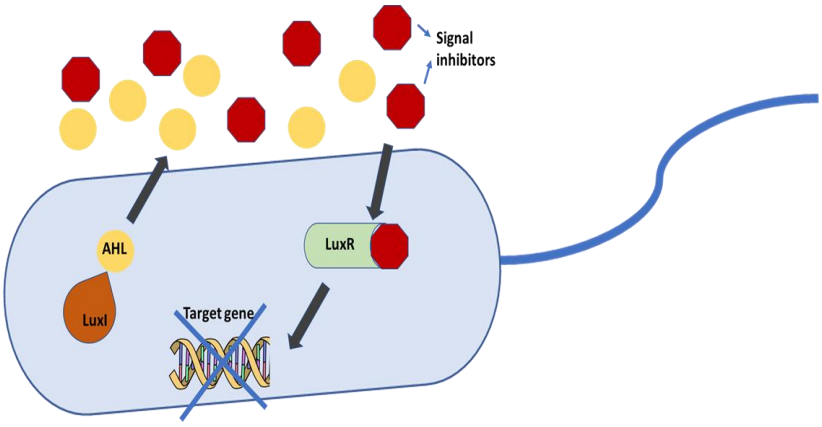

Figure 4. Representation of targeting quorum sensing (QS)

Techniques targeting QS system involve inhibition or degradation of the signal molecules such as the ones mentioned above. Quorum quenching (QQ) enzymes are used for the degradation of QS signal molecules. Quorum sensing inhibitors (QSIs) are used for the inhibition of AIs (Rémy et al., 2018). Previous researches have indicated that the use of these molecules successfully inhibits the QS system and prevents the formation of biofilms. However, it has been observed that most of these compounds are not very suitable for usage because they are either toxic or do not act successfully at tolerable doses (Koo et al., 2017).

Another method/strategy to combat biofilms is based on targeting the EPS matrix, which protects the biofilm from external factors and acts as a 3D scaffold for the cells, as previously mentioned. In addition, EPSs provide optimum ambient conditions (pH, nutrition, chemical gradient, etc.) for bacterial cells so that the biofilm can easily grow within the EPS matrix. Considering all these features, targeting the EPS matrix can be an effective method for fighting biofilms (Kaplan, 2010; Koo et al., 2017). Various extracellular and intracellular signaling networks and non-signaling mechanisms promote EPS production. In this respect, matrix production can be inhibited by targeting nucleotide-signal molecules such as exoenzymes, polysaccharides and adhesins that control the production of the EPS. For example, these signaling molecules regulate glucan-producing exoenzymes (such as glucosyltransferase) of Gram-positive bacteria and exopolysaccharides (Ps1 and Pel) of Gram-negative bacteria. For adhesins, ring-fused 2-pyridones are responsible for the inhibition of curli and type-1 pili synthesis (Koo et al., 2017). The effect of these inhibitors is not superior to chemicals used to combat biofilms. However, the

combination of chemicals and EPS synthesis inhibitors can greatly increase the therapeutic effects. Unfortunately, it is not suitable to use chemicals in every system. So, the use of inhibitors alone may also be insufficient to combat mature biofilms (Falsetta et al., 2012). In addition to inhibition of EPS synthesis, biofilm matrix degrading enzymes have been used to prevent the maturation of the biofilm or to induce the biofilm dispersion (Fleming, and Rumbaugh, 2017). These enzymes are also called anti-matrix molecules and can be categorized as polysaccharide degrading enzymes (Dispersin-B and Alfa amylase), nuclease enzymes (deoxyribonucleases) and protease enzymes. Many studies have shown that these enzymes are effective in biofilm dispersion. However, this method has some disadvantages such that the EPS matrix differs according to biofilm types and has a rather complex structure in biofilms containing heterogeneous bacterial species (Di Martino, 2018). Therefore, the use of matrix degrading enzymes for different types of biofilms can be very difficult and time consuming. EPS degrading based biofilm dispersal strategy is shown in Figure 5.

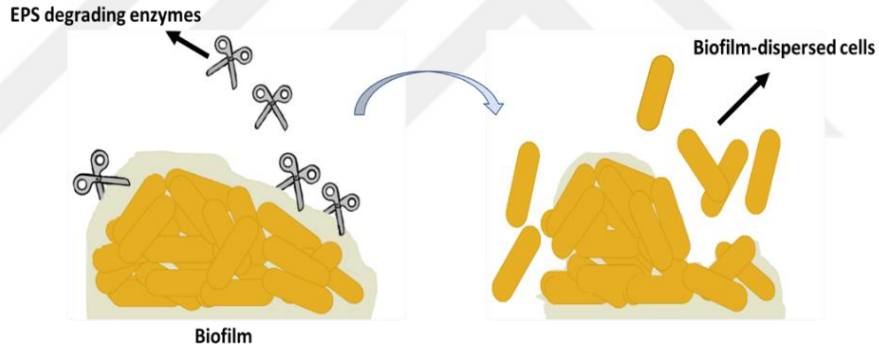

Figure 5. Representation of targeting EPS matrix by EPS degrading methods

Second messenger signaling (especially nucleotide-based ones) mechanisms are common in cellular systems. Cyclic dinucleotides regulate various processes in the bacterial cell. In 1987, a cyclic nucleotide was discovered in the *Acetobacter xylinum*, which appears to have a regulatory role in cellulose synthesis (Ross et al., 1987). In the following process, this nucleotide called cyclic dimeric (3 ′ → 5 ′) guanosine monophosphate (cyclic di GMP or c-di GMP) was found to be involved in many bacterial processes. Cyclic di GMP acts as a regulator in cellular interaction, proliferation, motility, EPS production, the bacterial cell division steps, adhesion, biofilm formation and other processes (Ha, and O'Toole, 2015; Romling et al., 2013).

This nucleotide can also be defined as the main element of a signal transmission network that regulates the dispersion of biofilm and transition to planktonic existence in response to signals between environmental factors and bacterial cells. C-di GMP is a very common signaling molecule, and many bacteria have the genes that recognize proteins containing this molecule. In addition, c-di GMP has effects in processes such as regulating flagella behavior, preventing flagellar motility of cells in biofilm, and synthesis of new flagella. This molecule is thought to play an important role in bacterial adhesion and biofilm formation with its functions on the expression of various polymeric adhesins and exopolysaccharides (EPSs) (Romling et al., 2013). Considering all these functions, targeting c-di GMP signaling pathways for biofilm dispersion is seemed as an effective method. Basically, an increase in the intracellular c-di GMP level encourages bacteria to remain in biofilm mode, while a decrease in the c-di GMP level causes the biofilm dispersal (Barraud et al., 2009; Yu, and Chua, 2019). The level of intracellular c-di GMP is determined by diguanylate cyclase (DGC), which synthesize c-di GMP, and phosphodiesterase (PDE) that degrade c-di GMP (Figure 6). There is an inverse relationship between motility and c-di GMP, DGC activity will suppress motility, whereas PDE activity will support motility (Ha, and O'Toole, 2015; Yu, and Chua, 2019).

Bacteria can quickly adjust the amount of intracellular c-di GMP as an adaptation to the changes in the environmental conditions. For example, in stress-generating conditions such as starvation, bacterial cells can activate specific PDEs, thereby reducing the content of intracellular c-di GMP that causes biofilm dispersion (Koo et al., 2017). So that, bacterial cells that disperse from the biofilm can spread to new environments and find necessary nutrients. Accordingly, DGC inhibition is a convenient way to reduce c-di GMP level and prevent biofilm formation/maturation. In some studies, DGC inhibitors have been used for the deactivation of c-di GMP pathways and biofilm dispersion has been observed (Sambanthamoorthy et al., 2014; Sarenko et al., 2017). However, the low biofilm matrix permeability of DGC inhibitors significantly limits their use. One way to target c-di GMP routes is to use PDE activators. PDEs provide the degradation of c-di GMP, so they induce the dispersion of biofilms. Not all PDEs in bacteria control biofilm dispersion, for example, some PDEs are active in virulence. Therefore, activators should be designed for PDEs with known dispersion roles (Yu, and Chua, 2019).

C-di GMP mediates the regulation of downstream cellular mechanisms (Figure 6). These mediated cellular mechanisms include signal-receptor interactions as transcriptional regulators or effectors such as, FleQ, BrlR or Pel (Chang, 2018). The flagella master transcriptional regulator FleQ plays an activator or a suppressor role in biofilm formation by binding to c-di GMP or ATP. Especially, it represses EPS components genes (pel or psl) and activates flagellar motility genes at low concentrations of intracellular c-di GMP. At high c-di GMP concentrations, FleQ binds to the ATP binding site and promotes biofilm formation (Baraquet et al., 2012; Chang, 2018). Increased intracellular levels of c-di GMP also result in antibiotic resistance by inducing the expression of BrlR (a transcriptional activator of the multi-drug efflux pump operons) (Gupta et al., 2014). C-di GMP also modulates PelD (responsible for pel production) and a membrane-related protein Alg44 (responsible for alginate polymerization). Thus it plays an active role in EPS synthesis, biofilm formation and/or dispersion (Chang, 2018).

A well-defined PDE activation approach to modulate the c-di GMP levels in the bacterial cell is the use of nitric oxide (NO). Nitric oxide is a signal molecule (nitrogen monoxide structure) formed by the combination of nitrogen (N) and oxygen (O) gases. This molecule, which is a short-lived and highly reactive free radical, can easily pass through the membranes through diffusion (Ignarro et al., 2001). NO can be produced in cells endogenously or exogenously. Appropriate NO concentrations regulate some genetic pathways related to planktonic existence and biofilm formation. Low and non-toxic NO concentrations produced by endogenous or external sources play an important role in the biofilm dispersion (Barraud et al., 2009). In addition, it has been reported that NO stimulates dispersion in biofilms formed by *E. coli*, *Pseudomonas aeruginosa*, *Vibrio cholerae*, *Staphylococcus aureus*, *Serratia marcescens*, *Bacillus subtilis* and *Legionella pneumophila*. NO-producing agents are preferred for exogenous production of NO. Sodium nitroprusside (SNP), S-nitroso-N-acetyl penicillamine (SNAP) and S-nitroso-L-glutathione (GSNO) are the main agents that produce extracellular NO production. It has been shown that these agents induce biofilm dispersion by lowering the intracellular c-di GMP level. In a study examining the effect of NO on biofilm formation, biofilm dispersion of *P. aeruginosa* in the presence and absence of GSNO, SNP and SNAP agents was investigated. All three agents were found to be effective in biofilm dispersion. However, it has been observed

that the most effective dispersion was provided by SNP compared to GSNO and SNAP (Barraud et al., 2006). Other studies have also shown that the low doses (in micromolar levels) of SNP is very effective in dispersion of biofilms (Chua et al., 2014; Howlin et al., 2017). Apart from the *in vitro* studies, it has been found that targeting c-di GMP pathways in the *in vivo* conditions also provides biofilm dispersion. These studies demonstrate that c-di GMP can be used therapeutically *in vivo* (Christensen et al., 2013; Chua et al., 2015). In other words, providing biofilm dispersion by targeting c-di GMP signaling pathways seems to be a very successful strategy to combat biofilms both *in vivo* and *in vitro*.

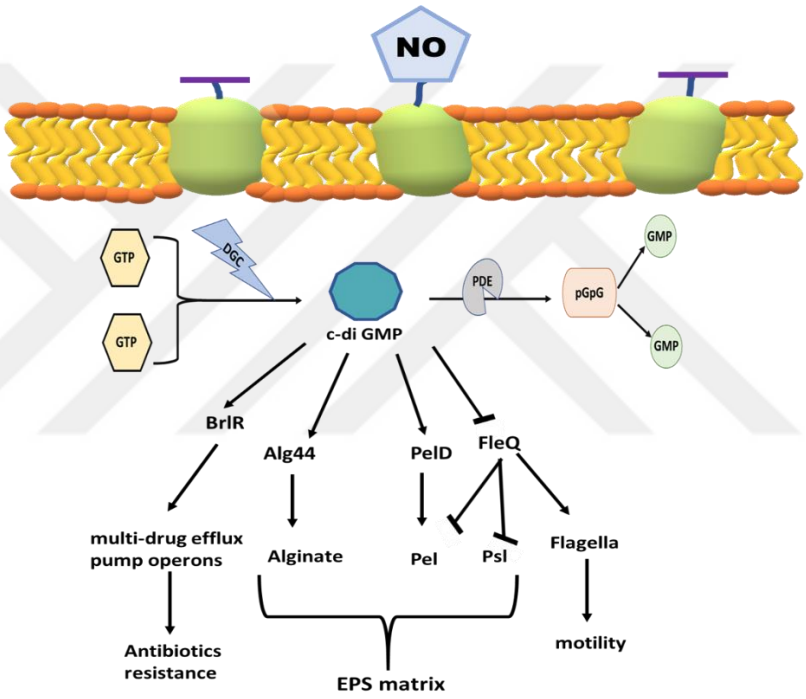

Figure 6. Representation of targeting c-di GMP pathway by using NO (Source: Adapted from Chang, 2018)

Bacteria dispersed from biofilms using the methods mentioned above are generally identified as planktonic cells. However, a few studies have shown that these biofilm-dispersed cells have different physiology than the planktonic cells (Chua et al., 2014; Guilhen et al., 2016; Guilhen et al., 2019; Pettigrew et al., 2014). In a study by Chua et al. (2014), the effects of dispersed cells from *P. aeruginosa* biofilms (by decreasing the level of c-di GMP) and planktonic *P. aeruginosa* cells on macrophages and *Caenorhabditis elegans* (*C. elegans*) have been investigated. After 2 hours of incubation of macrophage and bacterial coculture, it was observed that the

phagocytosis of planktonic cells by macrophages was approximately 100-fold less than that of dispersed cells. In other words, the resistance of dispersed cells against macrophages was higher than planktonic cells. As a result of fluorescent staining, they also showed that dispersed cells have a higher cytotoxic effect on macrophages than planktonic bacteria. In the same study, *C. elegans* liquid killing assay has been performed to determine the effect of dispersed cells *in vivo*, and it was found that dispersed cells killed 2.25 times more worms than planktonic cells. Inferentially, it has been observed that biofilm-dispersed cells were more lethal (virulent) than planktonic cells both *in vitro* and *in vivo* (Chua et al., 2014).

Ruhal et al. examined the effects of dispersed cells on lung infection mouse model and reported that NO-based dispersed cells had significant effects on infections. This study has shown that dispersed cells spread from the lung to the spleen and liver through blood, as well as increase the amount of infection and death (Ruhal et al., 2019). Based on the information provided by the mentioned studies, it can be said that the biofilm-dispersed cells make the biofilm related infections more complicated. Until recently, it was thought that the biofilm would be cleaned from the surface by using biofilm dispersion techniques, and the killing of the dispersed cells with antibiotics would be successful. However, the high virulence capability of dispersed cells raised the question of a treatment based on the dispersion of biofilm *in vivo* would be reliable or not. Such a dispersion based treatment method may result in septic shock or spread of infection by the dispersed cells (Chua et al., 2014; Fleming, and Rumbaugh, 2017; Ruhal et al., 2019).

In another study with *Klebsiella pneumoniae* cells, it has been discovered that biofilm-dispersed cells have better colonization ability on biotic (tooth surface, bone, skin, mucosa) and abiotic (plastics, ceramics, metals, composites) surfaces than the planktonic cells. Surface colonization kinetics were analyzed by real-time confocal imaging after 100 minutes of incubation of planktonic and biofilm-dispersed cells on the glass surface. It has been observed that dispersed cells produce higher biomass (approximately 5 times) than planktonic cells in a shorter time. It has also been shown that bacteria derived from biofilm-dispersed cells co-cultured with lung (A549) epithelial cells and pharyngeal (FaDu) have significantly higher colonization capacity than planktonic bacteria. *In vivo*, it has been observed that dispersed bacteria elicit a

less natural immune response in the murine lungs than planktonic bacteria. In addition to these findings, SEM images showed that morphological structures of dispersed cells were different from the planktonic cells and their surfaces were covered with extracellular material (Guilhen et al., 2019).

In essence, c-di GMP controls exoenzymes producing biopolymers on the bacterial surfaces such as EPSs, polysaccharides, different polymeric adhesins and bacterial motility. All these features can vary depending on the types of bacteria and the way the bacteria exist (planktonic, biofilm and dispersed). So that planktonic and biofilm-dispersed cells have different levels of c-di GMP content suggests that there can be differences in their adhesion capacities. To investigate the differences in the adhesion capacities of planktonic and biofilm-dispersed cells, their adhesion characteristics should be studied especially at the nanoscale. This is because, the initial attachment of both planktonic and biofilm-dispersed cells take place at the molecular level, which is also the first step in their biofilm formation processes. Understanding the molecular mechanisms that control the initial bacterial adhesion to surfaces will provide the necessary information to develop effective strategies for preventing bacterial adhesion and hence biofilm formation.

2.3 Description of bacterial adhesion phenomenon

The adhesion of bacteria to surfaces is a natural phenomenon required for the use of nutrients associated with solid surfaces. The fact that bacteria form more resistant and complex structures creates a great burden on human health and the continuity of industrial applications. The key step in the formation of these powerful bacterial communities is the first attachment of the planktonic bacterial cell to a surface. The adhesion of bacteria to the surface is a time-dependent formation and can be examined in two steps; reversible and irreversible attachment (An, and Friedman, 2000; Gottenbos et al., 2002).

When a planktonic bacterial cell living freely in an environment gets close enough to a surface, some physicochemical interactions occur between the surface and bacterial cell. At a separation distance of approximately < 100 nm, the bacterium will be only exposed to nonspecific and long-distance weak interactions without being in full contact with the surface (Figure 7). These nonspecific interactions are electrostatic,

hydrophobic, steric, gravitational and van der Waals forces (Gottenbos et al., 2002; Katsikogianni, and Missirlis, 2004). Among these interactions, hydrophobic forces which are both effective at long and short ranges are believed to have a predominant feature in attaching bacterial cell to the surface (Krasowska, and Sigler, 2014). Electrostatic forces generally act as repulsive forces because most of the bacteria and inert surfaces are negatively charged in aqueous environments (Singh et al., 2018).

Bacterial cells are brought closer to the surface by above mentioned long-range interactions, and when they come closer to the surface, specific short-range interactions enable the molecular or cellular phase of bacterial adhesion to surfaces. At a separation distance of about < 5 nm, ionic and covalent bonds, dipole-dipole, hydrophobic, ion-dipole and hydrogen interactions, as well as ligand-receptor interactions which are short-distance interactions with the surface, play roles in this irreversible adhesion (Figure 7). Bacterial cells can firmly and irreversibly attach to surfaces by using their surface biopolymers since those biopolymers are the binding arms of bacterial cells to the surfaces. Thus, short range interactions are actually between the specific surface biopolymers of bacterial cells and the surfaces.

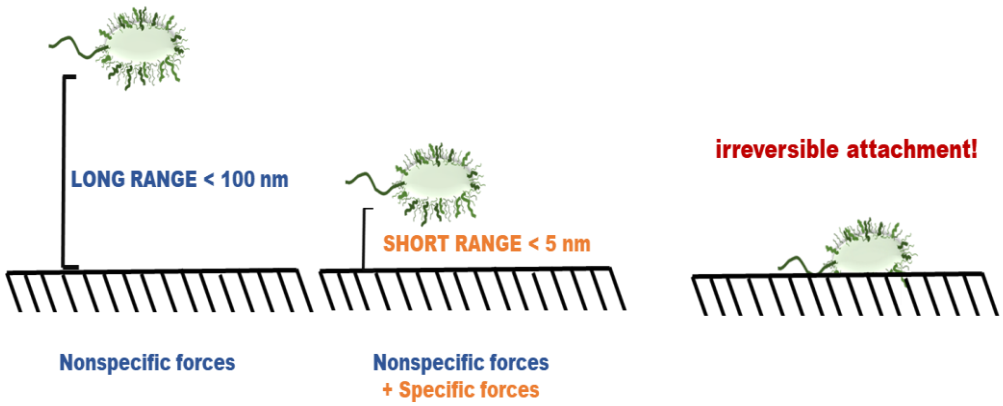

Figure 7. Representation of initial bacterial adhesion steps

2.3.1 Main factors affecting bacterial adhesion to surfaces

The nature of the attachment surface, the physical and chemical properties of the environment in which the adhesion process is taking place, hydrodynamic conditions, and various chemical and physical features of the cell surface are all effective in the attachment of microorganisms to surfaces and in their biofilm formation (Katsikogianni, and Missirlis, 2004; Moraes et al., 2013).

Bacteria can cling to different types of surfaces. It has been determined that many bacterial species develop into biofilms on materials such as wood, soil, glass, stainless steel and plastics (Galié et al., 2018a). Even on these surfaces, topographic differences cause different amounts of bacterial attachment and growth. Bacterial cells generally prefer to adhere to rough surfaces rather than flat ones. Bacteria tend to adhere to the porous and rough surfaces more than polished surfaces due to the increase in total area and better bacterial adaptation to similar-sized pores (Cheng et al., 2019; Katsikogianni, and Missirlis, 2004). It should also be noted that, material surface hydrophobicity and charge are also important factors that affect bacterial adhesion (An, and Friedman, 2000; Cheng et al., 2019).

Differences in environmental factors also affect the adhesion tendency of the bacteria. Bacteria regulate their tendency to adhere to the surfaces depending on the ambient circumstances (such as pH, temperature, oxygen level, amount of nutrients, presence of antibiotics and bacterial concentrations) (Moraes et al., 2013). In addition, flow conditions are important factors that influence the bacterial attachment rate in continuous flow systems. For example, increasing shear force along with the flow rate has been shown to reduce bacterial adhesion and biofilm development (Katsikogianni, and Missirlis, 2004). Ionic strength, temperature and pH of the growth environment also affect the strength of bacterial adhesion to surfaces (Gordesli, and Abu-Lail, 2012b; Park et al., 2014). Another environmental factor that affects bacterial adhesion is the presence or absence of antibiotic drugs in the environment. Antibiotics cannot totally eliminate but can decrease the level of bacterial adhesion and biofilm formation.

All bacterial species have different physicochemical surface characteristics which depend on the amount or diversity of the biopolymers on the bacterial surfaces. The differences in the physicochemical surface characteristics of the bacteria result in differences in their adhesion strengths and/or capacities to a particular surface. For example, hydrophilic cells adhere more firmly to hydrophilic surfaces, similarly hydrophobic ones like to adhere to hydrophobic surfaces (Krasowska, and Sigler, 2014). Apart from bacterial surface hydrophobicity, bacterial surface charge is also an effective physicochemical surface property on the adhesion of bacterial cells. The surface charge of bacteria varies with the ionic strength and pH of the environment, as well as with the bacterial species. Since the bacteria that float in aqueous environments

and the substrates that the bacteria usually adhere to under such environments are negatively charged in nature, bacterial cells are subjected to long-range repulsive electrostatic forces when they are approaching to the surfaces in aqueous environments. The degree of the repulsive force between those interacting surfaces depends in part the degree of the negative surface charge distribution on the bacterial surface and hence on the amount of negatively charged molecules on the bacterial surface. It was found that when the bacterial surface is less negatively charged, the bacterial adhesion strength to the negatively charged inert surface of silicon nitride in water increases (Gordesli, and Abu-Lail, 2012a; Gordesli, and Abu-Lail, 2012c). However, the repulsive forces cannot powerful enough to eliminate the bacterial adhesion to surfaces. Bacterial cells always find ways to overcome the repulsive long-range forces to get close to molecular contact with the surfaces. Afterwards, bacterial cells irreversibly attach to the surfaces with the help of their adhesive surface biopolymers and colonize on the surfaces. They mediate their molecular adhesion with the surfaces by using their specific surface proteins (adhesins), proteinaceous extensions (flagella, fimbriae, or pili), and surface polysaccharides. The types, amounts and sizes of the adhesive biopolymers differ according to the bacterial species and strains (Berne et al., 2015). In addition, conformational properties of the bacterial surface biopolymers such as the length and the grafting density of biopolymers were found to have major roles in their adhesion (Eskhan, and Abu-Lail, 2013; Gordesli, and Abu-Lail, 2012b; Ofek et al., 2013; Park et al., 2014). It was shown that *L. monocytogenes* strains possessing longer and extended biopolymers on their surfaces had better adhesion capabilities compared to strains with shorter surface biopolymers (Eskhan, and Abu-Lail, 2013).

2.3.2 Quantification of bacterial adhesion using atomic force microscopy (AFM) technique

From the past to the present day, many different techniques are used to evaluate bacterial adhesion. These methods can be presented in two basic categories: direct and indirect methods.

Indirect methods are based on total internal reflection without direct force probes. Spectrophotometric methods, bio-timer (BTA), quartz crystal microbalance (QCM) are some of the indirect techniques. Spectrophotometric methods are based

on the staining of adhering cells and the spectrophotometric measure of the dye. The BTA method allows to stain cells with phenol red and indirectly count the adhered live bacterial cells. QCM is a special biosensor that detects the mass and energy changes of the material connected to the sensor crystal in the nanogram-microgram range per unit area. Although indirect methods are useful due to their ability to detect individual adhered bacterial cells, they have limitations in the sensitivity and accuracy of the measurements (Camesano et al., 2007).

Direct methods are based on the exact quantification of the adhesive force. There are many direct measurement techniques to measure cell adhesion. Optical tweezers are one of the methods used to measure cellular adhesion forces. These are the devices that allow to capture and move micro-sized objects using laser beams. The technique uses the ability of radiation pressure generated by a focused laser beam to capture small particles. In addition to capturing and manipulating bacteria, they are also used to measure the adhesion forces of bacteria to surfaces (Alam et al., 2019; Ungai-Salánki et al., 2019). However, given that the laser light has to pass through the sample, the application areas of this method are limited. The thermal effect of the high laser density and the possible damage of the cell that might be caused due to the laser absorption by the sample should also be considered. Besides, this technique provides the best results for small, spherical particles. Therefore, optical tweezers are difficult to use for long or stick-shaped bacterial cells (Camesano et al., 2007).

Microscopes are one of the direct methods for observing bacterial adhesion. Atomic force microscope (AFM) is one step ahead of other microscopes with its functions such as determining the number of adherent bacteria and measuring adhesion forces between bacteria and the surface with nano to pico newton sensitivity and in close-native environments such as aqueous solutions. This high-tech microscope is widely used in all areas of surface science, including microbiological studies. Using AFM, direct biological structures can be examined in aqueous solutions and three-dimensional morphological images can be obtained in nanometer or sub-nanometer scales (Camesano et al., 2007; Ungai-Salánki et al., 2019). In addition to imaging, it is possible to measure the physical properties of the sample with AFM. Thus, it provides excellent application potential for quantitative measurements of the morphology of bacterial cells and the interaction forces of

bacterial surface biopolymers with the surfaces in water. In addition, information such as the conformation, flexibility, hydrophilic/hydrophobic nature, and heterogeneity of bacterial biopolymers can be obtained by using AFM (Abu-Lail, and Camesano, 2003).

AFM measurement is based on the interactions between the sample surface and a probe (Alam et al., 2019). This probe, also called as the as the *AFM probe* or the *AFM tip*, is placed at the end of a flexible cantilever and able to sense the attractive or repulsive forces between the sample and itself. These forces can be monitored by measuring the deflection of the cantilever.

AFM includes different modes for different applications. These modes can generally be presented in 2 categories: contact and dynamic fluid modes. In contact mode, the cantilever is drifted across the sample surface and surface trends and/or forces are recorded directly as the deviation of the cantilever. In other words, the sample and the probe are in direct contact. Dynamic fluid mode (DFM), also called as the *tapping mode* is the method where the cantilever (the console) vibrates or oscillates near the resonance frequency. This mode gives high resolution topographic images of sample surfaces without causing any damages, and the most frequently used AFM mode for imaging of samples in liquids. In particular, it is used for samples that are easily damaged or cannot be firmly attached to the surface.

The basic components of the AFM device are the sharp-tip cantilever, a piezo scanner that controls movements of the cantilever, a location-sensitive detector, and a laser diode (Figure 8). Among them, it can be said that the key component of AFM is the cantilever, particularly the probe (sharp tip) placed at the end of the cantilever. AFM probes vary according to the purpose of the experiment (such as imaging or force measurement), the AFM technique to be used (tapping mode, contact mode, etc.), the characteristics of the sample (like robust, soft, or fragile) and desired resolution level. Cantilevers of different sizes and shapes (such as triangular and rectangular) are available. Most AFM probes are made of silicon (Si), borosilicate glass and silicon nitride (Si_3N_4). Soft silicon nitride probes with suitable spring constants are generally preferred for biological sample measurements. Silicon nitride is known to provide a net negative charge in neutral solutions such as water, and

displays properties similar to that of soil and glass, which are the substrates bacterial cells generally adhere to in nature (Abu-Lail, and Camesano, 2003; An, and Friedman, 2000; Gordesli, and Abu-Lail, 2012c).

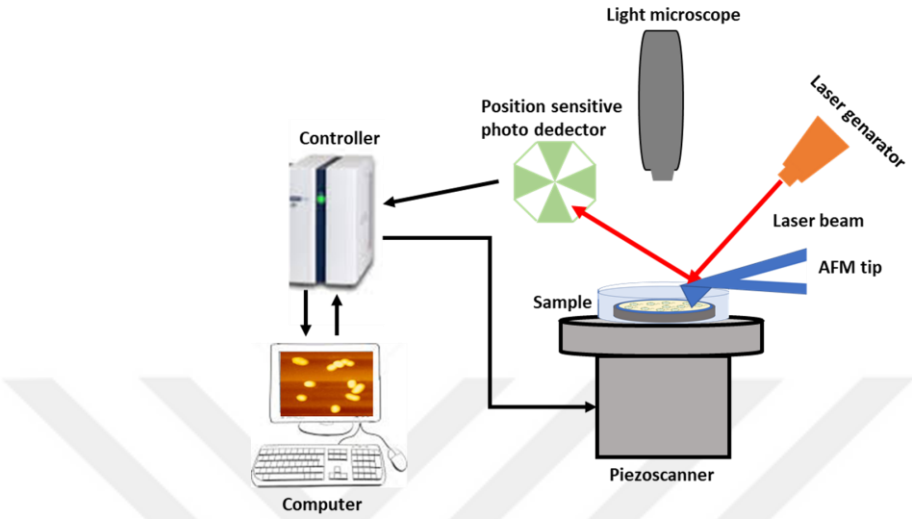

Figure 8. Components of atomic force microscope (AFM)

The sample is moved in the X, Y, Z direction by a piezo scanner but the cantilever does not move (the working principle of Hitachi 5100N). A laser beam focuses on the tip of the cantilever and is reflected back into the photodiode detector. With the location-sensitive photodiode, deviations in the console are detected. Thus, a topographic view of the sample surface is created. To measure forces, the tip must have physical contact with the surface. When the AFM tip/probe approaches to the sample surface, due to repulsion, an increase in the positive values of the forces is observed (red line, Figure 9). After the probe contacts the sample surface, the cantilever is retracted (pulled-off) from the sample surface. During retraction (blue line, Figure 9), *adhesion peaks* are observed which show 1) the *adhesion forces* that are needed to be applied to break-off the adhered molecules from the tip surface, 2) the distances at which the adhered molecules break-off from the tip surface. This distance is also called as the *pull-off distance*, representing the distance at which the AFM tip pulls-off the adhered molecules until they break-off from the tip. In this way, typical AFM force-distance curves are created.

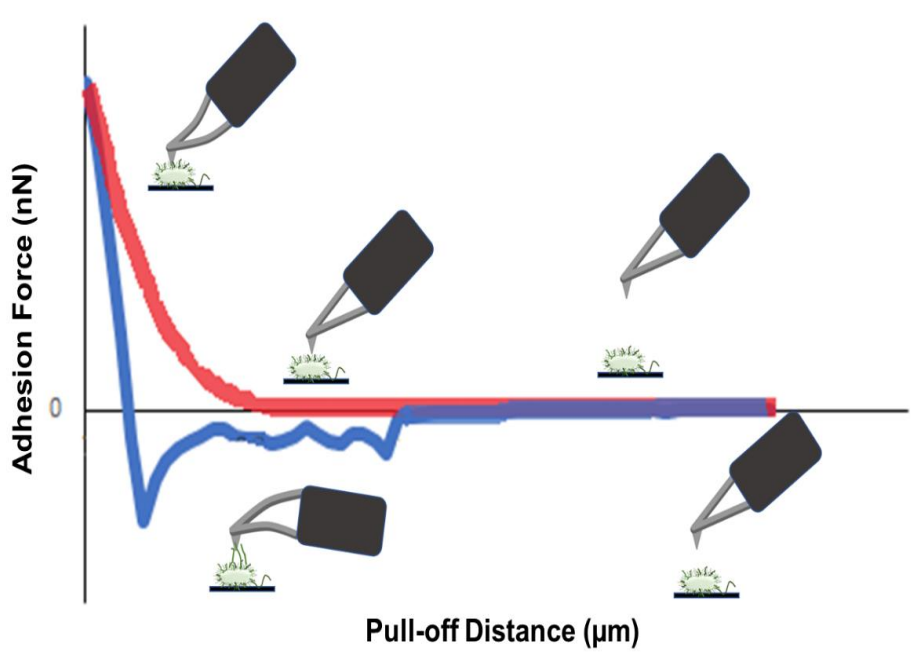

Figure 9. A typical AFM force-distance curve showing the interactions between bacterial cell and AFM tip during approach (red line) and retraction (blue line) of the AFM cantilever.

CHAPTER 3: MATERIALS AND METHODS

3.1 Preparation of the model micoorganism

Escherichia coli K-12 (ATCC 25404) was kindly provided by Prof. Dr. Thomas K. Wood, Biotechnology Endowed Chair and Professor of Chemical Engineering at the Pennsylvania State University, in the United States. *E. coli* ATCC 25404 was chosen as the model bacterial strain because its genome sequence and cell-wall characteristics are known from the previously published studies (Attila et al., 2009; Ren et al., 2005). In addition, many studies have shown that *E. coli* can form biofilms on many natural and man-made surfaces causing bioburden both in human health and industrial practices (Beloin et al., 2008; Sharma et al., 2016). *E. coli* strains are Gram-negative, rod-shaped and non-spore forming bacteria (Sharma et al., 2016), that can strongly adhere to surfaces through their extracellular biopolymers. These cellular extensions act as a mechanism to help overcome the repulsive forces and provide the first cell-to-surface contact for adhesion by enhancing the interaction between *E. coli* and the surfaces. After the pioneer bacterial cells adhere to the surface, they can easily form biofilms that will cause a wide variety of infections (Castonguay et al., 2006) and serious problems in the gastrointestinal and urogenital systems of the human body, as well in the medical devices, water systems and in the food industry (Beloin et al., 2008).

Particularly, *E. coli* ATCC 25404 was shown to form higher amount of biofilms compared to other biofilm-forming *E. coli* strains such as *E. coli* MG1655, which is another reason for its selection in the thesis (Wood et al., 2006).

E. coli ATCC 25404 cells were activated by growing in LB broth for 12-16 hours at 30°C in a temperature controlled shaker (IKA Incubator shaker KS 4000 i control) rotating at a 170 rotation per minute (rpm). Then, cells were diluted (1% v/v) in fresh medium and incubated at 37°C, 170 rpm (Moreira et al., 2017). The growth of the bacterial cells was monitored by reading the optical density (OD) of the bacterial culture in every 20-30 minutes at a wavelength of 600 nm using the UV/visible spectrophotometer (Figure 10). These experiments were repeated independently three times. According to the obtained typical bacteria-growth curves, *E. coli* ATCC 25404

reaches the late exponential growth phase after approximately 4-5 hours. Bacterial cells grown for 4 hours were centrifuged three times at 3000 rpm and harvested as the *planktonic cells* for use in the biofilm formation experiments, atomic force microscopy experiments (for the adhesion measurements of planktonic cells), and HPLC experiments (for the determination of extracted c-di GMP amount from the planktonic cells) or for storage.

The stock cultures were prepared as follows; cells that reached the late exponential phase were added into microfuge tubes with sterile glycerol solution (containing 50% glycerol and 50% distilled water) to a final cell concentration of 50% and stored at -80 °C.

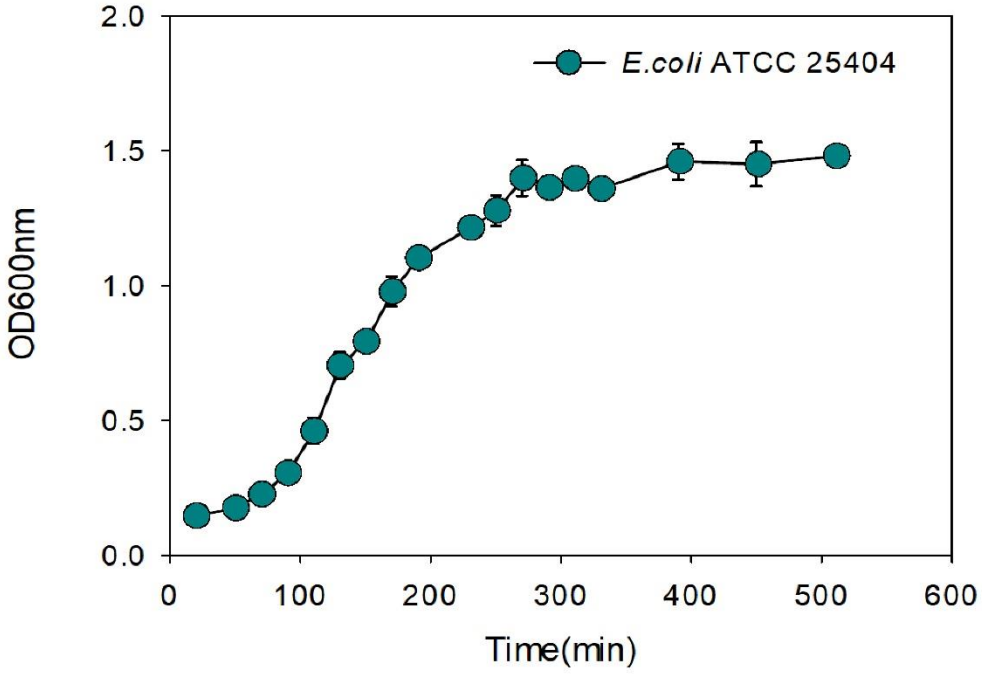

Figure 10. Growth curve of *E. coli* ATCC 25404 at 37 ºC in LB broth. Standard deviations of the measured OD600 values are shown in the figure.

3.2 Formation and quantification of biofilms in batch systems

Biofilms were grown either in the 12-well plates (Corning 3737, non-treated sterile 12-well plates) or in 96-well microplates (Corning 3788, non-treated sterile 96-well microplates). Firstly, planktonic *E. coli* ATCC 25404 cells stored at -80 °C were activated (%2 v/v) in fresh LB medium and incubated twelve hours at 37 °C, 170 rpm. Activated cells were diluted (1:100) with LB medium and transferred into the

polystyrene well plates. All wells were filled with the cell suspension (4 ml of cell suspension was added in each 12-well plates, and 200 µl of cell suspension was added in each 96-well microplates). Afterwards, the well plates were incubated for 17 hours at 37 °C, as seen in Figure 11. (O'Toole, 2011).

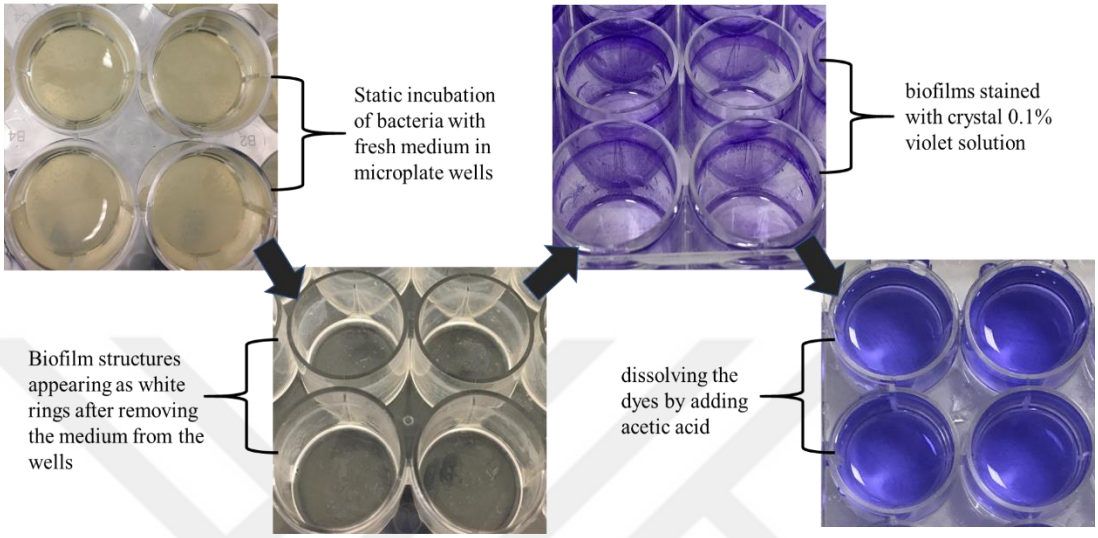

Figure 11. Representation of *E. coli* ATCC 25404 biofilm formation in batch cultures and quantification of the biofilm amount.

For the quantitative analysis of biofilm formation, *biofilm staining protocol* was used. After 17 hours of incubation, media containing unattached cells to the walls of the wells (the cells that did not contribute the formation of biofilms) was carefully removed by washing the wells twice with deionized (DI) water. The well plates were turned upside down on paper towels and left to dry for 5 minutes at room temperature. Then, 200 µl (or 4 ml) of 0.1% v/v crystal violet (CV) solution was added into each well and plates were incubated at 120 rpm for 10-15 minutes. The CV dye solutions were removed from wells by gently washing with DI water for three times and were allowed to air dry. To determine the amount of the dye absorbed by the biofilm, 200 µl (or 4 ml) of 30% acetic acid solution was added into each well and incubated for 10-15 minutes at room temperature. The solutions in the wells (containing the solubilized dye) were pipetted up and down for homogenization. Afterwards, the optical densities of the solutions which actually show the staining amounts of the biofilms with the CV solution, and hence the amounts of the biofilms formed, were measured at 595nm using ELISA reader (Li, Xi-Hui et al., 2017).

3.2.1 Procedure for obtaining biofilm-dispersed cells from batch cultures and quantification of remaining biofilms

After 17 hours of incubation period for biofilm formation, unattached cells were removed by washing twice with DI water, then fresh LB medium containing 15 different concentrations starting from 0.125 µM up to 100 mM (Figure 12) of the NO-producer sodium nitroprusside (SNP) was added into each well (for the control, only fresh LB medium was added). The main reason for using these concentrations was that the SNP concentrations in these ranges were previously tested in similar biofilm dispersion studies (Barraud, 2007a; Barraud et al., 2006; Barraud et al., 2009; Walker, and Keevil, 2015). Biofilm dispersion was induced by incubating the well plates at 120 rpm at 37 °C for 24 hours and dispersed cells were collected from the plates after incubation (Barraud et al., 2006).

The optimum SNP concentrations required for the dispersion of the batch culture *E. coli* ATCC 25404 biofilms were determined. Those concentrations were 0.5 µM (500 nM), 5 µM, and 50 µM of low dose SNP.

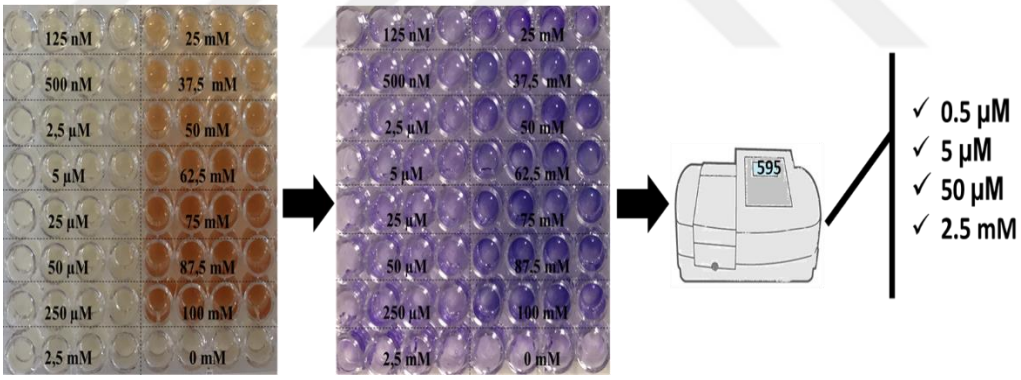

Figure 12. Determination of appropriate SNP concentrations for biofilm dispersion

To investigate whether such biofilm-dispersed cells obtained after the addition of high doses of SNP will have different adhesion properties and c-di GMP amounts compared to the biofilm-dispersed cells obtained after the addition of low doses of SNP, we have selected the cells dispersed from the batch grown biofilms at 2.5 mM SNP concentration. When the concentrations of added SNP to the batch cultures of biofilms were in the millimolar ranges (2.5 mM up to 100 mM), color changes in the cultures containing 25 mM-100 mM of SNP were observed after 24 hours of incubation, except for the cultures containing 2.5 mM of added SNP (Figure 12). It

was thought that this color change was probably arising from an increased toxic effect due to the higher doses of added SNP. Thus, among the high doses of SNP, 2.5 mM of SNP concentration was selected.

For the quantification of the remaining biofilms after dispersal, the *biofilm staining protocol*, which was described in detail in the previous section, was used. Briefly, after the collection of biofilm-dispersed cells from the wells of the plates, the microplates containing the remaining biofilms were washed twice with DI water. Then, each well was stained with the crystal violet solution. The addition of acetic acid dissolved the absorbed crystal violet (CV), and finally the OD values of the solutions containing solubilized CV were determined at 595 nm with the ELISA reader.

After the collection of cells dispersed from batch grown cultures, those freshly dispersed cells were directly prepared for atomic force microscopy measurements. The experiments regarding to the quantification of the remaining biofilms after dispersal and atomic force microscopy measurements on the freshly dispersed cells were done repeatedly at different times.

3.3 Formation and quantification of biofilms in continuous systems

E. coli ATCC 25404 cells were activated by growing in LB broth (2% v/v stock culture cells were transferred into 20 ml LB) for 12-16 hours at 30°C in a temperature controlled shaker rotating at 170 rpm, and used as the seed culture for biofilm formation in a continuous flow chamber system (FC284 Dual Channel Transmission Flow Cell, BioSurface Technologies Corp.). The continuous flow chamber system consists of medium bottle(s), a peristaltic pump (MasterFlex Pump System, Cole-Palmer), bubble traps, the flow chamber, a waste container, tubing (3 mm ID), and connectors (Figure 13).

The dual channel flow chamber (Figure 13) with dimensions 50×13mm with a depth of 2.35 mm was constructed in a sandwich of microscope cover slips and microscope slides on which the biofilms were formed. These glass windows were held in place by aluminum cover plate which also compressed silicone rubber gaskets to provide a leak-proof flow.

The seed culture equilibrated to an appropriate optical density was injected into the continuous flow chamber of two channels and it was kept for 1 hour without flow to allow the initial bacterial attachment to the surfaces. The flow of the fresh LB was initiated with the peristaltic pump at a rate of 0.4 ml/min (laminar flow) for the formation of biofilms for 48 hours at room temperature.

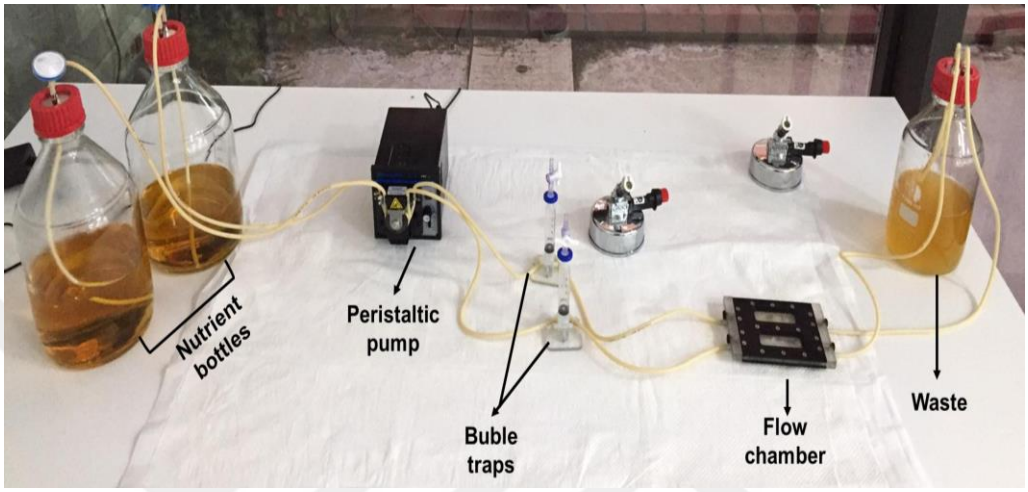

Figure 13. The continuous flow chamber system

After the biofilm formation, the glass slides were removed and washed 2 times with DI water to remove non-adherent bacteria and the medium components. The Live / Dead BacLight Bacterial Viability Kit (Invitrogen™) was used to visualize the biofilms, quantify their amounts (with the help of ImageJ software) and to investigate their viabilities. The kit includes two fluorescent dyes SYTO® 9 and propidium iodide (PI). PI gives red emission by staining dead or membrane-damaged cells, while SYTO9 gives green emission by staining living cells with intact membranes. For the quantification of biofilms, 0.75 µl of PI and SYTO9 stock solutions were added into 1 mL of 0.2 µm filtered DI water. Approximately 12-15 mm diameter circles were marked from the back side of the glasses on which the biofilms were formed. 200 µl of the prepared dye solution were added onto these areas. After adding the dye solution, slides were incubated in the dark for about 15 minutes. At the end of the incubation period, the glass slides were washed with the filtered DI water. The samples were placed in Petri dishes and DI water was added to them. Samples in water were imaged using an Oxion Inverso fluorescence microscope (Euromex, Arnhem, The Netherlands).

3.3.1 Procedure for obtaining biofilm-dispersed cells from continuous cultures and quantification of remaining biofilms

The biofilms were grown on the glass slides of the flow chamber as described above for 24 hours by continuously passing fresh LB broth through the flow channels at a rate of 0.4 ml/min. Afterwards, the NO-donor dispersion agent SNP was added to the medium bottle at a final concentration of 0.5 μM. Biofilm dispersion was induced at room temperature by continuous flow of the LB medium with 0.5 μM added SNP at the flow rate of 0.4 ml/min for 24 hours. Biofilm-dispersed cells were collected inside the waste bottle (Figure 13). However, only the dispersed cells for the last hour of the continuous dispersion process were collected from the waste bottle for further investigation. We have chosen 0.5 μM added SNP concentration to obtain the dispersed cells from the continuous cultures. This is because the most profound effect of SNP induced biofilm dispersal was observed at this concentration in the continuous flow system.

After the biofilm dispersion, to visualize the remaining biofilms, quantify their amounts (with the help of ImageJ software) and to investigate their viabilities, the protocol given in the previous section was followed. Briefly, the remaining biofilms on the glass slides (after the dispersion with SNP) were washed with DI water, stained with the two fluorescent dyes (SYTO® 9 and propidium iodide (PI)) and imaged using the fluorescence microscope.

3.4 Atomic force microscopy (AFM) experiments

3.4.1 AFM sample preparation

Bacterial cells must be firmly immobilized to a surface so that they do not move during the AFM imaging and force measurements. For this purpose, mica disks to which the cells were immobilized were first coated with the cationic polymer, poly-L-lysin (PLL) (Sigma-Aldrich, USA). PLL electrostatically interacts with the negative charges on the bacterial surface and has been successfully used to immobilize the cells on a surface for the AFM imaging and force measurements (Doktycz et al., 2003). Since mica surfaces can be easily cleaved and cleaned simply by using adhesive tapes, mica disks were selected to be used for the bacterial immobilization.

Prior to PLL coating, a mica disk was taken and fixed on an AFM magnetic coin using a double-sided tape, then the mica disk was cleaved several times to obtain a freshly cleaved and clean surface. Afterwards, approximately 100 µL of 0.01% (w/v) PLL solution (Sigma-Aldrich, USA) was spread over the mica surface (approximately 1.5 cm^2 surface area). The solution was allowed to sit on the mica surface, while the disk remained closed inside a petri dish. Then the disk was thoroughly washed off with DI water and allowed to dry at room temperature.

Planktonic cells and biofilm-dispersed cells, which were obtained as described previously, were centrifuged at 3000 rpm for 5 minutes. After the supernatant was removed from the bacterial pellet for each condition investigated, the cells were washed one more time with DI water. After washing, cells were suspended in water. The bacterial cell suspension was added onto the dried PLL-coated mica disc (prepared as described above) and incubated for 10-15 minutes to allow the bacterial cells to attach onto the PLL-coated mica surface and washed 3 times with DI water to remove the non-attached cells. After washing, the prepared sample was placed in a sterile plate and kept with the distilled water until the AFM measurements. This procedure was repeated for each condition investigated.

3.4.2 AFM imaging and adhesion force measurements

All AFM experiments were performed by HITACHI 5100N atomic force microscope (Hitachi High-Tech., Tokyo, Japan) using silicon nitride cantilevers (DNP-S cantilevers with 0.24 N/m nominal spring constant, Bruker AXS Inc., Santa Barbara, CA). Generally bacterial cells like to adhere to soil and glass surfaces in nature. Silicon nitride has similar surface properties to these two substances (Abu-Lail, and Camesano, 2003; Gordesli, and Abu-Lail, 2012c). In this study, the use of silicon nitride as the model inert surface was based on this reason.

Prior to AFM imaging and force measurements, PLL-coated mica disc with bacterial cells attached onto was placed on top of the AFM scanner and covered with distilled water. The cantilever was carefully placed in the cantilever holder, and the AFM tip was also immersed in water (Figure 14). Afterwards, the processes in the AFM software were initiated. The approach speed of the AFM cantilever to the sample surface was selected from the up-down section in the approach tab (high or low) of the

AFM software. Once the cantilever and the sample surface were close enough, the laser beam was aligned on the backside of the AFM tip, and ADD, DIF and FFM values were adjusted. ADD value was set to the maximum value that could be achieved in water and DIF/FFM values were adjusted to zero. Then the vibration spectrum of the AFM tip in water was obtained and resonance frequency of the AFM tip in water was determined (Q curve measurement in HITACHI 5100N).

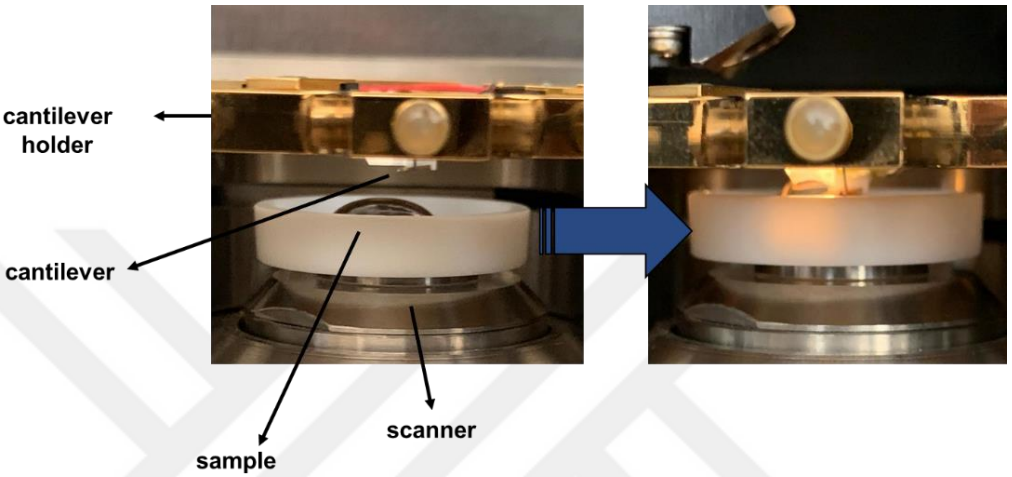

Figure 14. Immersion of AFM cantilever into water to get closer the sample surface

All topographical images were taken using dynamic fluid mode (DFM mode or the so called tapping mode) under water at a resolution of 256 pixels per line and 256 lines per image. In this mode, the cantilever oscillates nearby the surface of the bacterial cell, without contacting the surface. The image scanning was initiated with a low scanning speed (0.50 Hz) using sampling intelligent scan (SIS) topography method for all investigated, which is a method based on the DFM mode. The SIS mode is an intelligent measurement mode whose scanning speed can be freely controlled to match the topography of the sample. Since lateral AFM tip–sample forces are avoided by SIS-topography method, the resolution is much higher compared to normal DFM mode as well as to the classical contact mode.

After imaging, DFM mode was switched to the AFM contact mode and different points on the bacterial cells were selected for force measurements. Force-distance measurements were performed at different points/regions for each bacterium on a captured image. The black marks (+) shown on the bacterial surfaces are the spots where force measurements were performed (Figure 15). At least 20 cells taken from

different cultures were selected for AFM force measurements. On each cell, 9-12 points were located using the AFM software. After the force-distance curves were captured, the raw data and plots of these curves were saved for further analysis to obtain adhesion forces, pull-off distances and adhesion energies. In addition to the analysis of the force-distance curves, the captured bacterial images were analyzed using the AFM software to obtain cell dimensions (height, width and length) for all investigated. As can be seen in Figure 15, bacterial three-dimensional size analysis was performed on the topographic AFM images of the cells with the help of the line profile section analysis of the AFM software.

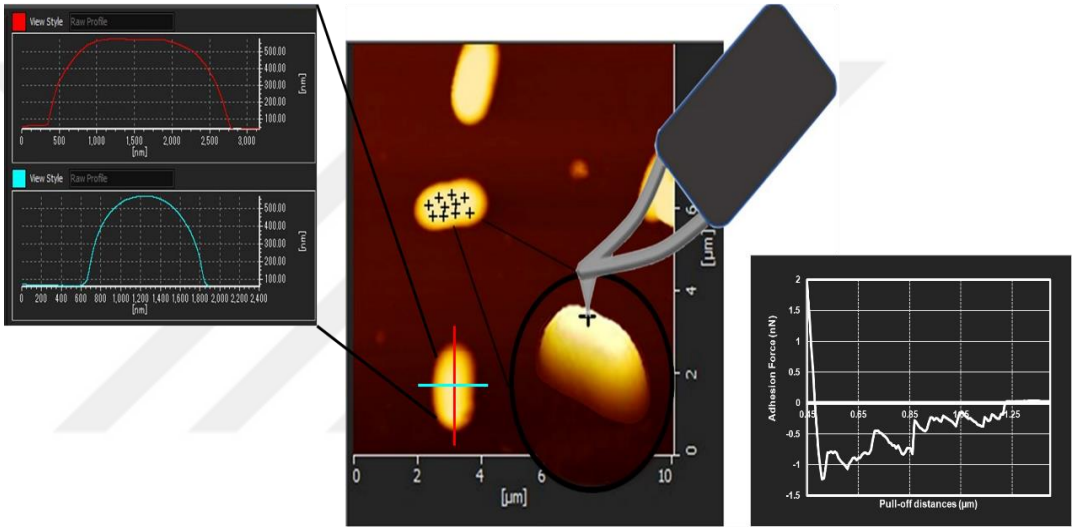

Figure 15. Topographical 10 × 10 µm AFM image of *E. coli* ATCC 25404 cells under water. The + signs in the images represent the regions on which the force measurements were performed. A retraction curve was obtained from a single region signed with +. The dimensional analysis of the bacterial cells were made on the images taken. The blue and red lines represent the width and length of a bacterial cell, respectively.

3.4.3 Analysis of AFM force-distance curves

AFM force-distance graphics consist of the approach and retraction curves. The retraction curve contains important information about bacterial adhesion such as adhesion forces and energies and pull-off distance values. This curve occurs as a result of interactions between the biopolymers on the bacterial surface and the AFM probe/tip when the tip retracts from the bacterial surface after touching it. The interactions between bacterial surface biopolymers and the silicon nitride tips are

complex and heterogeneous. Therefore, all retraction curves were handled separately. During retraction, biopolymers of bacterium are stretched until they remove from the tip. Biopolymers separated from the tip form the *adhesion peaks*. The properties of the biopolymer and the number of molecular extensions attached to the tip create differences in the adhesion peaks.

Bacterial adhesion was quantified by *adhesion forces* in nano-Newton (nN) and *adhesion energies* in attojoule (AJ). The forces and distances were obtained from the peaks in the curves. Each peak has two coordinates: pull-off distance (in the x axis) and the pull-off force or the adhesion force (in the y axis). The adhesion energies of bacterial cells were obtained from calculating the area between the retraction curve and the x-axis as simply given in equation 1. The negative sign was multiplied with the values of pull-off forces to convert them into positive adhesion forces. All the adhesion forces and energies are given in positive values in the thesis.

$$E_{adhesion} = -\int_{h_1}^{h_2} F dh \tag{1}$$

In equation 1, F is the adhesion force, h_1 and h_2 are the distance points that are also shown in the retraction curve (Figure 16). To quantify the adhesion energy, Trapezoidal rule was used (eq. 2).

$$E_{(adh)}(AFM) = -\int_{h_1}^{h_2} F dh \approx -\frac{h_2 - h_1}{n}\left[\frac{F(h_1)+F(h_2)}{2} + \sum_{k=1}^{n-1} F\left(h_1 + k\frac{h_2 - h_1}{n}\right)\right] \tag{2}$$

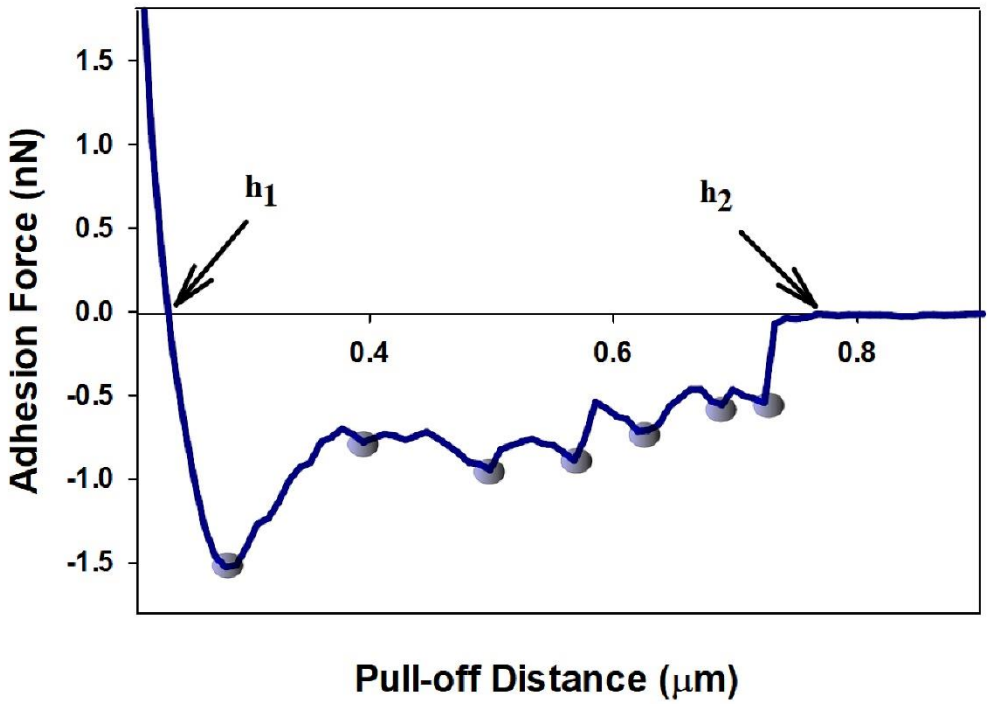

Figure 16. Bacterial adhesion force peaks and adhesion energy calculation on a typical AFM retraction curve.

It is important to measure the forces on different regions of the bacterial surface, and to repeat the same measurements on different bacterial cells for each investigated condition in order to obtain a mean value that can represent the adhesion strength of the bacterial cell to a surface. This is because the biopolymers on the bacterial surface are so heterogeneous (Abu-Lail, and Camesano, 2003; Gordesli, and Abu-Lail, 2012c; Park et al., 2014). Hence obtaining a single retraction curve from a single spot on a bacterial cell and evaluating the mean adhesion strength will not give a realistic result.

For each retraction curve collected from each region on a bacterial surface, the values of the adhesion peaks/forces (nN), distances (μm) and adhesion energies (AJ) were evaluated individually using a home-written MATLAB code. At least 200 retraction curves were examined to evaluate the adhesion forces for an investigated condition, and at least 856 adhesion forces (peaks) and pull-off distances were observed among the investigated conditions. The mean, median and standard error of the mean values of all adhesion forces, pull-off distances and adhesion energies were calculated for each investigated.

3.4.4 Statistical description of AFM data

In the literature, besides reporting mean or median values of AFM data, different statistical models have also been used to describe the heterogeneity of the AFM data which is based on the heterogeneity of bacterial surface biopolymers in our case. By applying (fitting) normal (Hu et al., 2009), log-normal (Hiratsuka et al., 2009), or Weibull (van der Mei et al., 2010), distributions to the probability histograms of adhesion forces, distances or energies, the most probable AFM adhesion event in the distribution can be found. In this way, by applying statistical distribution models to the histograms of adhesion data, the effect of heterogeneity can be minimized. In short, explaining the adhesion between bacterial cells and surfaces measured by AFM requires the statistical description of the AFM data such as calculations of mean, range, median, standard error of the mean values as well as the determination of the most probable values of the data obtained.

It was found that our AFM data can be considered as log-normal probability distributions. The log-normal probability distribution functions were applied to adhesion force, pull-off distance, and adhesion energy data of all investigated conditions. The qualities of the fittings were determined using the coefficient of correlation values (R^2), and the most probable values were obtained.

The log-normal distribution is a statistical method for the definition of the probability distribution of a normally distributed logarithm. In this study, log-normal distribution was used with 3 parameters as a, b and x_0 (eq. 3).

$$y = \frac{a}{x}.\exp\left[-0.5\left(\frac{\ln\left(x/x_0\right)}{b}\right)^2\right] \tag{3}$$

a: expressed as the amplitude of the distribution and is the parameter that predicts the maximum probability of occurrence.

b: called as a fitting parameter and has the role of an indicator in the width of the distribution function.

x_0: the parameter expressing the adhesion tendency with the maximum probability of occurrence

x: adhesion tendency

y: the probability of occurrence of adhesion

Sigma Plot version 14.0 (Systat Software, Inc., Chicago, IL) was used for the estimation of the most probable adhesion values by fitting with log-normal distribution function (eq. 3). In addition, independent one-way analysis of variance (ANOVA) (Sigma Plot 14.0, Systat Software, Inc) was used to determine if significant differences in the measured adhesion forces, energies, separation distances as well as in bacterial cell dimensions were present among the bacterial cells investigated. Tukey's or Dunn's pairwise comparison test and Kruskal−Wallis one way analysis of variance on ranks were performed for planktonic and biofilm-dispersed *E. coli* ATCC 25404 cells, where necessary.

3.5 Determination of intracellular c-di GMP levels of planktonic and biofilm-dispersed E. coli ATCC 25404 cells

The determination of the c-di GMP levels of planktonic and biofilm-dispersed *E. coli* ATCC 25404 cells in terms of pmol c-di GMP per mg of protein, were determined by following the protocol developed by (Petrova, and Sauer, 2017).

3.5.1 Extraction of c-di GMP

Planktonic cells and biofilm-dispersed cells (from -80°C stocks) were activated for 12-16 hours at 30°C and 170 rpm (2% v/v) in LB broth with appropriate concentration of added SNP, respectively. After that, cultures were transferred (1% v/v) separately in fresh medium. Main cultures were incubated until late exponential phase at 37°C and 170 rpm.

Optical density of the bacterial cells (planktonic cells and dispersed cells) were determined at 600nm. Cultures' volumes were adjusted to 1 ml with OD_{600} = 1.5-1.6. Then the cultures were centrifuged at 16,000 × g, 2 minutes, 4 ° C. After centrifugation, supernatants were removed from the cell pellets. Cell pellets were washed with 1 ml ice-cold PBS and centrifuged at 16,000 × g, 2 minutes, 4 ° C. Supernatants were removed again and the washing step was repeated one more time. The remaining cell

pellets were mixed with 100 µl ice-cold PBS for each condition, and incubated at 100°C for 5 min. After heat incubation, ice-cold ethanol, which was previously stored at −20°C, was added on the viscous cell pellet solution. Approximately 217 µl of 95 % ethanol was added and the tubes were vortexed for 15 seconds. Samples were centrifuged (at the same centrifugation conditions), and the supernatants containing extracted c-di GMP were transferred in new microfuge tubes. Tubes with the supernatants were stored on ice until the next step. Extraction step was repeated two more times and supernatants from the repeated three extractions were combined in one tube, for each investigated.

Approximately 900 µl of supernatants for each sample tube were prepared and freeze-dried for 22-24 hours. After drying, samples were stored at −80°C until the quantification of c-di GMP concentrations (pmol/µl). In addition to this, retained pellets in the tubes were kept at −20 °C for the quantification of their protein concentrations (mg/µl). A summary of the overall extraction procedure is given in Figure 17.

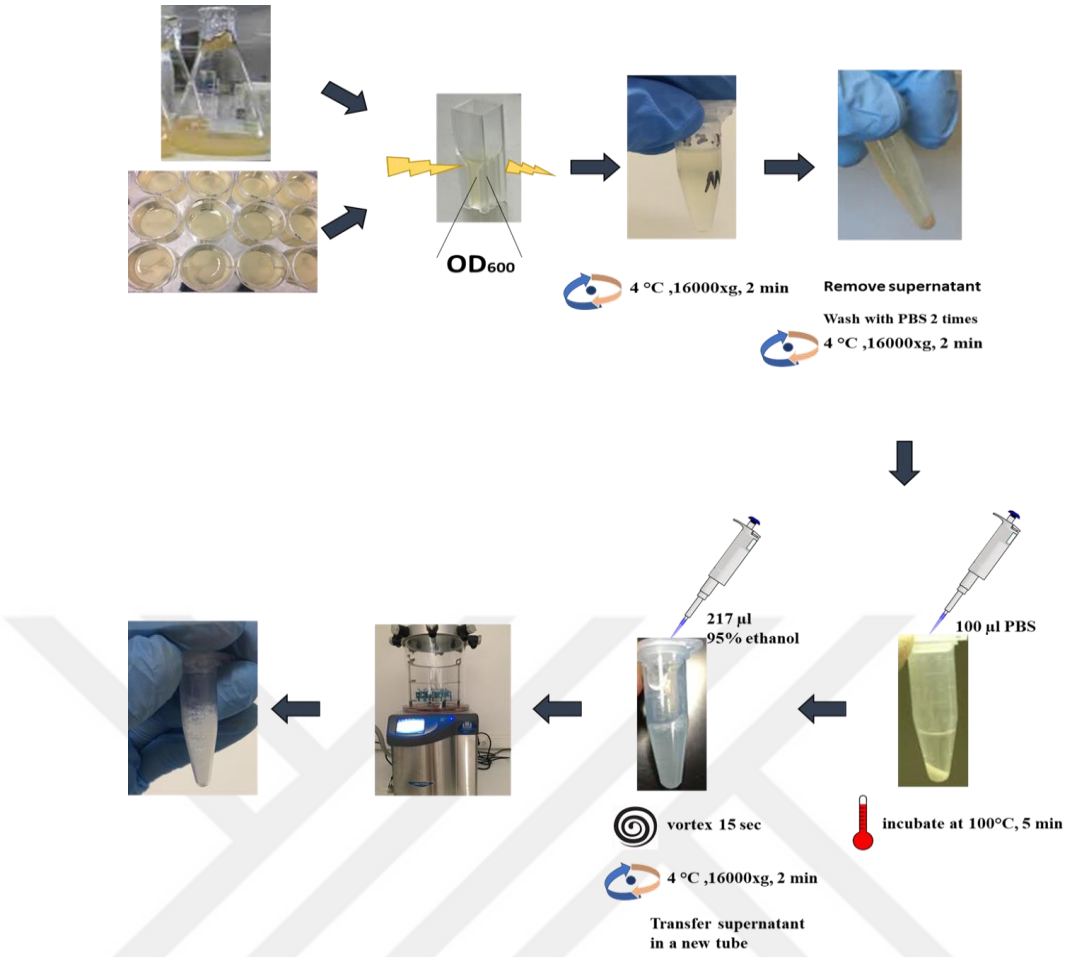

Figure 17. The extraction procedure of cellular c-di GMP

3.5.2 Measurement of extracted c-di GMP concentrations using high performance liquid chromatography (HPLC)

Separation of components from a column at different times originates the basis of the working principle of HPLC. This device mainly consists of: degasser, mobile phase, autosampler, column, column oven, pump, and the detector. The degasser provides removal of dissolved gases present in the mobile phase. The mobile phase is the liquid that carries the analytes/components that are of interest. The composition of the mobile phase and the pH value directly affect the separation. The sampler allows the injection of the sample. The column, usually made of steel and glass, and including a certain amount of stationary phase (such as silica), makes the elution of the components in the injected sample possible by the help of their chemical and physical properties. The components are first dissolved in an appropriate solvent and forced to pass through the chromatography column under high pressure.

The different stationary phase-analyte/component interactions and different speeds of components in the column cause their separation from the column at different times. The properties of the sample, solvent and stationary phase are also having important roles at the time of elution. If the components have strong interactions with the stationary phase, they exhibit long retention times or vice versa. As can be understood from its name, the column oven is used to keep the column at a constant temperature. Basically, the pump enables the mobile phase to move at high pressure in the HPLC system. Since the stationary phase of the column consists of µm sized particles, high pressure pumps are generally required to pass the mobile phase through the column. Finally, the components coming out of the column pass through the detector along with the mobile phase. The detector generates a signal based on the amount of the eluted component. Elution time and quantification signals are transferred to the software of the device and made it suitable for further analysis of the chromatograms generated. The basic working principle of HPLC is shown in the following figure (Figure 18).

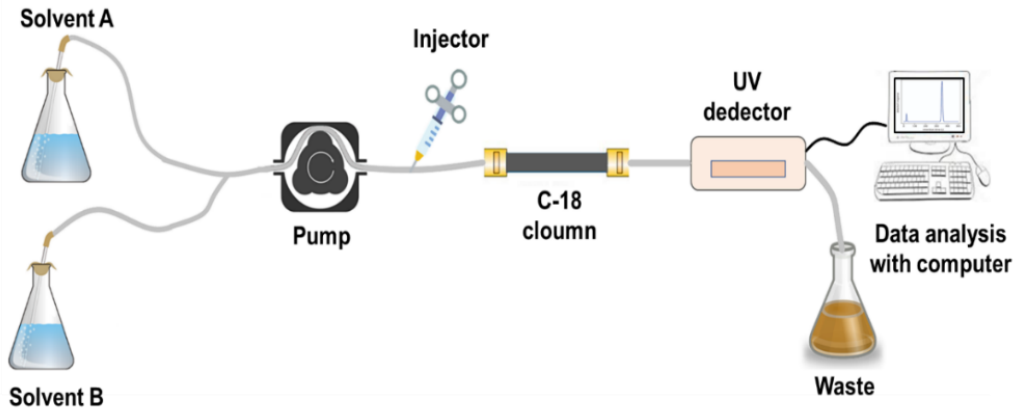

Figure 18. Representation of the basic working principle of HPLC

All liquid chromatography experiments in this study were performed with the Ultimate 3000 HPLC (Thermo Scientific, Massachusetts, USA) device and Chromeleon^{TM} 7.3 Chromotography Data System (CDS) software. For the detection of c-di GMP, reversed-phase C18 column (Thermo Scientific, USA) was used. The mobile phases (A, B) used were 10 mM ammonium acetate (MS grade) in ultrapure water (phase A) and 10 mM ammonium acetate (MS grade) in methanol (MS grade) (phase B). The solutions were filtered by using 0.2 µm filters before the experiments.

Used methodology includes a gradient program as given in Table 1, which was initiated with a flow rate of 0.5 ml min^{-1} and 20 µl of sample injection. The column temperature was 25 °C, and UV/Vis detector was set to 253 nm.

Table 1. HPLC mobile phase flow cycle

Time	Gradients of solvents
0 to 9 minutes	1% B and 99% A
9 to 14 minutes	15% B and 85% A
14 to 19 minutes	25% B and 75% A
19 to 26 minutes	90% B and 10% A
26 to 45 minutes	1% B and 99% A

To determine the elution time of c-di GMP and its concentration, first standard solutions of c-di GMP (1, 2, 5, 10 and 20 pmol/µl) were prepared from the authentic Bis-(3'–5')-cyclic diguanylic monophosphate (c-di GMP) (Bio-log) stock solution (200 pmol/µl). Also, another sample containing only nano pure water was used as the negative control (0 pmol/µl). 20 µl of all standard solutions were injected for run of HPLC and the coincident chromatogram of c-di GMP standards was created (Figure 19). Then the calibration plot (the standard curve) of c-di GMP standards was generated using the HPLC software (Figure 20).

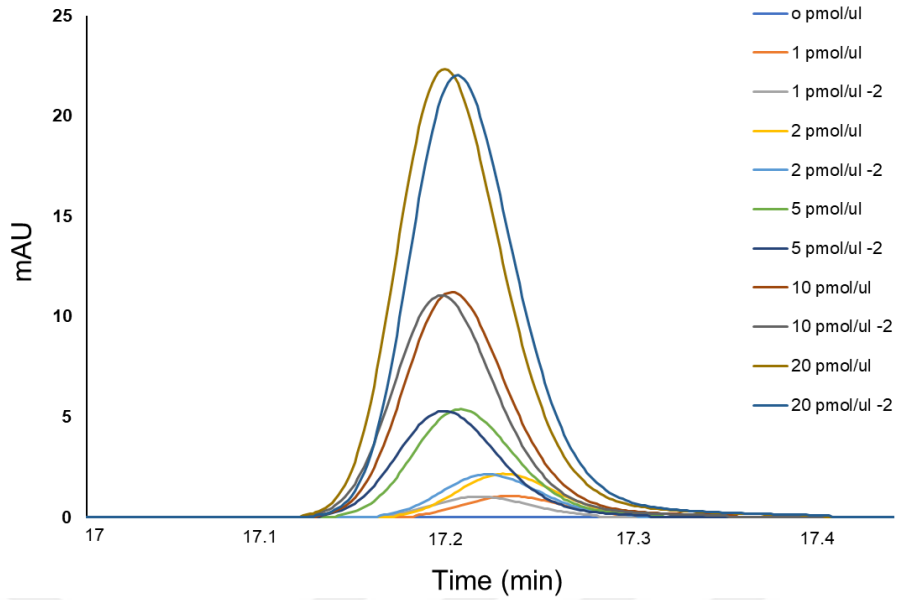

Figure 19. The coincident chromatogram of c-di GMP standards. 0 pmol/µl used as the negative control (no c-di GMP content, nano pure water). Each c-di GMP standard concentration was investigated in duplicate.

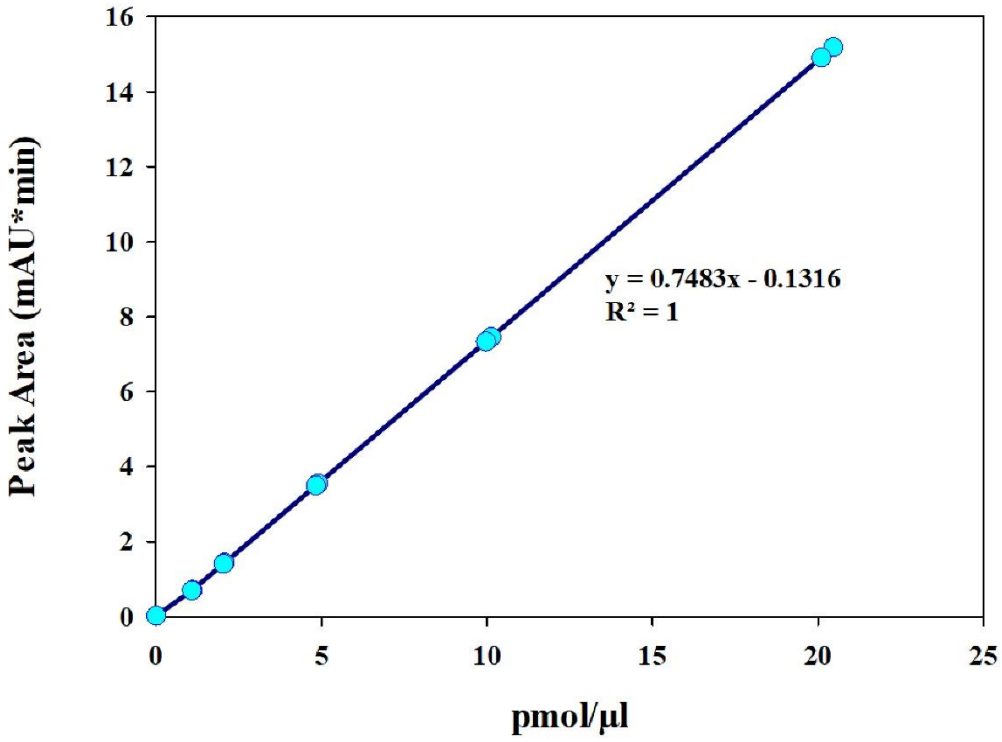

Figure 20. Calibration plot of c-di GMP standards. The calibration curve was plotted as the peak areas obtained following the separation of 20 µl samples of c-di GMP standards versus the c-di GMP concentrations.

For HPLC analysis of the extracted c-di GMP samples, dried c-di GMP extracts were suspended in 300 µl of water for each investigated and vortexed for 1 min. Then, suspensions were centrifuged at 16,000 × g for 2 minutes to remove the insoluble contents. Supernatants containing c-di GMP (just liquid part without insoluble contents) were filtered using 0.22 µm syringe filter and transferred into HPLC vials. 20 µl of the sample solution was injected and the concentration of c-di GMP per sample was determined using the standard curve previously generated.

3.5.3 Protein quantification assay

The modified Lowry protein assay procedure was performed for protein analysis of cell extracts as followed in Figure 21. Cell pellets retained after c-di GMP extraction were suspended in 500 µl of 0.2µm filtered DI water. Tubes were vortexed for 1 minute to distribute the pellets homogeneously in water. The suspensions were sonicated on ice for a total of 2 minutes including 10 seconds burst and 15 seconds stop intervals. 0.2 mL of replicates were transferred to labeled test tubes. At 15 second intervals, 1.0 mL of Modified Lowry reagent was added to the tubes and the mixtures were homogenized. They were incubated for exactly 10 minutes at room temperature. Then, 100 µL of prepared 1X Folin-Ciocalteu reagent was added to the tubes (maintaining the 15-second interval between the tubes) and the prepared mixtures were vortexed. After covering the tubes to protect them from light, they were incubated for 30 minutes under room conditions. After incubation, a water-soluble product whose amount is proportional to the protein amount of the cell suspension was formed in each tube. Absorbance measurements of the samples were done with a UV-visible spectrophotometer set to 750 nm. Bovine serum albumin (BSA) was used as the standard.

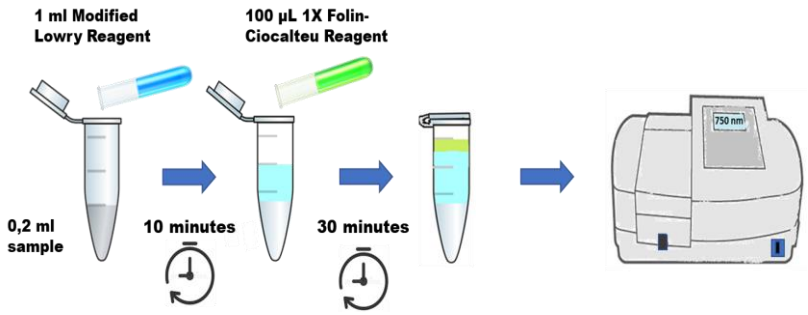

Figure 21. Representation of the Modified Lowry protein assay procedure

3.5.4 Normalization of c-di GMP concentrations

The concentration of c-di GMP was normalized with total cellular protein content of the bacterial cells (pmol/mg). Normalization was performed using the following calculations.

The c-di GMP quantified by HPLC analysis ($F_{c\text{-}di\ GMP}$) is the fraction (20 µl of 300 µl) of total c-di GMP in the extracted sample ($T_{c\text{-}di\ GMP}$). So, quantified c-di GMP amount was multiplied by 15 to find the total cellular c-di GMP amount:

$$T_{c-di-GMP} = 15 \times F_{c-di-GMP} \quad (4)$$

The total cellular protein content in the sample equals to the protein concentration ($C_{protein,}$ mg/ml) multiplied by 0.5 ml. This is because, in the protein quantification assay, cell pellets were suspended in 500 µl of water.

$$T_{protein} = C_{protein} \times 0.5ml \quad (5)$$

The cellular c-di GMP level in pmol normalized per mg of cellular protein ($N_{c\text{-}di\ GMP}$) was determined by using the following equation:

$$N_{c-di-GMP} = T_{c-di-GMP} / T_{protein} \quad (6)$$

CHAPTER 4: RESULTS AND DISCUSSION

4.1 Effect of added SNP concentration on the dispersion amounts of E. coli ATCC 25404 biofilms grown in batch systems

As was mentioned previously, NO regulates the biomass of biofilms by triggering the c-di GMP pathways and causes the dispersion of the biofilms. The effect of the addition of different doses of the NO donor, SNP, on biofilm dispersal was tested on *E. coli* ATCC 25404 biofilms grown in batch systems (Figure 22). A total of 15 different SNP concentrations starting from 0.125 µM up to 100 mM have been repeatedly tested on batch grown *E. coli* ATCC 25404 biofilms in 96-well plates.

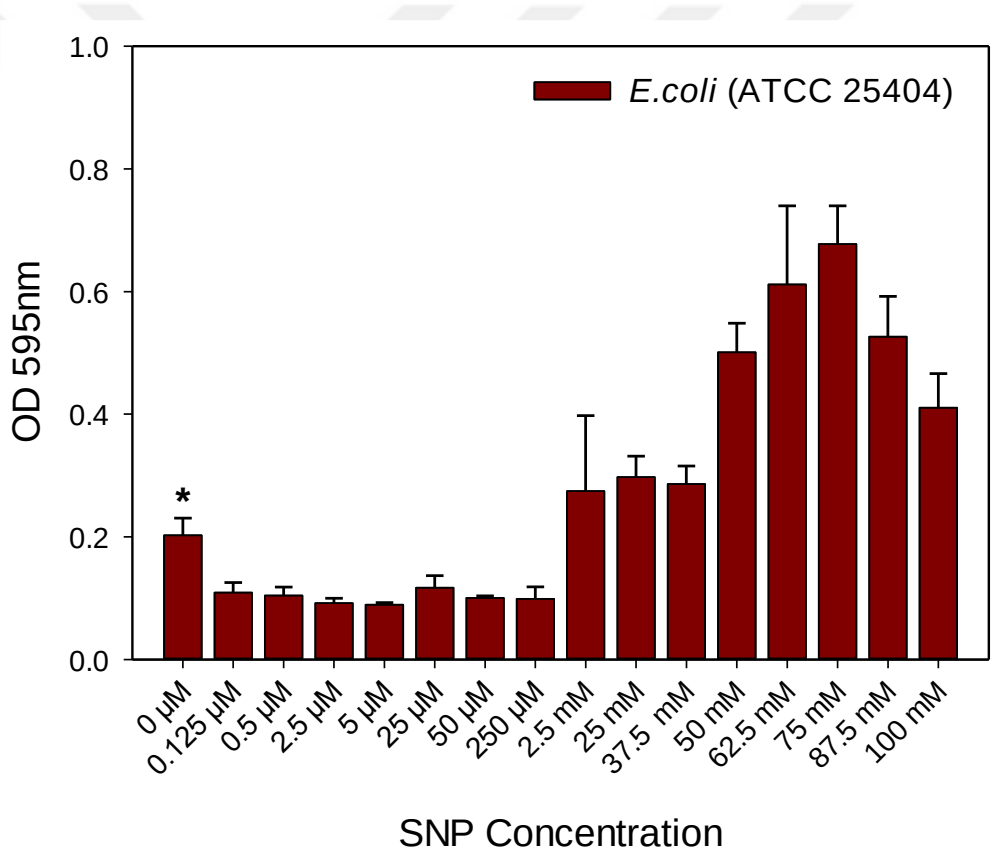

Figure 22. Comparison of optical densities of the remaining biofilms of *E. coli* ATCC 25404 after the addition of different SNP concentrations in batch grown biofilm cultures. The control (untreated biofilm, no SNP addition) given in the figure (0 µM) represents the optical density of the *E. coli* ATCC 25404 biofilm grown in LB medium in the batch system for 17+24 hours.

First, untreated biofilms were developed as batch cultures for 17 hours, and then each SNP concentration was added to the cultures of biofilms for 24 hours of incubation to allow the biofilms to disperse. The effect of each SNP concentration on the biofilm dispersal was investigated by crystal violet staining at the end of the incubation period. The control group (untreated biofilms) was grown for 17 + 24 hours (just in LB medium) and the biofilms unexposed to SNP (0 µM) showed normal development. Our results showed that exposure to low doses (in the micromolar ranges) of SNP significantly reduced the biofilm amount or, in other words, induced the dispersal of biofilms (Figures 22 and 23). The greatest dispersion effects were observed for the added SNP concentrations of 0.5 µM, 2.5 µM, 5 µM, 50 µM and 250 µM with 48.5 %, 54.5 %, 56 %, 50.5 % and 51 % decrease in the biofilm amount compared to the amount of control biofilm, respectively (Figure 23).

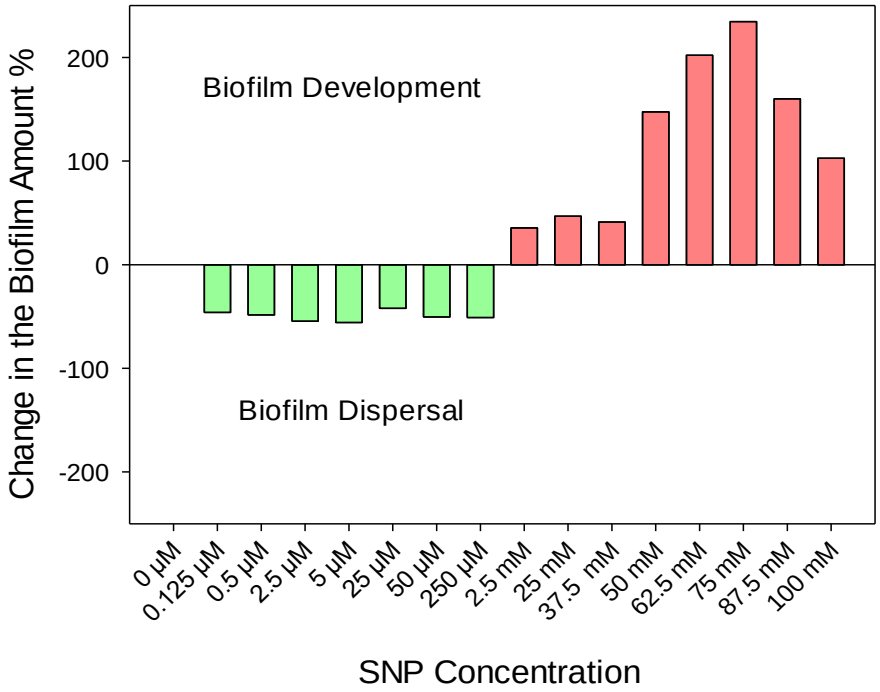

Figure 23. Comparison of the percentage changes of the biofilm amounts after the addition of different SNP concentrations in batch grown *E. coli* ATCC 25404 biofilm cultures. The percentage changes were calculated using the mean measured OD595nm values of the solubilized crystal violet solutions from the remaining biofilms and the control untreated-biofilms (Change % = ($OD595_{control\text{-}biofilm}$-$OD595_{remaining\text{-}biofilm}$) × 100 / $OD595_{control\text{-}biofilm}$)

Among these concentrations, all of which are in the micromolar range, we have chosen 0.5 μM, 5 μM, and 50 μM of SNP concentrations to disperse the biofilms and to get the biofilm-dispersed cells for further investigation. This is in part because, 0.5 μM of SNP concentration was previously suggested as the optimal low dose SNP concentration to disperse *E. coli* ATCC 25404 biofilms (Barraud et al., 2009) and *Pseudomonas aeruginosa* biofilms (Barraud et al., 2006). However, in our study, the optimum concentration of SNP to disperse the maximum amount of *E. coli* ATCC 25404 biofilm (56 % dispersal) was found to be 5 μM of added SNP concentration (Figure 23) in the batch system. In addition, 50 μM of SNP was also shown to significantly reduce the formation of marine biofilms compared with the control (Barraud et al., 2006; Barraud et al., 2009; Walker, and Keevil, 2015). On the other hand, it can be seen that biofilm formation substantially increased with the use of high SNP concentrations (millimolar ranges) as shown in Figures 22 and 23. For instance, the biofilm biomass with the usage of 2.5 mM and 75 mM SNP was 35 % and 234 % higher than the biomass of control biofilms, respectively. As was given in Materials and Methods section, when the concentrations of added SNP to the batch cultures of biofilms were in the range between 25 mM-100 mM, color changes in the cultures were observed after 24 hours of incubation. It was thought that this color change was probably arising from an increased toxic effect due to the higher doses of added SNP.

Despite the increase in biofilm biomass at high doses of SNP, dispersed cells were also observed in the wells of these groups. Thus, millimolar ranges of added SNP concentrations in the batch grown biofilm cultures both caused cell dispersion from the biofilms as well as the genesis of the biofilms on the walls of the well plates. In other words, while biofilms continued to grow at high SNP concentrations, bacterial cells also dispersed from the biofilms. Previously, Barraud and colleagues also observed a similar effect of the usage of high SNP concentrations (in millimolar ranges) in their study of dispersing *P. aeruginosa* biofilms. They used different concentrations of SNP (0.025 μm up to 100 mM of SNP) to disperse the biofilms and concluded that the use of low doses of SNP (in the micromolar range) result in biofilm dispersal, while the use of high doses of SNP (in millimolar ranges) caused an increase in the biofilm biomass. They considered that the increase in the biofilm biomass might have been related to the adaptation response of the bacterial cells to the toxic amounts of NO and other forms produced such as NO_2^- and NO_3^- (Barraud et al., 2006).

To investigate whether such biofilm-dispersed cells obtained after the addition of high doses of SNP will have different adhesion properties compared to the biofilm-dispersed cells obtained after the addition of low doses of SNP, 2.5 mM of SNP concentration was chosen as the model SNP concentration representing its toxic effect on the biofilms. This is because, more dispersed cells, less biofilm development and almost no color change in the biofilm cultures were observed after the addition of 2.5 mM SNP to batch grown biofilm cultures compared to those observed when other higher doses of SNP were used.

Consequently, a total of 4 different concentrations of added SNP were used to get the biofilm-dispersed cells from the batch cultures for further investigation (0.5 μM, 5 μM, and 50 μM of low doses of SNP and 2.5 mM of high dose of SNP).

4.2 Effect of added SNP concentration on the dispersion amounts of E. coli ATCC 25404 biofilms grown in continuous flow systems

Although researches have been focused on batch grown biofilms and biofilm-dispersed cells from the batch systems due to the simplicity and productivity of such experiments, it is also important to investigate the cells dispersed from biofilms grown in continuous systems. This is because biofilms observed in the industrial systems as well as on implants in the body generally develop under the continuous nutrient flow conditions. In order to investigate the differences between biofilm-dispersed cells from continuous and batch systems, biofilms were also formed in a continuous flow chamber, and dispersed using SNP. The dispersed cells were collected for further investigation.

As a result of the batch culture experiments, it was observed that low SNP concentrations caused the dispersion of the *E. coli* ATCC 25404 biofilm. In the continuous culture system, the effect of 0.5 μM of added SNP concentration on the dispersion of biofilms was investigated. While biofilms without SNP exposure showed normal development in this system for 48 hours. Exposure of 24-hour old biofilms to LB media with 0.5 μM SNP for 24 hours, reversed the biofilm formation and caused the dispersal of biofilm cells. The highest dispersal effect was repeatedly observed at 0.5 μM SNP on *E. coli* ATCC 25404 biofilms in the continuous flow chamber system.

A 46.8 % reduction in the biofilm surface coverage was observed with the use of SNP after dispersion (Figure 24). Also, an increase in the number of biofilm-dispersed cells in the waste bottle was observed after the addition of SNP to the continuous culture medium. This finding demonstrated that the reduction in biofilm biomass was associated with the SNP-dependent dispersal. Furthermore, biofilms and remaining biofilms were significantly viable when stained with the LIVE/DEAD BacLight bacterial viability stains as observed from the images taken by the fluorescence microscope (Figure 25). All experiments were repeatedly tested independently at different times. The untreated biofilm and remaining biofilm viability rates were found as 96 % and 80 %, respectively.

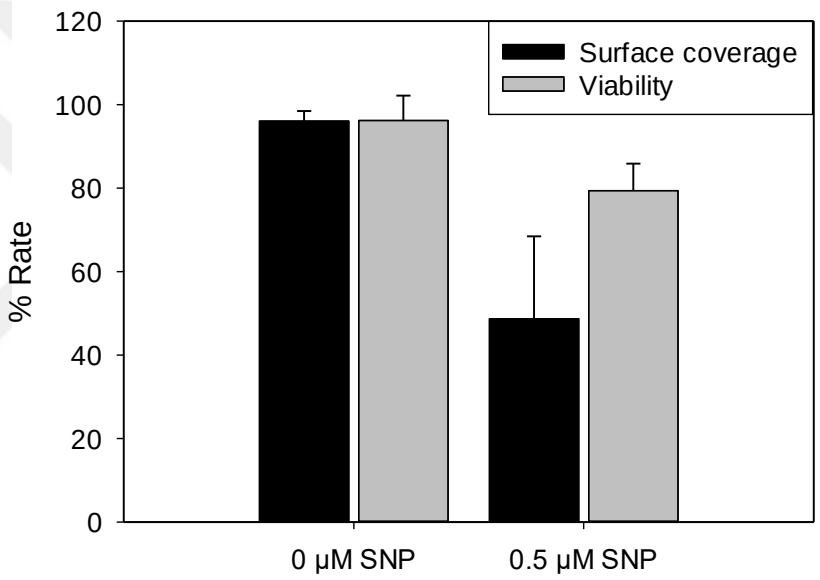

Figure 24. Surface coverage and viability rates of *E. coli* ATCC 25404 biofilms grown in continuous flow system (control, 0 µM SNP) and the remaining biofilms after the dispersal with 0.5 µM of added SNP treatment fluorescence images were quantified using ImageJ analysis to compare surface coverage and viability. Error bars represent standard error (n = 10).

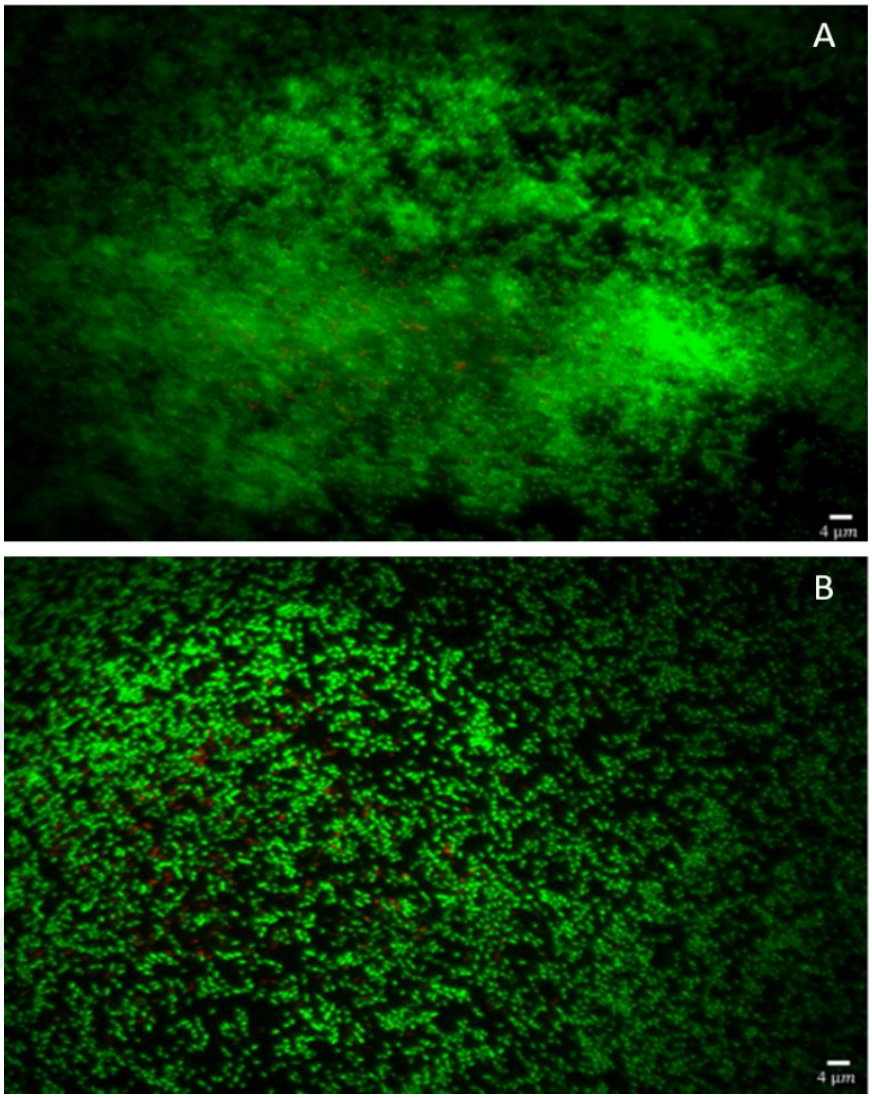

Figure 25. Fluorescence images of A) untreated biofilm (control, 0 µM SNP), and B) remaining biofilm after the dispersal with 0.5 µM of added SNP in the continuous culture system. Scale bars represents 4 µm size.

4.3 Dimensions of planktonic and biofilm-dispersed E. coli ATCC 25404 cells as a function of the SNP concentration added to cultures grown in batch and continuous systems

Bacteria can be imaged in air or in liquid. In general, AFM images of bacterial cells obtained in the air have better resolutions than those obtained in water. However, since bacterial cells form biofilms and disperse from the biofilms generally under aqueous environments, AFM imaging and force measurements on the bacterial cells investigated were performed in water. Performing AFM scanning and measurements in water will provide more realistic results than in air. Therefore, to visualize planktonic and biofilm-dispersed *E. coli* ATCC 25404 cells, DFM mode (tapping

mode) topographical image scans were performed under water. As can be seen from the images given in Figure 26, bacterial cells were intact and possessed their typical rod shape morphology when observed in water by AFM.

Using the topographic images of bacteria taken by AFM under water, dimensions of planktonic and biofilm-dispersed *E. coli* ATCC 25404 cells as a function of the SNP concentration added to cultures grown in batch and continuous systems were measured using the AFM software and compared to each other (Table 2, Figure 27). Pairwise comparison procedure indicated that there were not significant differences among the height values, as can also be seen from Figure 27 (A). However, when the width and length values were compared (Figure 27 (B and C)), significant differences were observed (Dunn's test). For example, although the widths and lengths of the dispersed cells from batch grown biofilms at 0.5 μM and 2.5 mM added SNP concentrations were similar to each other, they were statistically different ($P < 0.05$) and significantly higher than the widths and lengths of other cells investigated. Following the cells dispersed at the concentrations of 2.5 mM and 0.5 μM added SNP in the batch system, as can be seen from the respective box plots, the highest dimension increase was observed for cells dispersed in the continuous systems at 0.5 μM added SNP concentration (Table 2 and Figure 27 (B and C)).

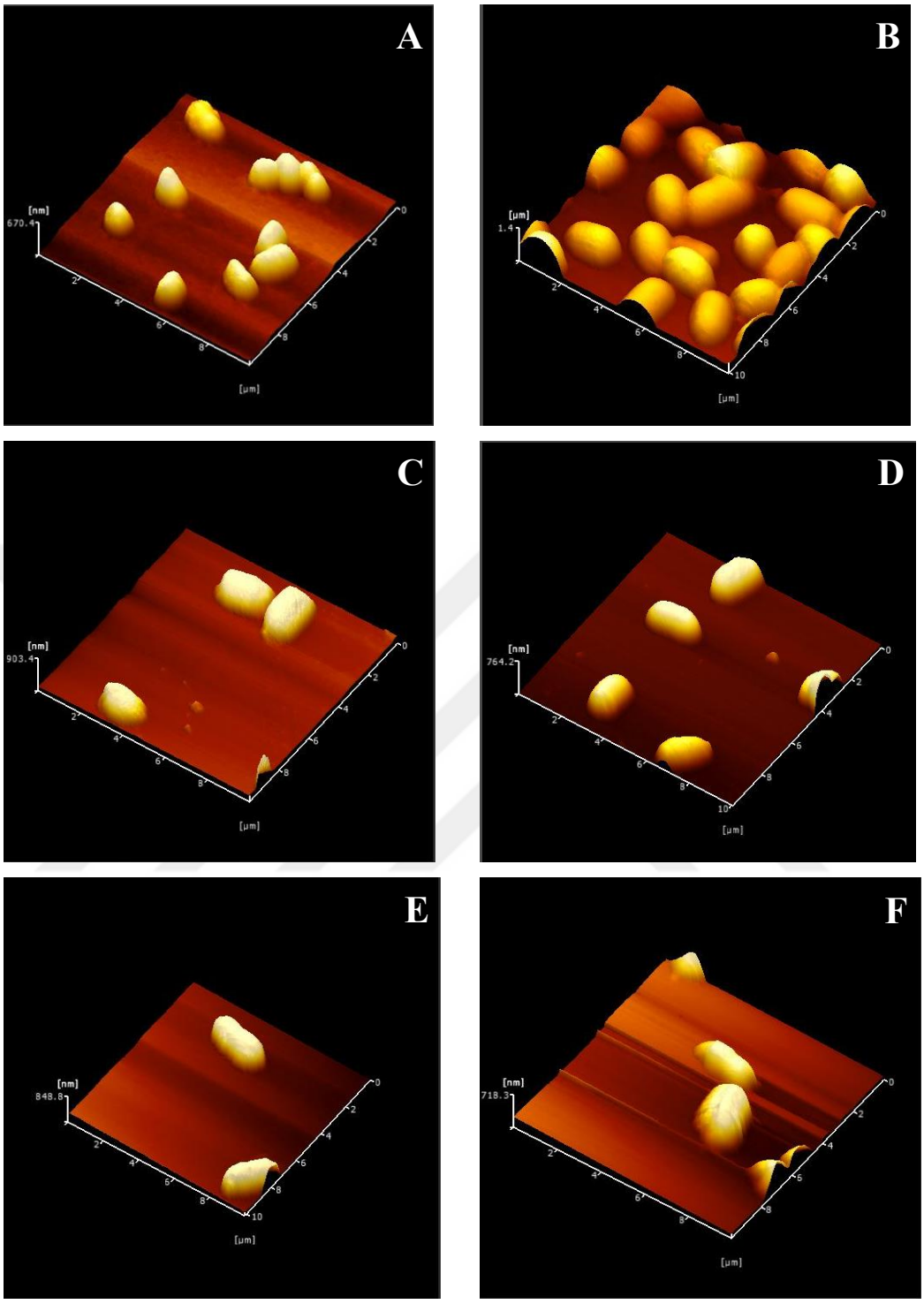

Figure 26. AFM topographical images of *E. coli* ATCC 25404 cells under water. The images are 10 × 10 µm in size. (A) 3D image of planktonic cells. (B), (C), (D) and (E) are the 3D images of biofilm-dispersed cells from batch cultures with the addition of 0.5 µM, 5 µM, 50 µM, and 2.5 mM SNP, respectively. (F) is the 3D image of biofilm-dispersed cells from the continuous culture with the addition of 0.5 µM SNP.

The width and length values of the biofilm-dispersed cells at 0.5 μM added SNP concentration both in batch and continuous systems were also statistically and significantly different from each other ($P < 0.05$). With the addition of 0.5 μM SNP in both batch and continuous systems, resulted in the dispersion of cells which were 76% and 38% wider, and 108% and 37% longer than the planktonic cells, respectively. However, cells dispersed from batch grown biofilms at 5 μM and 50 μM added SNP concentrations showed less increase in their widths and lengths compared to those observed for the cells dispersed at 0.5 μM and 2.5 mM added SNP. It was also understood from the similar box plot ranges that the widths and lengths of planktonic cells and biofilm-dispersed cells at 5 μM added SNP concentration in the batch system were not significantly different from each other, as was also observed for their heights. Whereas, there were statistically significant differences in the length and width values between planktonic cells and dispersed cells at 50 μM added SNP concentration.

Overall, it can be said that addition of SNP to the biofilm cultures resulted in the release of cells from the biofilms with increased cell dimensions (on average) compared to the dimensions of planktonic cells. The most profound effect was observed for the cells dispersed from batch grown biofilms at 2.5 mM toxic SNP concentration followed by the cells dispersed at 0.5 μM added SNP concentration.

Table 2. Average dimensions of 18 bacterial cells measured by AFM in water for each group investigated.

	Height (μm)	*Width (μm)*	*Length (μm)*
Planktonic (0 μM)	0.85 ± 0.08	1.10 ± 0.11	1.82 ± 0.27
0.5 μM (batch)	0.77 ± 0.22	1.94 ± 0.53	3.80 ± 0.95
5 μM (batch)	0.71 ± 0.26	1.17 ± 0.09	2.02 ± 0.23
50 μM (batch)	0.94 ± 0.23	1.32 ± 0.20	2.4 ± 0.37
2.5 mM (batch)	0.93 ± 0.28	2.16 ± 0.58	3.87 ± 1.18
0.5 μM (continuous)	0.75 ± 0.12	1.52 ± 0.29	2.49 ± 0.43

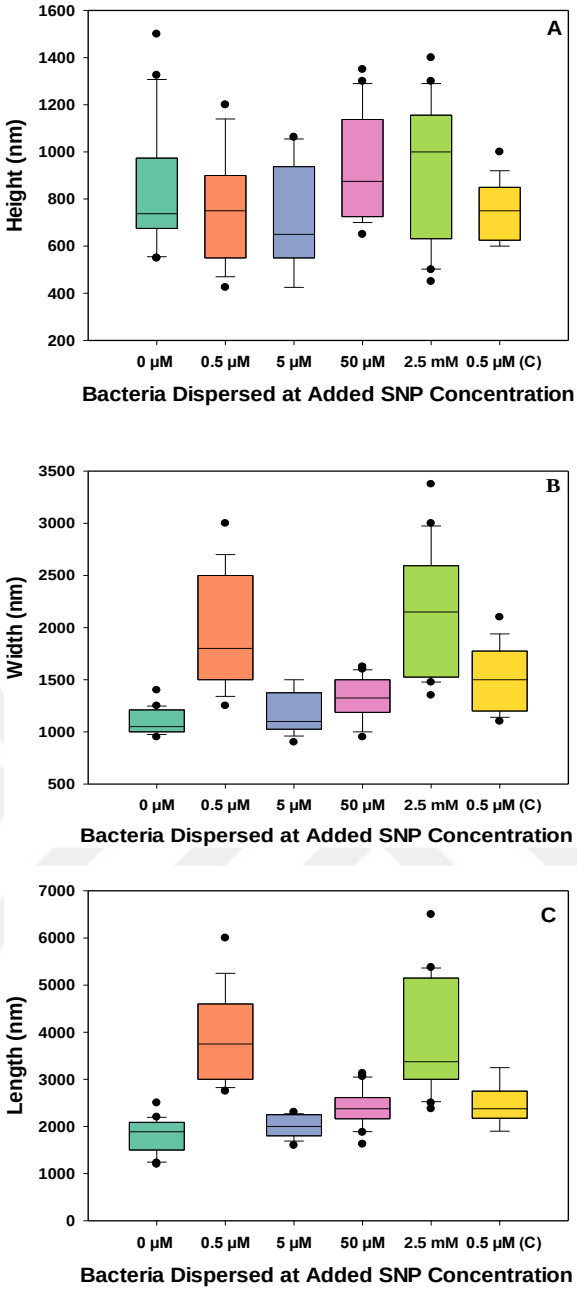

Figure 27. Box plots of (A) height, (B) width, and (C) length of planktonic and biofilm-dispersed *E. coli* ATCC 25404 cells at different added SNP concentrations. Black points indicate 5th/95th percentile outliers. 0 µM added SNP concentration refers to the planktonic cells (control), and 0.5 µM, 5 µM, 50 µM and 2.5 mM added SNP concentrations refer to biofilm-dispersed cells from batch cultures at respective added SNP concentrations. 0.5 µM (C) refers to biofilm-dispersed cells from the continuous culture.

It is known that the FtsZ protein is involved in the mechanism responsible for coordinating bacterial cell size with the growth rate. During cell division, the cell size first increases, and then the cell divides into two daughter cells along with the FtsZ protein aggregating in the division site. It was also shown that the inhibition of the assembly of FtsZ proteins in the division region in the bacterial cell causes an increase in the cell size (Weart et al., 2007). Kim and Harshey (2016) demonstrated that the diguanylate cyclase (DGC) YfiN protein in *E. coli* is associated with c-di GMP and acts as a division inhibitor by interacting with cell division proteins. The YfiN protein stops the division process by settling in the localization area of division proteins after the cell expands to divide. A bacterial cell whose division is inhibited will continue to live in a larger cellular size. In addition, they also stated that high intracellular c-di GMP levels are required for this protein to interact with the cell division protein FtsZ (Kim, and Harshey, 2016). Since, NO regulates the biomass of biofilms by triggering the c-di GMP pathways and causes the dispersion of the biofilms, this may explain the observed differences in the dimensions of biofilm-dispersed cells, especially those of cells dispersed at 0.5 μM and 2.5 mM added SNP (NO donor) concentrations from batch cultures, compared to the dimensions of planktonic cells.

The size of a bacterial cell also affects its attachment to surfaces. Bacteria are known to aim for strong adhesion to the surface by changing their shape. In other words, the bacterial cell gets more contact points with the increased surface area. Increasing the number of contact points is one of the best ways to get a firm attachment with the surface (Young, 2006). As will be shown in the following pages, the increased cell sizes, especially observed for the biofilm-dispersed cells at 0.5 μM and 2.5 mM added SNP (NO donor) concentrations from batch cultures correlated with the increased adhesion and increased intracellular c-di GMP levels.

4.4 Distributions of adhesion forces, energies and pull-off distances of the surface biopolymers of planktonic and biofilm-dispersed E. coli ATCC 25404 cells as a function of the SNP concentration added to cultures grown in batch and continuous systems

Force measurements were performed on the intact bacterial cells (Figure 26) using AFM in water. The distributions of adhesion forces and energies measured between the surface biopolymers of planktonic and biofilm-dispersed *E. coli* ATCC

25404 cells and silicon nitride AFM tips under water can be seen in the probability histograms as shown in Figures 28 and 29, respectively. The probability histograms of adhesion forces and energies can be used as well to compare the heterogeneities of the surface biopolymers present on the bacterial cells. More heterogeneous AFM data will be obtained when the bacterial surface is covered with a higher density and/or diversity of adhesive biopolymers. Since the value of each adhesion force or energy measured by AFM represents an adhesion event between the AFM tip and a biopolymer and/or a group of molecules on the bacterial surface, the chances of the AFM tip encountering an adhesive group will be high if the density and diversity of adhesive biopolymers on the bacterial surface are high.

Statistical comparisons indicated that adhesion force values measured for the planktonic cells, biofilm-dispersed cells at 5 μM added SNP concentration in batch system, and biofilm-dispersed cells at 0.5 μM added SNP concentration in continuous system were not significantly different from each other, as can also be seen from the similar distributions of their adhesion forces (Figure 28 (A, C and F)). However, adhesion forces measured for the other conditions investigated were statistically and significantly different from each other ($P < 0.05$). When compared, the highest heterogeneity and/or the widest distribution of the adhesion forces was observed for the biofilm-dispersed cells when 2.5 mM toxic SNP concentration was added to the biofilm culture grown in the batch system, followed by those observed for the biofilm-dispersed cells when 0.5 μM and 50 μM SNP was added to the cultures in the batch system (Figure 28 (B, D and E)), which can also be seen from the highest ranges of the adhesion forces (5.91 nN, 4.48 nN and 4.12 nN) identified for cells dispersed at 2.5 mM, 0.5 μM, and 50 μM added SNP concentrations, respectively.

When the calculated adhesion energies given in Figure 29 were statistically compared, it was found that adhesion energies of planktonic cells and biofilm-dispersed cells at 5 μM added SNP concentration in the batch system were not significantly different from each other, as was observed for their measured adhesion forces. However, the adhesion energies calculated for the biofilm-dispersed cells at 0.5 μM added SNP concentration in the continuous system were significantly different from those obtained for the other groups investigated, as can also be seen from their energy distributions (Figure 29 (F)). Although the adhesion forces obtained for the

biofilm-dispersed cells in the batch system at 0.5 μM and 2.5 mM added SNP concentrations were statistically different from each other, the adhesion energies calculated for those cell groups were not different. The highest heterogeneity and/or the widest distribution of the adhesion energies were observed for the biofilm-dispersed cells in batch systems at 0.5 μM and 2.5 mM added SNP concentrations, followed by those observed for the cells dispersed at 50 μM added SNP concentration in the batch system (Figure 29 (B, D and E)), as can be seen from the highest ranges of their respective adhesion energies (Table 3).

Since the heterogeneity in the adhesion data is related to the density and/or diversity of the biopolymers present on the bacterial surface, our results can also be interpreted as follows; the amounts and/or the compositions of the surface biopolymers of bacterial cells dispersed from the biofilms were dependent on the concentration of the SNP added in the biofilm cultures. This observation was more significant for the cells dispersed from the biofilms in the batch system at 0.5 μM, 50 μM, and 2.5 mM added SNP concentrations, compared to cells dispersed in continuous system at 0.5 μM added SNP concentration. Both adhesion force and energy data of biofilm-dispersed cells at 5 μM added SNP concentration in the batch system were similar to those data obtained for the control group, the planktonic *E. coli* ATCC 25404 cells (Figures 28 and 29 (A and C)).

As was mentioned previously, more heterogeneous AFM data corresponds to a higher density and/or diversity of adhesive biopolymers present on the bacterial surface. Thus, it can be said that, bacterial cells dispersed at 0.5 μM and 2.5 mM added SNP concentrations in the batch systems were possessing higher amounts and/or more different types of adhesive biopolymers on their surfaces compared to other cell groups investigated.

As can be seen in the probability histograms of Figure 30, the distributions of pull-off distances were also measured between the surface biopolymers of planktonic and biofilm-dispersed *E. coli* ATCC 25404 cells and silicon nitride AFM tips in water. Although the actual lengths of the surface biopolymers of bacterial cells might be longer or shorter, the pull-off distance values could be indicators of the lengths of the surface biopolymers of the bacterial cells (Abu-Lail, and Camesano, 2003). A range

of pull-off distances was observed starting at an average of 0.456 μm went up to 1.110 μm (Table 3). Our data show that each bacteria and AFM tip interaction under water were heterogeneous as well for the pull-off distances. As we mentioned earlier, heterogeneous pull-off distance AFM data might indicate that various lengths of adhesive biopolymers coexist on the bacterial surfaces. However, it should be noted that the pull-off distance is actually the separation distance at which the attached biopolymer to the AFM tip separated from it during retraction.

As a result of statistical comparisons, pull-off distance data measured for the planktonic cells, biofilm-dispersed cells at 50 μM added SNP concentration in the batch system were not significantly different from each other (Figure 30 (A and D)). As given in Table 3, the mean and median of pull-off distance values of these two groups were also very close to each other (mean values 0.620 μm, 0.629 μm and median values 0.592 μm, 0.573 μm, respectively). Similarly, pull-off distance values for the biofilm-dispersed cells in the batch system at 5 μM and 2.5 mM added SNP concentrations were also not statistically different from each other (Table 3, Figure 30 (C and E)). However, the pull-off distances of other experimental groups investigated were statistically and significantly different from each other ($P < 0.001$). Since the measured pull-off distance data gives information about the length of the bacterial surface biopolymers, the heterogeneity of our data can represent that planktonic and biofilm-dispersed *E. coli* ATCC 25404 cells have biopolymers of various lengths on their surfaces. According to our pull-off distance AFM data, it is understood that there are differences in the biopolymer lengths of bacteria due to varying SNP concentrations. This difference was most significant for cells dispersed from biofilms both in batch and continuous systems with the addition of 0.5 μM SNP.

To describe the heterogeneity in the distributions of adhesion and pull-off distance data, lognormal function was used. By fitting the lognormal function to the probability histograms of all data seen in Figures 28, 29 and 30, most probable values of adhesion forces, energies and pull-off distances were obtained. The most probable adhesion affinities and pull-off distances (x_0) and the coefficient of correlation values (r^2) are all given in Table 3 and compared in the following section.

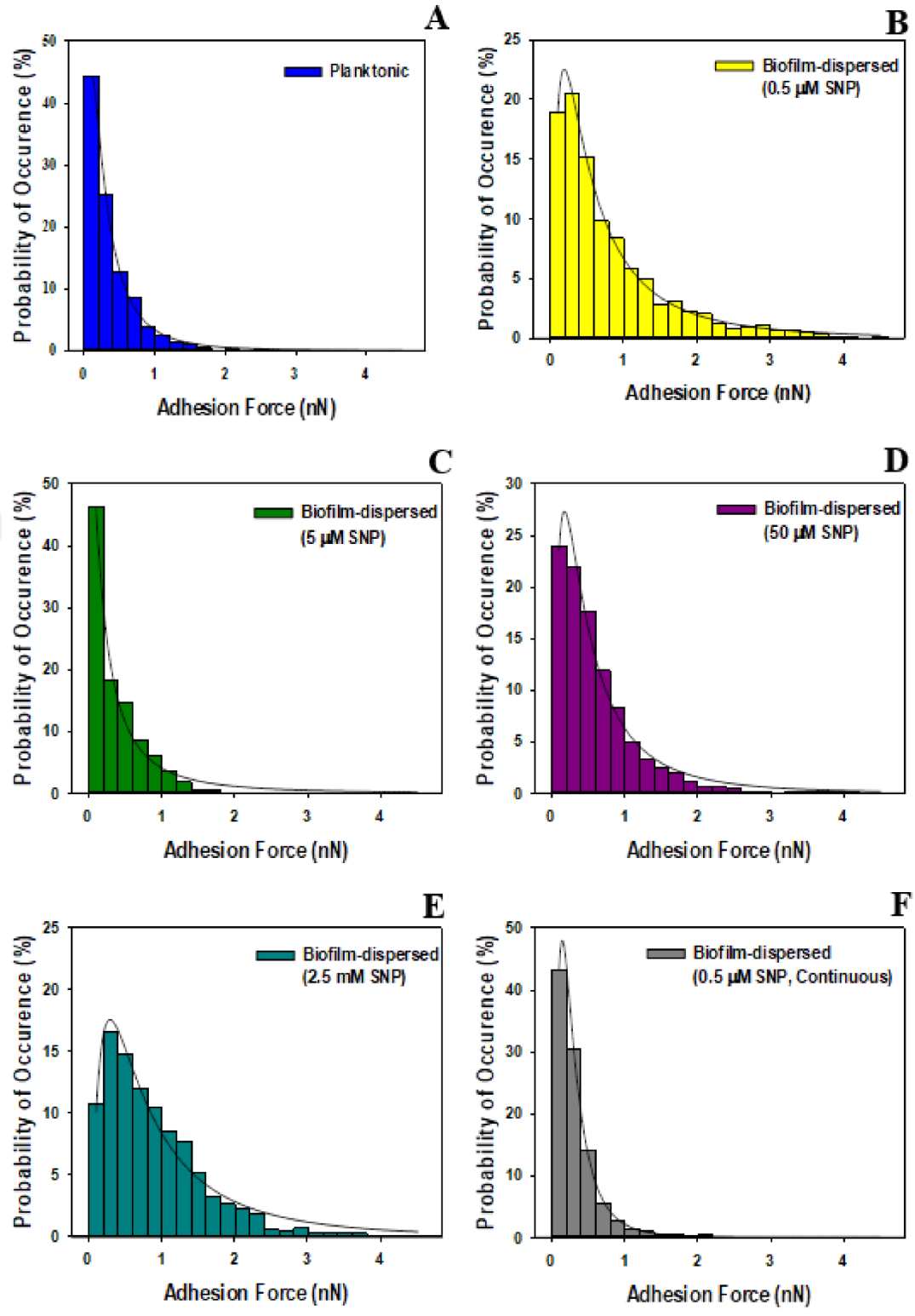

Figure 28. Histograms showing the distribution of adhesion forces (nN) of *E. coli* ATCC 25404 cells. Straight lines in histograms indicate that the lognormal probability distribution function fits the adhesion force values. Fitting qualities (r^2) are given in Table 3.

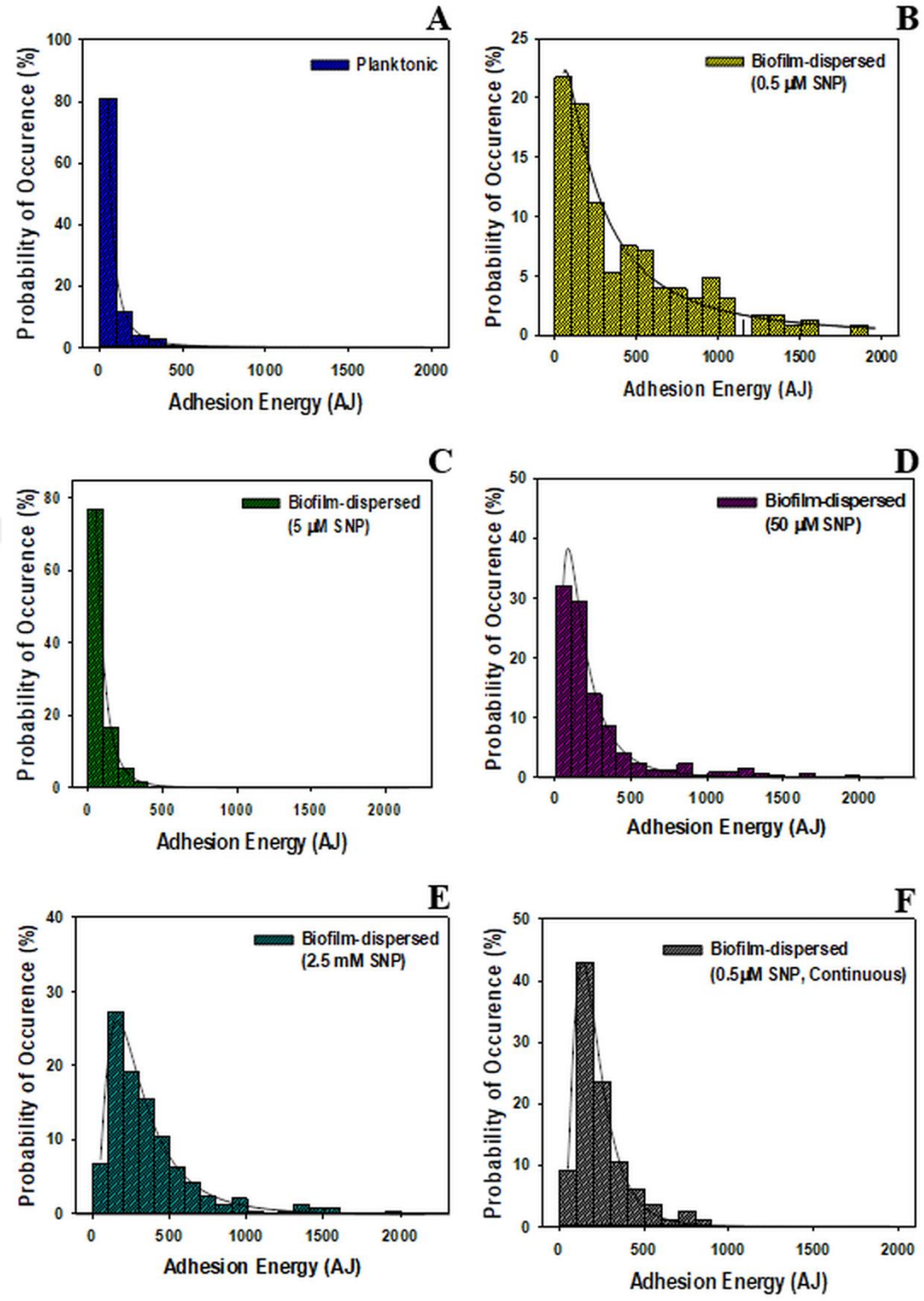

Figure 29. Histograms showing the distribution of adhesion energies (AJ) of *E. coli* ATCC 25404 cells. Straight lines in histograms indicate that the lognormal probability distribution function fits the adhesion energy values. Fitting qualities (r^2) are given in Table 3.

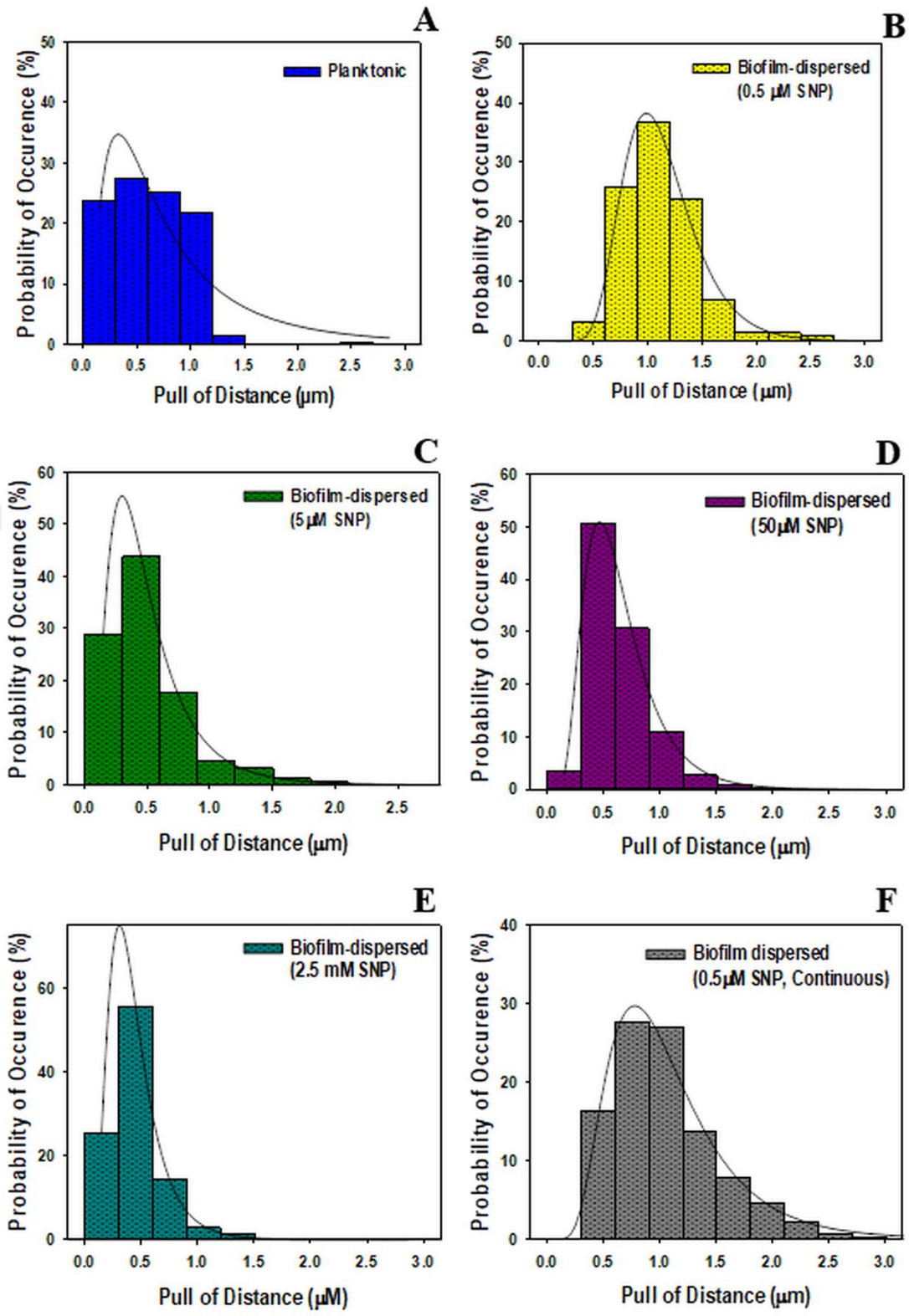

Figure 30. Histograms showing the distribution of pull-off distances (µm) of *E. coli* ATCC 25404 cells. Straight lines in histograms indicate that the lognormal probability distribution function fits the pull-off distance values. Fitting qualities (r^2) are given in Table 3.

Table 3. A summary of the most probable values (xo) quantified by fitting lognormal dynamic peak function to the adhesion force, adhesion energy and pull-off distance (PD) data collected between *E. coli* ATCC 25404 cells (planktonic and biofilm-dispersed) and silicon nitride under water. Lognormal fitting quality (r^2) values, and the mean, median, range, and standard error of the mean (SEM) of all the data shown in the probability histograms (Figures 28, 29 and 30) are given below.

	Planktonic cells	Biofilm-dispersed cells with the addition of SNP				
		Batch System				Continuous System
Added SNP concentration	0 μM	0.5 μM	5 μM	50 μM	2.5 mM	0.5 μM (C)
xo (nN)	0.279	0.590	0.287	0.492	0.812	0.263
r^2	0.998	0.996	0.988	0.991	0.978	0.987
Mean (nN)	0.347	0.799	0.358	0.594	0.917	0.327
SEM (nN)	0.008	0.019	0.011	0.011	0.017	0.008
Median (nN)	0.233	0.526	0.220	0.436	0.720	0.226
Range (nN)	2.475	4.479	1.637	4.120	5.909	3.034
# of adh peaks	1702	1615	856	2760	1974	1300
xo (AJ)	41.43	331.83	64.64	158.92	272.14	188.48
r^2	0.999	0.951	0.999	0.995	0.989	0.996
Mean (AJ)	65.28	443.62	60.19	253.70	384.31	245.22
SEM (AJ)	5.805	28.27	4.93	16.18	22.94	11.53
Median (AJ)	31.15	263.71	22.79	160.87	290.83	195.03
Range (AJ)	626.9	2062.0	395.6	1880.6	2455.7	878.7
# of adh energies	225	225	225	350	240	200
xo (μm)	0.638	1.075	0.428	0.578	0.392	0.969
r^2	0.851	0.991	0.998	0.999	0.999	0.999
Mean (μm)	0.620	1.110	0.496	0.629	0.456	1.042
SEM (μm)	0.008	0.009	0.011	0.005	0.005	0.013
Median (μm)	0.592	1.064	0.433	0.573	0.408	0.956
Range (μm)	2.646	2.258	1.924	2.258	1.832	3.149
# of PD peaks	1702	1615	856	2760	1974	1300
# of cells	25	25	25	35	25	20

4.5 Strengths of adhesion forces and energies measured between silicon nitride AFM tips and planktonic and biofilm-dispersed E. coli ATCC 25404 cells in water as a function of the SNP concentration added to cultures grown in batch and continuous systems

As can be seen from Table 3, the strengths of adhesion were described by using mean, median and the most probable values of adhesion forces and energies quantified between AFM tips and planktonic and biofilm-dispersed cells as a function of added SNP concentration for batch and continuous grown cultures.

Similar to the highest heterogeneities of adhesion forces and energies observed for the biofilm-dispersed cells in the batch systems at 2.5 mM and 0.5 μM added SNP concentrations, respectively, their most probable adhesion force and energy values (0.812 nN and 272.14, and 0.590 nN and 331.83 AJ, respectively) were also much higher than those observed for other experimental groups (Table 3). In the light of these results, it can be said that more heterogeneous data resulted in the higher most probable adhesion forces and energies. Following the most probable adhesion forces observed for the dispersed cells at 2.5 mM and 0.5 μM added SNP concentrations in the batch systems, the highest most probable adhesion force was observed for cells dispersed at 50 μM added SNP concentration in the batch system. However, the most probable adhesion energy was found as the 3rd highest value for the cells dispersed at the SNP concentration of 0.5 μM in the continuous system (Figure 31 (A and B)). In addition, it was observed that the biofilm-dispersed cells in the batch system at 5 μM added SNP concentration and planktonic cells had the lowest most probable adhesion energy values (Table 3 and Figure 31 (B)).

The mean and median values of the adhesion data are also presented in Table 3. The mean adhesion force and energy values were on average 19% and 31% higher than the most probable values (x_0), respectively. The mean values obtained for the adhesion force and energy were on average 31% and 40% higher than the median adhesion force and energy values obtained for the same data for all conditions investigated, respectively (Table 3 and Figures 31 (A and B)). As can be seen from the trends of mean, median, as well as most probable of adhesion values as functions of the SNP concentration added to cultures grown in batch and continuous systems in Figures 31 A and B, a transition in the adhesion affinity was observed for biofilm-

dispersed cells in the batch system at 0.5 µM and 2.5 mM added SNP concentrations in comparison to other conditions. According to the mean, median and most probable values, adhesion force and energy data of biofilm-dispersed cells at 5 µM added SNP concentration in the batch system were similar to those data obtained for the planktonic cells.

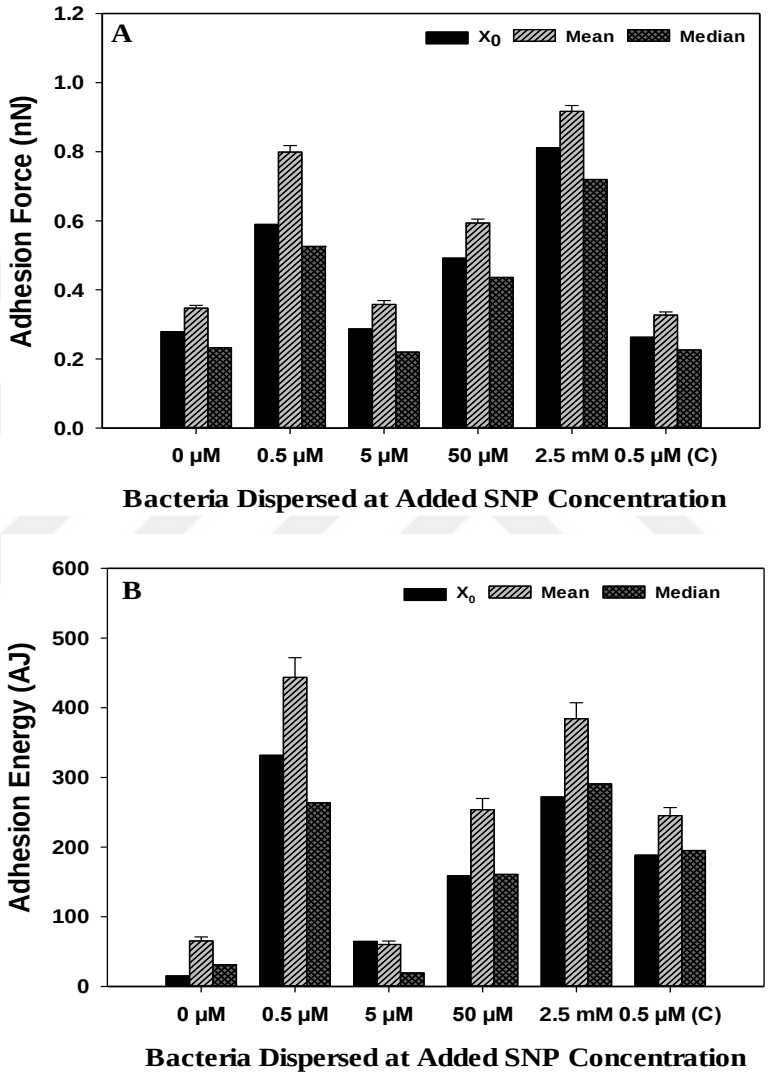

Figure 31. Comparison of the most probable, mean, and median values of adhesion forces (A) and energies (B) quantified for planktonic and biofilm-dispersed *E. coli* ATCC 25404 cells at different added SNP concentrations. 0 µM SNP concentration refers to the planktonic cells (control), and 0.5 µM, 5 µM, 50 µM and 2.5 mM SNP concentrations refer to biofilm-dispersed cells from batch cultures at respective added SNP concentrations. 0.5 µM (C) refers to biofilm-dispersed cells from the continuous culture. Error bars represent the standard error of the mean values.

Recent studies have shown that dispersed cells from biofilms have a distinct stage different from those planktonic and biofilm stages. Contrary to in-depth studies on the genetic structures of the biofilm-dispersed cells, literature is lacking the information regarding to their molecular adhesion properties and morphologies. In this study, we investigated the differences in the nanoscale adhesion forces and energies between planktonic and biofilm-dispersed cells with respect to different added SNP concentrations, or in other words, different intracellular c-di GMP contents by the use of added SNP. Our findings showed that adhesion strengths of planktonic and biofilm-dispersed *E. coli* ATCC 25404 cells in water as a function of the SNP concentration added to cultures grown in batch and continuous systems were not similar to each other. The observed differences appear to be highly consistent with the recent findings presented in the literature.

Previous studies indicated that the colonization and biofilm formation abilities of the cells dispersed naturally from biofilms were higher than those of planktonic existences at the macroscale. For example, Berlanga et al. (2017) compared the biofilm formation abilities of the dispersed cells with their planktonic counterparts and emphasized that the adhesivity and hydrophobicity of the biofilm-dispersed cells were higher than those of planktonic cells. They argued that the variations in the biofilm formation abilities of dispersed and planktonic cells could be associated with the variations in their cell surface heterogeneities and physicochemical surface properties (Berlanga et al., 2017). Similarly, the heterogeneity of our molecular level adhesion force and energy data was probably related to the changes and variations in the surface biopolymers of the bacteria. Higher heterogeneity observed in the adhesion data resulted in the higher adhesion strength in our study. Other studies showed that biofilm-dispersed *Klebsiella pneumoniae* cells had a strong ability to adhere and colonize onto both biotic and abiotic surfaces as confirmed by the confocal microscopy images of the cells. The higher colonization ability of biofilm-dispersed cells was related to the higher expressions of several genes involved in the colonization and biofilm formation compared to planktonic counterparts (Guilhen et al., 2016; Guilhen et al., 2019).

In this study, cells dispersed from the biofilms were obtained by targeting the intracellular c-di GMP molecules. Besides its control of biofilm dispersal, c-di GMP also acts as a regulator in bacterial adhesion by stimulating the biosynthesis of bacterial surface adhesins, lipopolysaccharides (LPSs) and exopolysaccharide matrix materials. The varying amount of intracellular c-di GMP during the biofilm dispersion process might have caused changes in the density, variety, and conformation of bacterial surface adhesins all of which affect the molecular level bacterial adhesion.

Increasing c-di GMP level enables LapA, a surface adhesin, to be localized on the cell surface, and thus the cell forms irreversible connections to the surface. Otherwise, LapA is released from the cell surface and the cell becomes a swimmer (Newell et al., 2011). In another study, it was observed that CsgD gene associated with c-di GMP in *E. coli* regulates the expression of curli fibers (Serra et al., 2013). The relationship between c-di GMP and exopolysaccharide production is very important for the bacteria to attach to the surface. Poly-β-1,6-N-acetylglucosamine (PGA), an exopolysaccharide, plays a role in the surface adhesion of *E. coli*. Varying levels of c-di GMP also regulate the amount and efficiency of PGA in the cell. The findings of all these studies suggest that there were differences in adhesion strengths of planktonic and biofilm-dispersed cells due to the changes in the diversity and/or amount of surface adhesins which were probably associated with the differences in c-di GMP levels of the cells after the biofilm dispersion.

According to our adhesion force and energy data, bacteria dispersed at 0.5 μM and 2.5 mM added SNP concentrations in the batch system were highly sticky cells. Their strong adhesion abilities could be related to the presence of higher amounts and/or diversities of surface adhesins or higher amounts of LPSs compared to other cell groups investigated.

Environmental conditions as temperature and nutrient availability as well as the shear stress due to continuous flow of the media can affect the adhesion or adaptation to the environmental conditions. The adhesion strength of dispersed cells collected from both continuous and batch systems was measured to compare the adhesion capacity of cells dispersed from the biofilm with the SNP in the presence and absence of nutrient flow. Although the cells dispersed from biofilms in both batch and

continuous systems with the addition of 0.5 μM SNP showed higher adhesion strengths than the planktonic cells, the adhesion capacity of 0.5 μM SNP-dispersed cells in the batch system was higher than that observed for the continuous system counterparts. The differences observed between the dispersed cells from batch and continuous cultures at 0.5 μM added SNP concentration could be arising in part from the different environmental conditions of batch and continuous systems.

Batch and continuous systems have different nutrient levels. Since continuous systems have a continuous flow of the growth media, those systems are rich in nutrient availability. The nutrient availability can elevate or disrupt the adhesion tendency of the bacterial cells to the surfaces (Petrova, and Sauer, 2012). In other words, the different amount of nutrients in the batch and continuous systems could be the reason of the observed differences in the adhesion strengths of the cells dispersed from the batch and continuous grown biofilms. It was observed that when the planktonic bacterial cells can not escape from the environment, they would tend to form biofilms under continuous environmental stresses such as starvation (also it was observed that cells tend to disperse from biofilms under starvation to find new environments with available nutrients). Since those cells would probably possess high levels of c-di GMP just before forming biofilms, it was expected that dispersed cells from batch cultures (in general) would show increased levels of c-di GMP compared to the cells dispersed from continuous cultures.

Chemotaxis is a fundamental strategy that bacteria use to find food, create biofilms, or escape harsh environmental conditions. It was mentioned in the literature that bacterial chemotactic ability could be diminished by shear-induced trapping and therefore the bacterium might not follow chemical signals. A study showed that the chemotactic response of *B. subtilis* to oxygen was suppressed in the presence of flow (Rusconi et al., 2014). Chemotactic ability is thought to be related to changes in c-di GMP levels of bacterial cells (Russell et al., 2013). In the light of all the given information, it is possible that there were differences in the c-di GMP levels and adhesion capacities of the bacterial cells dispersed from continuous cultures compared to those dispersed from batch cultures, despite the use of the same dispersal agent concentration, considering the flow and nutrient availability in the continuous system.

4.6 Relationship between pull-off distances and adhesion forces and energies obtained for planktonic and biofilm-dispersed cells as a function of the SNP concentration added to cultures grown in batch and continuous systems

As mentioned in section 4.4, the values of the pull-off distances can be used to get information about the length of the surface biopolymers of bacterial cells. The mean, median and most probable values of pull-off distances quantified between planktonic and biofilm-dispersed cells as a function of added SNP concentration for batch and continuous biofilm systems were used for further description of differences in the bacterial surface biopolymer lengths (Table 3).

The trends of the mean, median and the most probable values of pull-off distances were very similar for each condition. The difference between mean and both the median and most likely values were on average 8%. In addition, the difference between the median and the most probable values was only 2% on average. When pull-off distance data of planktonic and biofilm-dispersed cells as a function of added SNP concentration for batch and continuous biofilm systems were compared, the mean, median, and most probable value of pull-off distance data for biofilm-dispersed cells in both systems at 0.5 μM added SNP concentration was close to each other, as seen in Table 3. Therefore, regardless of the biofilm culture system, it can be considered that bacteria dispersed at a concentration of 0.5 μM added SNP concentration possessed longer adhesive biopolymers on their surfaces than those observed for planktonic and biofilm-dispersed cells in the batch system at 5 μM, 50 μM and 2.5 mM added SNP concentrations. Although the adhesion forces and energies obtained for the biofilm-dispersed cells in the batch system at 2.5 mM added toxic SNP concentration showed one of the highest values in comparisons, the pull-off distances calculated for this cell group was lower (most probable value 0.392 μm, mean 0.456 μm, median 0.408 μm) than other experimental groups. As we mentioned earlier, the lowest pull-off distance values (in terms of most probable, mean and median) of 2.5 mM SNP concentration could be related to the toxic effect of SNP on *E. coli* ATCC 25404 cells, and could be resulted in collapsed biopolymers (not extended) with a high grafting density on the bacterial surface.

Surface biopolymers are effective in attaching bacteria to both abiotic and biotic surfaces. The grafting density, length, and diversity of these biopolymers vary

due to genetic deviations of the bacteria and environmental factors. Changes in the properties and diversity of these biopolymers cause differences in their adhesive strength (Moradali, and Rehm, 2020; Rehm, 2010). In previous studies, bacterial adhesion was described as a function of the lengths and grafting densities of surface biopolymers. It was shown that increased biopolymer lengths enabled bacteria to adhere more tightly to surfaces (Gordesli, and Abu-Lail, 2012b; Uzoechi, and Abu-Lail, 2019). It was also observed that the adhesion strengths measured in AFM increased in consistent with the lengths of the bacterial pili (Dorobantu et al., 2008). Both long extended biopolymers and high grafting density of the biopolymers on the bacterial surface were previously shown to be correlating with high bacterial adhesion. Since the adhesion affinity of cells dispersed at 2.5 mM of SNP concentration was high and the biopolymers on the cell surfaces were short, probably their grafting densities were high on the bacterial surface. Further analyses related to the AFM approach curves using models such as steric model (which predicts the length and grafting density of polymers) could explain the observed differences in the pull-off distances.

Overall, it can be said from our results that the changes in the intracellular c-di GMP levels of bacteria (induced by the addition of SNP at different concentrations) had an effect on the conformation and production of cellular extensions by stimulating different transcriptional mechanisms, as was shown previously (Jenal et al., 2017). The length of Type IV pili, which is an important surface structure modulated by c-di GMP in *E. coli* (Vogeleer et al., 2014) was shown to be dependent on the level of c-di GMP. A decrease in the length of the type IV pili was observed at low levels of intracellular c-di GMP (Floyd et al., 2020). With this information and the presented variations in the pull-off distances, it can be said that by targeting c-di GMP pathways with different SNP concentrations, cells dispersed from biofilm might have differences in the lengths of their surface biopolymers.

4.7 Determination of NO donor SNP-mediated intracellular c-di GMP levels of planktonic and biofilm-dispersed E. coli ATCC 25404 cells grown in batch and continuous systems

Changes occur in c-di GMP levels throughout the life-cycle of bacteria. These changes, which affect functions such as mobility, virulence and dispersal, also show

their effect on planktonic existence and biofilm cells. It is known that c-di GMP has important effects on bacterial adhesion and synthesis of cellular surface biopolymers and EPS (Romling et al., 2013). Therefore, it can be said that this molecule will have important functions to combat biofilms, especially considering its impact on the dispersion of biofilms, which is a huge burden on health and industry. Knowing the c-di GMP levels is a piece of decisive information to understand the physiological changes of bacteria in some periods, such as before forming biofilms, during biofilm lifestyle and after biofilm dispersion.

To evaluate the role of c-di GMP in NO-regulated biofilm dispersion and bacterial adhesion, cell extracts of planktonic and biofilm dispersed cells were analyzed by HPLC, as described in Chapter 3. For accurate determination of c-di GMP in cell extracts, standards containing different concentrations of authentic c-di GMP were analyzed and c-di GMP peaks were observed at a retention time of around 17.2 minutes, as seen in Figure 17. Hence this retention time was used to define c-di GMP for further HPLC analysis of cell extracts. The amounts of c-di GMP determined in all samples were normalized to their total protein content.

As seen in Figure 32, it was observed that the extracts of all analyzed groups contained different intracellular c-di GMP amounts. 8.4 pmol c-di GMP/mg protein was detected in planktonic *E. coli* ATCC 25404 cell extracts (in the late exponential phase). In the batch biofilm system, it was observed that extracts of biofilm-dispersed cells at 0.5 μM concentration of SNP contained 19.6 pmol c-di GMP/mg protein which was 2.3 times higher than that observed for planktonic cells. An excessive expression of c-di GMP was detected for the biofilm-dispersed cells when 2.5 mM toxic SNP concentration was added to the biofilm culture grown in the batch system. This overexpression with 2.5 mM SNP concentration corresponded to approximately 8-fold the intracellular level of c-di GMP of planktonic cells. The addition of 5 μM and 50 μM SNP concentrations to the batch biofilm culture resulted in a 1.5 and 2.9-fold increase in the c-di GMP level for dispersed cells compared to planktonic cells (Figure 32). In addition, it was observed that the c-di GMP levels of biofilm-dispersed cells when 0.5 μm SNP concentration was added to the biofilm grown in the continuous system were similar to the planktonic counterparts.

It is generally accepted that an increase in the intracellular c-di GMP level encourages bacteria to remain in the biofilm mode, while a decrease in the c-di GMP level causes the biofilm dispersal. According to the previous studies performed using SNP, *P. aeruginosa* cells dispersed from biofilms contained lower amounts of c-di GMP compared to the planktonic cells (Barraud et al., 2009; Chua et al., 2014). However, in another study, actively dispersed *P. aeruginosa* cells from continuous system biofilms using SNP were reported to have slightly higher concentrations of c-di GMP than planktonic cells (Wille et al., 2020). In the study, it was also reported that the passively dispersed *P. aeruginosa* biofilm cells had significantly lower intracellular c-di GMP. Similarly, in a study conducted with *Legionella pneumophila* biofilms grown in batch cultures, it was reported that a decrease in the c-di GMP pool was compatible with an increase of the capacity to form a biofilm in *L. pneumophila* (Pécastaings et al., 2016), contrary to what is generally observed in the literature.

Many molecular mechanisms of detection and downstream signaling events of NO are still not fully elucidated. NO-based biofilm dispersion mechanisms include events that lead to a change in cellular c-di GMP levels, as well as subsequent events (Cutruzzola, and Frankenberg-Dinkel, 2016). Previously, it was shown that the amount of produced NO increased linearly with the added SNP concentrations in PBS in the ranges between 250 μM up to 1 mM SNP (Barraud, 2007a). So, it was expected for the intracellular c-di GMP levels to show an increasing or a decreasing trend as the added SNP concentrations to the biofilm cultures increased. When our findings were examined, it was shown that with the addition of 0.5 μM SNP, the c-di GMP levels of the cells dispersed from the batch system biofilms were higher than our 5 μM SNP group. Those differences might be related to the adequacy of the SNP concentrations and hence produced NO amounts. In other words, the amount of NO produced with the 0.5 μM SNP concentration might have been insufficient in the process of c-di GMP degradation although inducing the biofilm dispersion. In addition, the fact that the cells dispersed at added 5 μM SNP concentration contained c-di GMP levels similar to planktonic cells might indicate that this concentration produced the optimal nitric oxide amount. On the other hand, the addition of 50 μm and 2.5 mM SNP concentrations might have caused nitrosative stress in the dispersed bacterial cells. Cells might have tended to form biofilms to avoid this stress. Thus, an increase in

intracellular c-di GMP levels of the dispersed cells at 50 μm and 2.5 mM added SNP concentrations were observed.

In our study, we used two different experimental setups (batch and continuous systems) to obtain biofilm-dispersed *E. coli* ATCC 25404 cells. Our experimental results in the batch culture system showed that biofilm-dispersed cells with SNP showed higher levels of c-di GMP than the c-di GMP level of planktonic cells. On the other hand, c-di GMP levels of planktonic and biofilm-dispersed cells in the continuous system at 0.5 μM added SNP concentration was close to each other. The differences observed in the c-di GMP levels of bacterial cells could be arising from the use of different systems (batch and continuous). Further investigations of the effects of batch and continuous growth conditions on the biofilm formation and dispersion can detail the observed differences in the c-di GMP levels and adhesion affinities of biofilm-dispersed cells in our study.

In addition, previously it was reported that the amount of c-di GMP in the planktonic cells depended on the growth phase of the cells. It has been also shown that the change in the c-di GMP level occurs almost throughout the life of the bacterium (Spangler et al., 2010). The low amount of c-di GMP extracted from planktonic *E. coli* ATCC 25404 cells in our study might be due to the growth phase in which we harvested the planktonic bacterial cells. When the planktonic cells were harvested from different growth phases, there could have been differences in their c-di GMP amounts, as also previously reported by other studies.

As can be understood from our study and also from all the mentioned studies, the c-di GMP levels of bacteria can vary according to the bacterial strain used, growth phase of the cells at which they were harvested (for planktonic cells), the biofilm culture system (batch or continuous), as well as the dispersion method used (active or passive dispersion). In future studies, investigation of c-di GMP levels of both biofilms and post-biofilms for both batch and continuous culture systems may also provide a better understanding of the effectiveness of this molecule in the biofilm life-cycle.

As can be seen from the linear correlation (r^2=0.8322) between cellular c-di GMP amounts and adhesion strengths of planktonic and biofilm-dispersed *E. coli* ATCC 25404 cells investigated, it can be concluded that molecular adhesion of *E. coli* ATCC 25404 was mediated by the amount of intracellular c-di GMP, increased intracellular c-di GMP levels enhanced the initial attachment of bacteria to the surface (Figure 33).

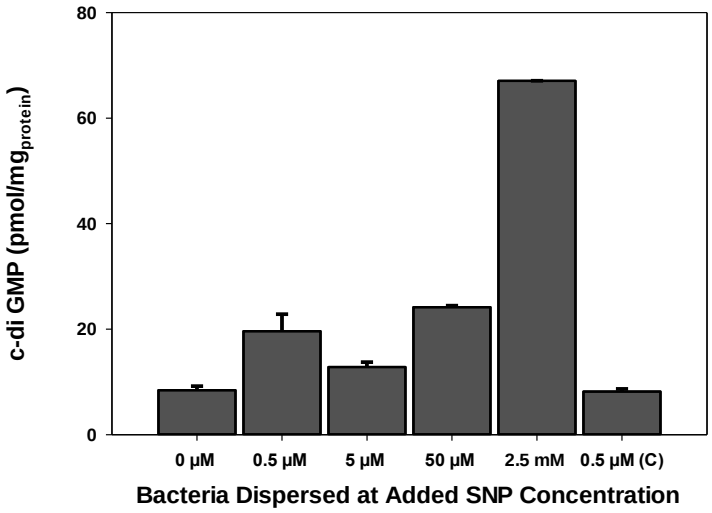

Figure 32. Intracellular c-di GMP amounts of planktonic and biofilm-dispersed *E.coli* ATCC 25404 cells as a function of the SNP concentration added to cultures grown in batch and continuous system.

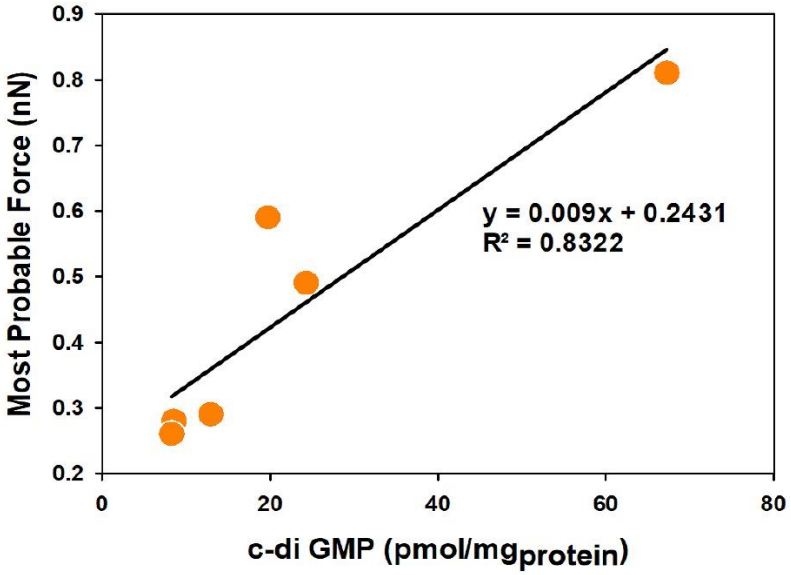

Figure 33. Correlation between the most probable adhesion forces and c-di GMP amounts of planktonic and biofilm-dispersed cells.

CHAPTER 5: CONCLUSION

The main intention of this thesis was to reveal a description of changes in the molecular adhesion mechanisms of biofilm-dispersed cells, which have a distinct existence in the biofilm life-cycle compared to their planktonic counterparts. To accomplish this, the planktonic *E. coli* ATCC 25404 cells were cultured in batch and continuous systems to form biofilms, and optimum SNP concentrations were determined to ensure the biofilm dispersion. Measurements of topographical imaging of planktonic and biofilm-dispersed *E. coli* ATCC 25404 cells and their adhesion affinities to silicon nitride as a function of the SNP concentration added to cultures grown in batch and continuous systems were performed under water using AFM. Changes in bacterial size depending on the SNP concentration were determined and compared to each. The comparison showed that addition of SNP to the biofilm cultures resulted in the release of cells from the biofilms with increased cell dimensions (on average) compared to the dimensions of planktonic cells. The most profound effect was observed for the cells dispersed from batch grown biofilms at 2.5 mM toxic SNP concentration followed by the cells dispersed at 0.5 μM added SNP concentration. These changes were related to the cells having different c-di GMP levels due to the introduction of different concentrations of SNP to biofilm cultures.

The adhesion forces, energies, and pull-off distances of the surface biopolymers of intact planktonic and biofilm-dispersed *E. coli* ATCC 25404 cells were measured as functions of the SNP concentration added to biofilm cultures grown in batch and continuous systems. Our AFM data showed that planktonic cells and SNP induced biofilm-dispersed bacterial cells possessed different molecular adhesion capacities due to different levels of heterogeneities in the composition and/or amounts of their surface biopolymers. The highest heterogeneity and/or the widest distribution of the measured adhesion forces and energies was observed for the biofilm-dispersed cells in batch systems at 0.5 μM and 2.5 mM added SNP concentrations which resulted in the highest adhesion strengths compared to other cell groups investigated. The adhesion force and energy distributions of the biofilm-dispersed cells at a concentration of 5 μM added SNP in the batch system were found to be similar to those of the control group, planktonic cells.

Although the cells dispersed from biofilms in both batch and continuous systems with the addition of 0.5 μM SNP showed higher adhesion strengths than the planktonic cells, the adhesion capacity of 0.5 μM SNP-dispersed cells in the batch system was higher than that observed for the continuous system counterparts. The differences observed between the dispersed cells from batch and continuous cultures at 0.5 μM added SNP concentration could be arising in part from the different environmental conditions of batch and continuous systems.

In order to obtain information about the length of bacterial surface biopolymers, the analysis of pull-off distance data obtained from AFM was also performed and compared. The heterogeneity in the histograms of pull-of distance data indicated that planktonic and biofilm dispersed *E. coli* ATCC 25404 cells had biopolymers of varying lengths on their surfaces. The difference in the biopolymer lengths was most significant for biofilm-dispersed cells obtained after the addition of 0.5 μM SNP in both batch and continuous systems.

The diversity in the bacterial surface biopolymers is regulated by the genetic deviations in bacteria and differences in the environmental factors. The sodium nitroprusside (SNP) used as the agent to induce biofilm dispersion in this study is a nitric oxide generator and targets bacteria's c-di GMP pathways. C-di GMP is a second messenger signallling molecule that enables communication between bacterial cells. Many bacteria contain genes that recognize proteins containing this molecule. In addition, it plays a very important role in the regulation of cellular processes such as bacterial molecular adhesion mechanisms by stimulating bacterial surface biopolymers and EPS production. HPLC analysis was performed to compare the fluctuations in intracellular levels of c-di GMP due to varying SNP concentrations. After the addition of different SNP concentrations in batch system biofilms, an increase was observed in the c-di GMP levels of the biofilm-dispersed cells compared to their planktonic counterparts. The c-di GMP level of cells dispersed with 0.5 μM SNP from continuous system biofilm was very similar to that of planktonic cells. Overall, our results showed that molecular adhesion strength and intracellular c-di GMP level was well correlated.

Consequently, the chronic nature of biofilms and their resistance to antimicrobial methods make it very difficult to combat them. Up to the present, methods developed to combat biofilms generally contain target points in line with the characteristics of planktonic bacteria. However, bacteria go through different stages during the biofilm life-cycle, so it is likely that the cells separated from the biofilm will have different genetic and physiological characteristics compared to planktonic cells. In this study, we investigated the differences in the molecular adhesion mechanisms of biofilm dispersed cells in comparison to their planktonic equivalents by using the capability of AFM measurements of the bacterial adhesion. We showed that the heterogeneity of the surface biopolymers of the biofilm dispersed cells, and hence the adhesion capacities of them, were significantly different from those of planktonic cells. More importantly, these differences were due to the concentration of the dispersing agent SNP and the conditions of the system in which the biofilm was formed. Based on our results, it can be said that the concentration of the dispersion agent is very important in biofilm-combating techniques. Agents not used in the optimum concentrations might lead to increased bacterial adhesion and the formation of new and more dense biofilms. As was shown in the previous chapter, the use of high doses (millimolar range) of SNP induced biofilm formation, and its toxic effect caused the biofilm-dispersed cells to become much more sticky. On the other hand, although 0.5 μM SNP was one of the low dose agent concentrations, it also induced biopolymer synthesis of the dispersed cells and increased the initial adhesion strength.

Determining the molecular adhesion mechanisms of biofilm-dispersed bacteria can shed light on developing stronger methods for preventing biofilms. Our study shows that it is possible to disperse biofilms and release more or less adhesive cells with the use of dispersion agents at the optimum concentrations. This finding could help developing better strategies to decrease biofilms-related problems in the industry and healthcare environments. In addition, for the applications that use the advantages of biofilms such as bioremediation and waste water systems, our findings would be beneficial as it was shown that using the appropriate dispersion agent concentration could result in the production of more biofilms. Further investigations regarding the concentration-dependent effects of different biofilm-dispersal agents on the adhesion mechanisms of biofilm-dispersed cells could help developing universal methods for both combating biofilms or promoting the formation of biofilms.

REFERENCES

Abu-Lail, N. I., and Camesano, T. A. (2003). *Role of lipopolysaccharides in the adhesion, retention, and transport of Escherichia coli JM109*. Environmental Science & Technology, Vol. 37, pp. 2173-2183.

Alam, F., Kumar, S., and Varadarajan, K. M. (2019). *Quantification of Adhesion Force of Bacteria on the Surface of Biomaterials: Techniques and Assays*. ACS Biomaterials Science & Engineering, Vol. 5, pp. 2093-2110.

Allesen-Holm, M., Barken, K. B., Yang, L., Klausen, M., Webb, J. S., Kjelleberg, S., Molin, S., Givskov, M., Tolker-Nielsen, T. (2006). *A characterization of DNA release in Pseudomonas aeruginosa cultures and biofilms*. Mol Microbiol, Vol. 59, pp. 1114-1128.

An, Y. H., and Friedman, R. J. (2000). *Handbook of bacterial adhesion: principles, methods, and applications*. Springer Science & Business Media.

Attila, C., Ueda, A., and Wood, T. K. (2009). *5-Fluorouracil reduces biofilm formation in Escherichia coli K-12 through global regulator AriR as an antivirulence compound*. Appl Microbiol Biotechnol, Vol. 82, pp. 525-533.

Baraquet, C., Murakami, K., Parsek, M. R., and Harwood, C. S. (2012). *The FleQ protein from Pseudomonas aeruginosa functions as both a repressor and an activator to control gene expression from the pel operon promoter in response to c-di-GMP*. Nucleic Acids Res, Vol. 40, pp. 7207-7218.

Barraud, N. (2007a). *Nitric oxide-mediated differentiation and dispersal in bacterial biofilms.* (Doctoral Thesis), The University of New South Wales, Sydney, Australia.

Barraud, N., Hassett, D. J., Hwang, S.-H., Rice, S. A., Kjelleberg, S., and Webb, J. S. (2006). *Involvement of nitric oxide in biofilm dispersal of Pseudomonas aeruginosa*. Journal of bacteriology, Vol. 188, pp. 7344-7353.

Barraud, N., Schleheck, D., Klebensberger, J., Webb, J. S., Hassett, D. J., Rice, S. A., and Kjelleberg, S. (2009). *Nitric oxide signaling in Pseudomonas aeruginosa biofilms mediates phosphodiesterase activity, decreased cyclic di-GMP levels, and enhanced dispersal*. Journal of bacteriology, Vol. 191, pp. 7333-7342.

Beloin, C., Roux, A., and Ghigo, J. M. (2008). *Escherichia coli biofilms*. Current topics in microbiology and immunology, Vol. 322, pp. 249-289.

Berlanga, M., Gomez-Perez, L., and Guerrero, R. (2017). *Biofilm formation and antibiotic susceptibility in dispersed cells versus planktonic cells from clinical, industry and environmental origins*. Antonie Van Leeuwenhoek, Vol. 110, pp. 1691-1704.

Berlanga, M., and Guerrero, R. (2016). *Living together in biofilms: the microbial cell factory and its biotechnological implications*. Microbial cell factories, Vol. 15, pp. 165-165.

Berne, C., Ducret, A., Hardy, G. G., and Brun, Y. V. (2015). *Adhesins Involved in Attachment to Abiotic Surfaces by Gram-Negative Bacteria*. Microbiology spectrum, Vol. 3, pp. 163-199.

Biswas, D., and Micallef, S. A. (2019). *Safety and Practice for Organic Food*. Academic Press.

Blanchette, K. A., and Wenke, J. C. (2018). *Current therapies in treatment and prevention of fracture wound biofilms: why a multifaceted approach is essential for resolving persistent infections*. Journal of bone and joint infection, Vol. 3, pp. 50-67.

Burmølle, M., Webb, J. S., Rao, D., Hansen, L. H., Sørensen, S. J., and Kjelleberg, S. (2006). *Enhanced biofilm formation and increased resistance to antimicrobial agents and bacterial invasion are caused by synergistic interactions in multispecies biofilms*. Applied and environmental microbiology, Vol. 72, pp. 3916-3923.

Camesano, T. A., Liu, Y., and Datta, M. (2007). *Measuring bacterial adhesion at environmental interfaces with single-cell and single-molecule techniques*. Advances in Water Resources, Vol. 30, pp. 1470-1491.

Castonguay, M. H., van der Schaaf, S., Koester, W., Krooneman, J., van der Meer, W., Harmsen, H., and Landini, P. (2006). *Biofilm formation by Escherichia coli is stimulated by synergistic interactions and co-adhesion mechanisms with adherence-proficient bacteria*. Res Microbiol, Vol. 157, pp. 471-478.

Chang, C.-Y. (2018). *Surface Sensing for Biofilm Formation in Pseudomonas aeruginosa*. Frontiers in microbiology, Vol. 8, pp. 2671-2671.

Characklis, W. G. (1973). *Attached microbial growths-II. Frictional resistance due to microbial slimes*. Water Research, Vol. 7, pp. 1249-1258.

Cheng, Y., Feng, G., and Moraru, C. I. (2019). *Micro-and nanotopography sensitive bacterial attachment mechanisms: A review*. Frontiers in microbiology, Vol. 10, pp. 191-208.

Choi, N.-Y., Bae, Y.-M., and Lee, S.-Y. (2015). *Cell surface properties and biofilm formation of pathogenic bacteria*. Food science and biotechnology, Vol. 24, pp. 2257-2264.

Christensen, L. D., van Gennip, M., Rybtke, M. T., Wu, H., Chiang, W. C., Alhede, M., Høiby, N., Nielsen, T.E., Givskov, M., Tolker-Nielsen, T. (2013). *Clearance of Pseudomonas aeruginosa foreign-body biofilm infections through reduction of the cyclic Di-GMP level in the bacteria*. Infect Immun, Vol. 81, pp. 2705-2713.

Chua, S. L., Hultqvist, L. D., Yuan, M., Rybtke, M., Nielsen, T. E., Givskov, M., Tolker-Nielsen, T., Yang, L. (2015). *In vitro and in vivo generation and characterization of Pseudomonas aeruginosa biofilm–dispersed cells via c-di-GMP manipulation*. Nature Protocols, Vol. 10, pp. 1165-1180.

Chua, S. L., Liu, Y., Yam, J. K. H., Chen, Y., Vejborg, R. M., Tan, B. G. C., Kjelleberg, S., Tolker-Nielsen, T., Givskov, M., Yang, L. (2014). *Dispersed cells represent a distinct stage in the transition from bacterial biofilm to planktonic lifestyles*. Nature communications, Vol. 5, pp. 4462-4474.

Costerton, J. W. (1999). *Introduction to biofilm*. Int J Antimicrob Agents, Vol. 11, pp. 217-221; discussion 237-219.

Costerton, J. W., Lewandowski, Z., Caldwell, D. E., Korber, D. R., and Lappin-Scott, H. M. (1995). *Microbial biofilms*. Annual Review of Microbiology, Vol. 49, pp. 711-745.

Cutruzzola, F., and Frankenberg-Dinkel, N. (2016). *Origin and impact of nitric oxide in Pseudomonas aeruginosa biofilms*. Journal of bacteriology, Vol. 198, pp. 55-65.

Di Martino, P. (2018). *Extracellular polymeric substances, a key element in understanding biofilm phenotype*. AIMS microbiology, Vol. 4, pp. 274-288.

Dochitoiu, R., Vodnar, D., and Socaciu, C. (2014). *Efficiency of Edible Films Containing Bioactive Antimicrobials on Refrigerated Pork Meat*. Bulletin of University of Agricultural Sciences and Veterinary Medicine Cluj-Napoca: Food Science and Technology, Vol. 71, pp. 68-72.

Doktycz, M. J., Sullivan, C. J., Hoyt, P. R., Pelletier, D. A., Wu, S., and Allison, D. P. (2003). *AFM imaging of bacteria in liquid media immobilized on gelatin coated mica surfaces*. Ultramicroscopy, Vol. 97, pp. 209-216.

Donlan, R. M. (2000). *Role of biofilms in antimicrobial resistance*. ASAIO journal, Vol. 46, pp. 47-52.

Donlan, R. M. (2002). *Biofilms: microbial life on surfaces*. Emerging infectious diseases, Vol. 8, pp. 881-890.

Donlan, R. M. (2009). *Preventing biofilms of clinically relevant organisms using bacteriophage*. Trends Microbiol, Vol. 17, pp. 66-72.

Donlan, R. M., and Costerton, J. W. (2002). *Biofilms: Survival Mechanisms of Clinically Relevant Microorganisms*. Clinical microbiology reviews, Vol. 15, pp. 167-193.

Dorobantu, L. S., Bhattacharjee, S., Foght, J. M., and Gray, M. R. (2008). *Atomic Force Microscopy Measurement of Heterogeneity in Bacterial Surface Hydrophobicity*. Langmuir, Vol. 24, pp. 4944-4951.

Eskhan, A. O., and Abu-Lail, N. I. (2013). *Cellular and molecular investigations of the adhesion and mechanics of Listeria monocytogenes lineages' I and II environmental and epidemic strains*. Journal of colloid and interface science, Vol. 394, pp. 554-563.

Fabbri, S., Johnston, D. A., Rmaile, A., Gottenbos, B., De Jager, M., Aspiras, M., Starke, E.M., Ward, M.T., Stoodley, P. (2016). *Streptococcus mutans biofilm transient viscoelastic fluid behaviour during high-velocity microsprays*. Journal of the Mechanical Behavior of Biomedical Materials, Vol. 59, pp. 197-206.

Falsetta, M. L., Klein, M. I., Lemos, J. A., Silva, B. B., Agidi, S., Scott-Anne, K. K., and Koo, H. (2012). *Novel antibiofilm chemotherapy targets exopolysaccharide synthesis and stress tolerance in Streptococcus mutans to modulate virulence expression in vivo*. Antimicrobial agents and chemotherapy, Vol. 56, pp. 6201-6211.

Fleming, D., and Rumbaugh, K. P. (2017). *Approaches to Dispersing Medical Biofilms*. Microorganisms, Vol. 5, pp. 15-31.

Flemming, H.-C., Neu, T. R., and Wozniak, D. J. (2007). *The EPS matrix: the "house of biofilm cells"*. Journal of bacteriology, Vol. 189, pp. 7945-7947.

Flemming, H.-C., Wingender, J., Griegbe, T., and Mayer, C. (2000). Physico-chemical properties of biofilms. Harwood Academic Publishers.

Flemming, H. C., and Wingender, J. (2010). *The biofilm matrix*. Nat Rev Microbiol, Vol. 8, pp. 623-633.

Floyd, K. A., Lee, C. K., Xian, W., Nametalla, M., Valentine, A., Crair, B., Zhu, S., Hughes, H.Q., Chlebek, J.L., Wu, D.C., Hwan Park, J., Farhat, A.M., Lomba, C.J., Ellison, C.K., Brun, Y.V., Campos-Gomez, J., Dalia, A.B., Liu, J., Biais, N., Wong, G.C.L., Yildiz, F. H. (2020). *c-di-GMP modulates type IV MSHA pilus retraction and*

surface attachment in Vibrio cholerae. Nature communications, Vol. 11, pp. 1549.

Galié, S., García-Gutiérrez, C., Miguélez, E. M., Villar, C. J., and Lombó, F. (2018). *Biofilms in the Food Industry: Health Aspects and Control Methods*. Frontiers in microbiology, Vol. 9, pp. 898-916.

Garrett, T. R., Bhakoo, M., and Zhang, Z. (2008). *Bacterial adhesion and biofilms on surfaces*. Progress in Natural Science, Vol. 18, pp. 1049-1056.

Getchis, T., Bouchard, D. A., Buttner, J., Ewart, J., Faulds, A., Flimlin, G. E., Hicks, D., Hollingsworth, C., Lazur, A., Leavitt, D. (2015). *A New Resource to Aid In the Identification and Management of Aquaculture Production Hazards.* Paper presented at the Journal of Shellfish Research, Vol. 34, pp. 633-634.

Gordesli, F. P., and Abu-Lail, N. I. (2012a). *Combined Poisson and soft-particle DLVO analysis of the specific and nonspecific adhesion forces measured between L. monocytogenes grown at various temperatures and silicon nitride*. Environmental Science & Technology, Vol. 46, pp. 10089-10098.

Gordesli, F. P., and Abu-Lail, N. I. (2012b). *Impact of ionic strength of growth on the physiochemical properties, structure, and adhesion of Listeria monocytogenes polyelectrolyte brushes to a silicon nitride surface in water*. Journal of colloid and interface science, Vol. 388, pp. 257-267.

Gordesli, F. P., and Abu-Lail, N. I. (2012c). *The Role of Growth Temperature in the Adhesion and Mechanics of Pathogenic L. monocytogenes: An AFM Study*. Langmuir, Vol. 28, pp. 1360-1373.

Gottenbos, B., Busscher, H. J., van der Mei, H. C., and Nieuwenhuis, P. (2002). *Pathogenesis and prevention of biomaterial centered infections*. Journal of Materials Science: Materials in Medicine, Vol. 13, pp. 717-722.

Guilhen, C., Charbonnel, N., Parisot, N., Gueguen, N., Iltis, A., Forestier, C., and Balestrino, D. (2016). *Transcriptional profiling of Klebsiella pneumoniae defines signatures for planktonic, sessile and biofilm-dispersed cells*. BMC Genomics, Vol. 17, pp. 237-252.

Guilhen, C., Miquel, S., Charbonnel, N., Joseph, L., Carrier, G., Forestier, C., and Balestrino, D. (2019). *Colonization and immune modulation properties of Klebsiella pneumoniae biofilm-dispersed cells*. NPJ biofilms and microbiomes, Vol. 5, pp. 25-36.

Gupta, K., Liao, J., Petrova, O. E., Cherny, K. E., and Sauer, K. (2014). *Elevated levels of the second messenger c-di-GMP contribute to antimicrobial resistance of*

Pseudomonas aeruginosa. Mol Microbiol, Vol. 92, pp. 488-506.

Ha, D.-G., and O'Toole, G. A. (2015). *c-di-GMP and its Effects on Biofilm Formation and Dispersion: a Pseudomonas Aeruginosa Review*. Microbiology spectrum, Vol. 3, pp. 301-317.

Hall-Stoodley, L., Costerton, J. W., and Stoodley, P. (2004). *Bacterial biofilms: from the natural environment to infectious diseases*. Nature reviews microbiology, Vol. 2, pp. 95-108.

Hawver, L. A., Jung, S. A., and Ng, W.-L. (2016). *Specificity and complexity in bacterial quorum-sensing systems*. FEMS microbiology reviews, Vol. 40, pp. 738-752.

EFSA BIOHAZ Panel (EFSA Panel on Biological Hazards) (2015). *Public health risks associated with Enteroaggregative Escherichia coli (EAEC) as a food-borne pathogen*. EFSA Journal, Vol. 13, pp. 4330-4418.

Hiratsuka, S., Mizutani, Y., Tsuchiya, M., Kawahara, K., Tokumoto, H., and Okajima, T. (2009). *The number distribution of complex shear modulus of single cells measured by atomic force microscopy*. Ultramicroscopy, Vol. 109, pp. 937-941.

Howlin, R. P., Cathie, K., Hall-Stoodley, L., Cornelius, V., Duignan, C., Allan, R. N., Fernandez, B.O., Barraud, N., Bruce, K.D., Jefferies, J., Kelso, M., Kjelleberg, S., Rice, S.A., Rogers, G.B., Pink, S., Smith, C., Sukhtankar, P.S., Salib, R., Legg, J., Carroll, M., Daniels, T., Feelisch, M., Stoodley, P., Clarke, S.C., Connett, G., Faust, S.N., Webb, J.S. (2017). *Low-dose nitric oxide as targeted anti-biofilm adjunctive therapy to treat chronic Pseudomonas aeruginosa infection in cystic fibrosis*. Molecular Therapy, Vol. 25, pp. 2104-2116.

Hu, M., Chen, J., Wang, J., Wang, X., Ma, S., Cai, J., Chen, C.Y., Chen, Z. W. (2009). *AFM-and NSOM-based force spectroscopy and distribution analysis of CD69 molecules on human CD4+ T cell membrane*. Journal of Molecular Recognition: An Interdisciplinary Journal, Vol. 22, pp. 516-520.

Ignarro, L. J., Buga, G. M., Wei, L. H., Bauer, P. M., Wu, G., and del Soldato, P. (2001). *Role of the arginine-nitric oxide pathway in the regulation of vascular smooth muscle cell proliferation*. Proceedings of the National Academy of Sciences, Vol. 98, pp. 4202-4208.

Israelachvili, J. N. (2011). *Intermolecular and surface forces*. Academic press.

Iturriaga, M. H., Tamplin, M. L., and Escartin, E. F. (2007). *Colonization of tomatoes by Salmonella Montevideo is affected by relative humidity and storage temperature*. Journal of food protection, Vol. 70, pp. 30-34.

Jamal, M., Ahmad, W., Andleeb, S., Jalil, F., Imran, M., Nawaz, M. A., Hussain, T., Ali, M., Rafiq M., Kamil, M. A. (2018). *Bacterial biofilm and associated infections*. Journal of the Chinese Medical Association, Vol. 81, pp. 7-11.

James, G. A., Swogger, E., Wolcott, R., Pulcini, E. d., Secor, P., Sestrich, J., Costerton, J.W., Stewart, P. S. (2008). *Biofilms in chronic wounds*. Wound Repair and regeneration, Vol. 16, pp. 37-44.

Jenal, U., Reinders, A., and Lori, C. (2017). *Cyclic di-GMP: second messenger extraordinaire*. Nature reviews microbiology, Vol. 15, pp. 271-284.

Jiang, Q., Chen, J., Yang, C., Yin, Y., and Yao, K. (2019). *Quorum sensing: a prospective therapeutic target for bacterial diseases*. BioMed research international, Vol. 2019, pp.1-15.

Jones, H., Roth, I., and Sanders, W. (1969). *Electron microscopic study of a slime layer*. Journal of bacteriology, Vol. 99, pp. 316-325.

Kaplan, J. B. (2010). *Biofilm dispersal: mechanisms, clinical implications, and potential therapeutic uses*. J Dent Res, Vol. 89, pp. 205-218.

Karygianni, L., Ren, Z., Koo, H., and Thurnheer, T. (2020). *Biofilm Matrixome: Extracellular Components in Structured Microbial Communities*. Trends Microbiol, Vol. 28, pp. 668-681.

Katsikogianni, M., and Missirlis, Y. F. (2004). *Concise review of mechanisms of bacterial adhesion to biomaterials and of techniques used in estimating bacteria-material interactions*. Eur Cell Mater, Vol. 8, pp. 37-57.

Kikuchi, T., Mizunoe, Y., Takade, A., Naito, S., and Yoshida, S. (2005). *Curli fibers are required for development of biofilm architecture in Escherichia coli K-12 and enhance bacterial adherence to human uroepithelial cells*. Microbiol Immunol, Vol. 49, pp. 875-884.

Kim, H. K., and Harshey, R. M. (2016). *A diguanylate cyclase acts as a cell division inhibitor in a two-step response to reductive and envelope stresses*. mBio, Vol. 7, pp. 1-13.

Knott, J. (2019). *Clinical Problem-Solving in Tracheoesophageal Puncture Voice Restoration*. Clinical Care and Rehabilitation in Head and Neck Cancer (pp. 189-207): Springer.

Koo, H., Allan, R. N., Howlin, R. P., Stoodley, P., and Hall-Stoodley, L. (2017). *Targeting microbial biofilms: current and prospective therapeutic strategies*. Nat Rev Microbiol, Vol. 15, pp. 740-755.

Kostakioti, M., Hadjifrangiskou, M., and Hultgren, S. J. (2013). *Bacterial biofilms: development, dispersal, and therapeutic strategies in the dawn of the postantibiotic era*. Cold Spring Harbor perspectives in medicine, Vol. 3, pp. 1-23.

Krasowska, A., and Sigler, K. (2014). *How microorganisms use hydrophobicity and what does this mean for human needs?* Frontiers in Cellular and Infection Microbiology, Vol. 4, pp. 112-119.

Lebeaux, D., Ghigo, J.-M., and Beloin, C. (2014). *Biofilm-related infections: bridging the gap between clinical management and fundamental aspects of recalcitrance toward antibiotics*. Microbiology and molecular biology reviews : MMBR, Vol. 78, pp. 510-543.

Lenselink, E., and Andriessen, A. (2011). *A cohort study on the efficacy of a polyhexanide-containing biocellulose dressing in the treatment of biofilms in wounds*. journal of wound care, Vol. 20, pp. 534-539.

Li, K., Whitfield, M., and Van Vliet, K. (2013). *Beating the bugs: Roles of microbial biofilms in corrosion*. Corrosion Reviews, Vol. 31(3-6), pp. 73-84.

Li, X.-H., Kim, S.-K., and Lee, J.-H. (2017). *Anti-biofilm effects of anthranilate on a broad range of bacteria*. Scientific reports, Vol. 7, pp. 8604-8616.

Mangwani, N., Dash, H. R., Chauhan, A., and Das, S. (2012). *Bacterial quorum sensing: functional features and potential applications in biotechnology*. Journal of molecular microbiology and biotechnology, Vol. 22, pp. 215-227.

Marino, M., Maifreni, M., Baggio, A., and Innocente, N. (2018). *Inactivation of Foodborne Bacteria Biofilms by Aqueous and Gaseous Ozone*. Frontiers in microbiology, Vol. 9, pp. 1-12.

Moradali, M. F., and Rehm, B. H. A. (2020). *Bacterial biopolymers: from pathogenesis to advanced materials*. Nature reviews microbiology, Vol. 18, pp. 195-210.

Moraes, M. N., Silveira, W., Teixeira, L. E. M., and Araújo, I. D. (2013). *Mechanisms of bacterial adhesion to biomaterials*. Revista Médica de Minas Gerais, Vol. 23, pp. 99-104.

Moreira, R. N., Dressaire, C., Barahona, S., Galego, L., Kaever, V., Jenal, U., and Arraiano, C. M. (2017). *BolA Is Required for the Accurate Regulation of c-di-GMP, a Central Player in Biofilm Formation*. mBio, Vol. 8(5), pp. e00443-00417.

Müller, D. J., and Dufrêne, Y. F. (2011). *Atomic force microscopy: a nanoscopic window on the cell surface*. Trends in Cell Biology, Vol. 21, pp. 461-469.

Newell, P. D., Boyd, C. D., Sondermann, H., and O'Toole, G. A. (2011). *A c-di-GMP effector system controls cell adhesion by inside-out signaling and surface protein cleavage*. PLoS Biol, Vol. 9, pp. 1-17.

O'Toole, G. A. (2011). *Microtiter dish biofilm formation assay*. Journal of visualized experiments : JoVE, Vol. 47, pp. 2437-2438.

Ofek, I., Edward, B., and Abraham, S. (2013). *Bacterial adhesion*. The Prokaryotes: Human Microbiology, pp. 107-123.

Park, B.-J., Gordesli, F. P., and Abu-Lail, N. I. (2014). *The Role of pH Conditions of Growth in the Specificity of Interaction Forces Measured Between Pathogenic L. monocytogenes and Silicon Nitride*. Journal of Bionanoscience, Vol. 8, pp. 473-484.

Pécastaings, S., Allombert, J., Lajoie, B., Doublet, P., Roques, C., and Vianney, A. (2016). *New insights into Legionella pneumophila biofilm regulation by c-di-GMP signaling*. Biofouling, Vol. 32, pp. 935-948.

Petrova, O. E., and Sauer, K. (2012). *Sticky situations: key components that control bacterial surface attachment*. Journal of bacteriology, Vol. 194, pp. 2413-2425.

Petrova, O. E., and Sauer, K. (2017). *High-Performance Liquid Chromatography (HPLC)-Based Detection and Quantitation of Cellular c-di-GMP*. Methods in molecular biology (Clifton, N.J.), Vol. 1657, pp. 33-43.

Pettigrew, M. M., Marks, L. R., Kong, Y., Gent, J. F., Roche-Hakansson, H., and Hakansson, A. P. (2014). *Dynamic changes in the Streptococcus pneumoniae transcriptome during transition from biofilm formation to invasive disease upon influenza A virus infection*. Infect Immun, Vol. 82, pp. 4607-4619.

Rehm, B. H. (2010). *Bacterial polymers: biosynthesis, modifications and applications*. Nature reviews microbiology, Vol. 8, pp. 578-592.

Rémy, B., Mion, S., Plener, L., Elias, M., Chabrière, E., and Daudé, D. (2018). *Interference in Bacterial Quorum Sensing: A Biopharmaceutical Perspective*. Frontiers in Pharmacology, Vol. 9, pp. 203-220.

Ren, D., Zuo, R., Barrios, A. F. G., Bedzyk, L. A., Eldridge, G. R., Pasmore, M. E., and Wood, T. K. (2005). *Differential gene expression for investigation of Escherichia coli biofilm inhibition by plant extract ursolic acid*. Applied and environmental microbiology, Vol. 71, pp. 4022-4034.

Romling, U., Galperin, M. Y., and Gomelsky, M. (2013). *Cyclic di-GMP: the first 25 years of a universal bacterial second messenger*. Microbiology and molecular biology reviews : MMBR, Vol. 77, pp. 1-52.

Ross, P., Weinhouse, H., Aloni, Y., Michaeli, D., Weinberger-Ohana, P., Mayer, R., . . . Benziman, M. (1987). *Regulation of cellulose synthesis in Acetobacter xylinum by cyclic diguanylic acid*. Nature, Vol. 325, pp. 279-281.

Ruas-Madiedo, P., Hugenholtz, J., and Zoon, P. (2002). *An overview of the functionality of exopolysaccharides produced by lactic acid bacteria*. International Dairy Journal, Vol. 12, pp. 163-171.

Ruhal, R., De Winter, F., de Jonger, B., Xavier, B. B., Goossens, H., Singh, S. K., and Malhotra-Kumar, S. (2019). *Comparison of biofilm dispersal approaches in Pseudomonas aeruginosa and evaluation of dispersed cells in acute infection mouse model*. bioRxiv, pp. 1-35.

Rusconi, R., Guasto, J. S., and Stocker, R. (2014). *Bacterial transport suppressed by fluid shear*. Nature Physics, Vol. 10, pp. 212-217.

Russell, M. H., Bible, A. N., Fang, X., Gooding, J. R., Campagna, S. R., Gomelsky, M., and Alexandre, G. (2013). *Integration of the second messenger c-di-GMP into the chemotactic signaling pathway*. mBio, Vol. 4, pp. e00001-e00013.

Sambanthamoorthy, K., Luo, C., Pattabiraman, N., Feng, X., Koestler, B., Waters, C. M., and Palys, T. J. (2014). *Identification of small molecules inhibiting diguanylate cyclases to control bacterial biofilm development*. Biofouling, Vol. 30, pp. 17-28.

Sarenko, O., Klauck, G., Wilke, F. M., Pfiffer, V., Richter, A. M., Herbst, S., . . . Hengge, R. (2017). *More than Enzymes That Make or Break Cyclic Di-GMP-Local Signaling in the Interactome of GGDEF/EAL Domain Proteins of Escherichia coli*. mBio, Vol. 8, pp. 1-18.

Scott, E., Bloomfield, S. F., and Barlow, C. (1984). *Evaluation of disinfectants in the domestic environment under 'in use'conditions*. Epidemiology & Infection, Vol. 92, pp. 193-203.

Serra, D. O., Richter, A. M., Klauck, G., Mika, F., and Hengge, R. (2013). *Microanatomy at cellular resolution and spatial order of physiological differentiation in a bacterial biofilm*. mBio, Vol. 4, pp. e00103-00113.

Sharma, G., Sharma, S., Sharma, P., Chandola, D., Dang, S., Gupta, S., and Gabrani, R. (2016). *Escherichia coli biofilm: development and therapeutic strategies*. J Appl Microbiol, Vol. 121, pp. 309-319.

Sihorkar, V., and Vyas, S. P. (2001). *Biofilm Consortia on Biomedical and Biological Surfaces: Delivery and Targeting Strategies*. Pharmaceutical Research, Vol. 18, pp. 1247-1254.

Singh, A., Tiwari, A., Bajpai, J., and Bajpai, A. K. (2018). *3 - Polymer-Based Antimicrobial Coatings as Potential Biomaterials: From Action to Application*. Handbook of Antimicrobial Coatings (pp. 27-61): Elsevier.

Song, F., Koo, H., and Ren, D. (2015). *Effects of material properties on bacterial adhesion and biofilm formation*. J Dent Res, Vol. 94, pp. 1027-1034.

Spangler, C., Böhm, A., Jenal, U., Seifert, R., and Kaever, V. (2010). *A liquid chromatography-coupled tandem mass spectrometry method for quantitation of cyclic di-guanosine monophosphate*. J Microbiol Methods, Vol. 81, pp. 226-231.

Stones, D. H., and Krachler, A. M. (2016). *Against the tide: the role of bacterial adhesion in host colonization*. Biochemical Society transactions, Vol. 44, pp. 1571-1580.

Stoodley, P., Wilson, S., Cargo, R., Piscitteli, C., and Rupp, C. J. (2001). *Detachment and other dynamic processes in bacterial biofilms*. pp. 189-192.

Toyofuku, M., Inaba, T., Kiyokawa, T., Obana, N., Yawata, Y., and Nomura, N. (2016). *Environmental factors that shape biofilm formation*. Biosci Biotechnol Biochem, Vol. 80, pp. 7-12.

Ungai-Salánki, R., Peter, B., Gerecsei, T., Orgovan, N., Horvath, R., and Szabó, B. (2019). *A practical review on the measurement tools for cellular adhesion force*. Advances in Colloid and Interface Science, Vol. 269, pp. 309-333.

Uzoechi, S. C., and Abu-Lail, N. I. (2019). *Changes in cellular elasticities and conformational properties of bacterial surface biopolymers of multidrug-resistant Escherichia coli (MDR-E. coli) strains in response to ampicillin*. The Cell Surface, Vol. 5, pp. 1-15.

Van der Mei, H. C., de Vries, J., and Busscher, H. J. (2010). *Weibull analyses of bacterial interaction forces measured using AFM*. Colloids and surfaces B: Biointerfaces, Vol. 78, pp. 372-375.

Van Houdt, R., and Michiels, C. W. (2010). *Biofilm formation and the food industry, a focus on the bacterial outer surface*. J Appl Microbiol, Vol. 109, pp. 1117-1131.

Vogeleer, P., Tremblay, Y. D., Mafu, A. A., Jacques, M., and Harel, J. (2014). *Life on the outside: role of biofilms in environmental persistence of Shiga-toxin producing Escherichia coli*. Frontiers in microbiology, Vol. 5, pp. 317-329.

Walker, D. I., and Keevil, C. W. (2015). *Low-concentration diffusible molecules affect the formation of biofilms by mixed marine communities*. Cogent Biology, Vol. 1, pp. 1-13.

Washio, J., Sato, T., Ikawa, K., Tanda, N., Iwakura, M., Koseki, T., and Takahashi, N. (2005). *Relationship between hydrogen sulfide-producing bacteria of the tongue coating and oral malodor*. International Congress Series, Vol. 1284, pp. 199-200.

Weart, R. B., Lee, A. H., Chien, A.C., Haeusser, D. P., Hill, N. S., and Levin, P. A. (2007). *A metabolic sensor governing cell size in bacteria*. Cell, Vol. 130, pp. 335-347.

Wille, J., Teirlinck, E., Sass, A., Van Nieuwerburgh, F., Kaever, V., Braeckmans, K., and Coenye, T. (2020). *Does the mode of dispersion determine the properties of dispersed Pseudomonas aeruginosa biofilm cells?* Int J Antimicrob Agents, Vol. 56, pp. 106194-106204.

Wood, T. K., Barrios, A. F. G., Herzberg, M., and Lee, J. (2006). *Motility influences biofilm architecture in Escherichia coli*. Appl Microbiol Biotechnol, Vol. 72, pp. 361-367.

Wu, Y.-K., Cheng, N.-C., and Cheng, C.-M. (2019). *Biofilms in chronic wounds: pathogenesis and diagnosis*. Trends in biotechnology, Vol. 37, pp. 505-517.

Yin, W., Wang, Y., Liu, L., and He, J. (2019). *Biofilms: The microbial "protective clothing" in extreme environments*. International journal of molecular sciences, Vol. 20, pp. 3423-3441.

Young, K. D. (2006). *The selective value of bacterial shape*. Microbiology and molecular biology reviews, Vol. 70, pp. 660-703.

Yu, M., and Chua, S. L. (2019). *Demolishing the great wall of biofilms in Gram-negative bacteria: To disrupt or disperse?* Medicinal research reviews, Vol. 40(3), pp. 1103-1116.

Zeraik, A. E., and Nitschke, M. (2012). *Influence of growth media and temperature on bacterial adhesion to polystyrene surfaces*. Brazilian Archives of Biology and Technology, Vol. 55, pp. 569-576.